Contributions of NHEJ and HRR in the processing of DNA double strand breaks and chromosome breaks throughout the cell cycle

Inaugural-Dissertation

zur

Erlangung des Doktorgrades

Dr. rer. nat.

der Fakultät für Biologie

an der

Universität Duisburg-Essen

Standort Essen

vorgelegt von

Maria Siemann

aus Telgte

Dezember, 2013

Die der vorliegenden Arbeit zugrunde liegenden Experimente wurden am Institut für Medizinische Strahlenbiologie an der Universität Duisburg-Essen, Standort Essen, durchgeführt.

1. Gutachter: Prof. Dr. George Iliakis

2. Gutachter: Prof. Dr. Hemmo Meyer

Vorsitzender des Prüfungsausschusses: PD Dr. Jürgen Thomale

Tag der mündlichen Prüfung: 19. März 2014

Die beste Bildung findet ein gescheiter Mensch auf Reisen.

Johann Wolfgang von Goethe (1749 – 1832)

Table of Contents

List of figures

List of tables

List of abbreviations

°C	Degree celsius
%	Percent
A	Ampere
Ab	Antibody
AFIGE	Asymmetric field inversion gel electrophoresis
aNHEJ	Alternative NHEJ
Aph	Aphidicolin
ATM	Ataxia-telangiectasia-mutated
ATR	Ataxia-telangiectasia and RAD3 related kinase
BER	Base excision repair
BLM	Bloom’s syndrome protein
B-NHEJ	Backup NHEJ
bp	Base pair
BRCA1/2	Breast cancer susceptibility protein 1/2
BrdU	Bromodeoxyuridine
CE	Chromosomal exchange
CHO	Chinese hamster ovary
cm	Centimeter
CO_2	Carbon dioxide
CT	Chromosomal translocation
CtIP	C-terminal binding interacting protein
DAPI	4',6-Diamidino-2-phenylindole
DDR	DNA damage response
DEQ	Dose equivalent
D-loop	Displacement loop

DMSO	Dimethyl sulfoxide
DNA	Deoxyribonucleic acid
DNA-PK	DNA-dependent protein kinase
DNA-PKcs	DNA-dependent protein kinase catalytic subunit
D-NHEJ	DNA-PK dependent non-homologous end-joining
DSB	Double strand break
EDTA	Ethylenediaminetetraacetic acid
e.g.	Exempli gratia
et al.	Et alii
EtBr	Ethidium bromide
eV	Electronvolt
FACS	Fluorescence activated cell sorting
FBS	Fetal bovine serum
FDR	Fraction of DNA released
FISH	fluorescence in situ hybridization
g	Gramm
Gy	Gray
OH•	Hydroxyl radical
h	hour
H_2O	Water
HCT	Human colorectal tumor
HEPES	4-(2-hydroxyethyl)-1-Piperazineethanesulfonic acid
HR	Homologous recombination
HRR	Homologues recombination repair
HST	Histogram
HTL	High temperature lysis
i.e.	Id est

Ig	Immunoglobulin
IR	Ionizing radiation
IRS	Insuline receptor substrate
kg	Kilogram
KO	Knock out
LET	Linear energy transfer
Lig	Ligase
M	Molar (mol/ L)
mA	Milliampere
MEF	Mouse embryonic stem cell
M-FISH	Multicolor-FISH
MT	microtubules
min	Minute
ml	Milliliter
Mm	Millimeter
mM	Millimolar
MMEJ	Microhomology-mediated end-joining
MRN	Mre11/Rad50/Nbs1
NBS	Nijmegen breakage syndrome
NE	Neurospora endonuclease
NEB	Nuclear envelope breakdown
NER	Nucleotide excision repair
NHEJ	Non-homolohuos end-joining
nM	Nanomolar
O_2	Oxygen
OH	Hydroxyl
PARP-1	Poly (ADP-ribose) polymerase 1

PBS	Phosphate-buffered saline
PCC	Premature chromosome condensation
PCR	Polymerase chain reaction
PFGE	Pulsed field gel electrophoresis
PI	Propidium iodide
Rad51	Radiation protein 51
RNA	Ribonucleic acid
ROS	Reactive oxygen species
RPA	Replication protein A
rpm	Rounds per minute
RT	Room temperature
ss	Single strand
SSB	Single strand break
SSC	Saline-sodium Citrate Buffer
Tris	Tris(hydroxymethyl)-amino methane
UV	Ultraviolet
wt	Wild type
XCP	XCyting Chromosome Paints
XRCC1/2/5	X-ray repair cross-complementing protein group 1/2/5
XRS	X-ray sensitive
α	Alpha
β	Beta
β-ME	β-Mercaptoethanol
γ	Gamma
µl	Microliter
µm	Micrometer

Abstract

DNA double strand breaks (DSBs) are the most deleterious lesions induced by ionizing radiation (IR), which if unrepaired or misrepaired can cause chromosomal aberrations and lead to genomic instability or cell death. In higher eukaryotic cells the two main repair pathways DNA-PK dependent non-homologous end joining (D-NHEJ) and homologous recombination repair (HRR) are responsible for the repair of DSBs. An alternative pathway of NHEJ termed B-NHEJ operates as a backup, when D-NHEJ is compromised.

In this work we want to elucidate the contributions and the interplay of the three repair pathways HRR, D-NHEJ and B-NHEJ in the processing of DNA DSBs and chromosomal breaks throughout the whole cell cycle and in G2-phase cells in particular. Additionally we want to investigate if a dose depended switch for the repair pathway choice exists.
Recent findings of our group show that RAD51 foci saturate after exposure to higher doses and that the repair of IR induced chromosomal breaks at small doses (0.5 - 2 Gy) is almost completely inhibited in HRR mutants. Nevertheless, normal repair of DNA DSBs is revealed in HRR mutants obtained by PFGE after high doses.

In order to further investigate this observation, we performed PFGE and G2-PCC experiments using a broad, overlapping dose-spectrum, analyzing repair outcomes after DNA damage induction at lower doses than typical for PFGE, and at higher doses than typical for G2-PCC. Our G2-PCC results show that the impaired repair of chromosomal breaks in HRR deficient cells at low doses recovers after exposure to 5 Gy of IR. This result gives additional evidence that at low doses HRR is the dominant pathway. Additionally the inhibition of PARP-1, an important component of B-NHEJ, results in a decrease in the repair of G2-PCC breaks, showing the involvement of B-NHEJ in the repair of lesions induced at high doses in HRR deficient cells.

It has been widely shown that B-NHEJ is responsible for the formation of chromosomal translocations (CTs) and chromosomal exchanges (CEs). We observed a strong increase in the frequency of CE formation at 5 Gy compared to the frequency of CEs in cells irradiated with 1 Gy that further strengthens the involvement of B-NHEJ in the repair of G2-PCC breaks in HRR deficient cells at 5 Gy.

In order to further investigate the involvement of B-NHEJ in DSB repair we analyzed CE formation after inhibiting B-NHEJ with PARP inhibitors in D-NHEJ deficient cells. In addition to our results showing that B-NHEJ is involved in the repair of DNA damage in HRR deficient cells resulting in high frequency of CEs formation, we show that wild type and D-NHEJ deficient cells have a lower frequency of CEs compared to HRR deficient cells. These experiments help us to elucidate potential interactions and/or mutual regulations between B-NHEJ and D-NHEJ.

Collectively, these results allow us to suggest that in the G2- phase of the cell cycle B-NHEJ backups HRR as efficiently as D-NHEJ. Furthermore we revealed the important role of PARP-1 in the formation of CEs in G2-phase at clinically relevant doses i.e. 1 or 2 Gy.

1 Introduction

1.1 Background of the subject

The maintenance of the integrity of genetic information and the genomic stability are very important for normal cell-function and also for the suppression of mutagenic events that can lead to cancer. Deoxyribonucleic acid (DNA) double strand breaks (DSBs) are considered as the most lethal form of DNA damage, whereby DNA damage is defined as any chemical change in the DNA molecule (Burma et al., 2006; Olive, 1998; Pastink et al., 2001).

There are several possibilities how DNA damages can be produced. External sources, such as exposure to ionizing radiation (IR) (Ward, 1988), ultraviolet radiation (UV), topoisomerase inhibitors and radiomimetic drugs (Ackland et al., 1988; Elmroth et al., 2003) contribute to break formation, as well as endogenous sources including cellular processes such as meiosis, V(D)J recombination, class switch recombination, meiotic recombination (Richardson et al., 2004), stalled DNA replication forks (Arnaudeau et al., 2001) and reactions that generate ROS (reactive oxygen species) (Helleday et al., 2007). All these events can produce a wide range of DNA lesions i.e. modification of bases or sugar residues, crosslinking of the DNA strands, the formation of DNA adducts and production of single- and double-strand breaks (Price and D'Andrea, 2013).

Cells have evolved different DNA repair pathways to handle these different types of DNA damage (Kennedy and D'Andrea, 2006; Mladenov and Iliakis, 2011). Among all types of lesions DSBs are considered to be the most lethal lesions, because they result in physical cleavage of the DNA backbone (Price and D'Andrea, 2013). Therefore DSBs severe entire chromosomes, which result in the loss of chromosomal fragments or even in chromosomal rearrangements through translocations, inversions or deletions (Friedl et al., 1998; van Gent et al., 2001). After exposure to a dose of 1 Gy of X-rays, there are about 1000 single strand breaks (SSBs), and an equal number of base damages generated, but only 20 - 40 DSBs (Ward, 1990). When a DSB remains unrepaired it can lead to permanent cell cycle arrest, induction of apoptosis, or cell killing (Olive, 1998), in misrepair-events or

it can result in mutations, genomic instability, deregulated growth and cancer development (Jackson, 2002).

For the detection and elimination of DNA DSBs a DNA damage response (DDR) mechanism is activated (Gospodinov and Herceg, 2013). This mechanism includes a repair network efficient enough to handle the bulk of DNA lesions, which are generated by ionizing irradiation to maintain the genomic integrity.

The two main repair pathways, DNA-PK dependent non-homologous end joining (D-NHEJ) and homologous recombination repair (HRR) are responsible for the repair of DSBs in higher eukaryotes. An alternative pathway of NHEJ operating as backup (B-NHEJ) also plays an important role when D-NHEJ is compromised (Mladenov and Iliakis, 2011; Pastink et al., 2001; Wu et al., 2008b).

D-NHEJ simply merges the ends of the broken DNA and ligates them after removing the damaged nucleotides. In this case it can happen that undamaged nucleotides are removed or new nucleotides are added, which do not fit to the original DNA sequences. Due to this limitation the original DNA sequence cannot always be restored. Therefore this repair pathway is considered to be error prone (Burma et al., 2006).

The second mechanism, HRR, repairs error free. Thereby a homologues template is needed, which can be used to restore the DNA sequence in the region of the DSB.

It is still unknown how cells make the choice over a certain repair pathway, although there are many details on the mechanisms and much information about the proteins involved are known (You and Bailis, 2010; Zhang et al., 2009). This information is important because D-NHEJ is very fast but potentially error-prone, whereas HRR works slower but error-free.

HRR had been known to be a minor pathway of DSB repair in higher eukaryotes. This hypothesis is based on the fact that none of the cell lines deficient in important HRR genes displayed DNA DSB repair defects in PFGE experiments (Wu et al., 2008a). Therefore it is believed that in higher eukaryotes IR induced DSB repair is almost completely undertaken by D-NHEJ. But it has also been shown that HRR mutant cells have a comparable radiosensitivity to D-NHEJ mutants (Soni, 2010).

As radiation therapy is widely used to treat cancer, understanding how cells repair DSBs created by IR, and how this process is altered in tumors, is of high significance (Price and D'Andrea, 2013).

1.2 Radiation and break induction by ionizing radiation

1.2.1 Physics of ionizing radiation

Radiation is a process in which energetic particles or waves come from a source and travel through vacuum or material. When the energy of radiation is absorbed by biological material it leads to excitation or ionization. In the process of ionization with X-rays, photons have enough energy to kick out electrons from atoms or molecules. The energy required per ionizing event in the absorbing material is 33eV.There are different kinds of radiation: the electromagnetic waves i.e. X-rays and γ-rays and the particulate radiations i.e. β- and α- radiation, neutrons, electrons and protons. Radiation is measured in units of Gray (Gy), which represent the amount of energy absorbed per unit of mass. The unit of 1 Gy is 1 J/kg (Hall and Giaccia, 2006).

LET (linear energy transfer) is the rate at which energy is transferred from ionizing radiation to absorbing material, which is expressed as kilo electron volts per micrometer (keV/ μm) of track length. Sparsely ionizing radiation is defined as low LET radiation, whereas densely ionizing radiation is defined as high LET radiation (Hall and Giaccia, 2006). The biological effect of a type of radiation strongly depends on its LET, biological effects of high LET are stronger compared to those of low LET (Kadhim et al., 2006). Low LET radiations are X- and γ-rays, whereas slowly moving charged particles, i.e. α-particles, are high LET radiations (Hall and Giaccia, 2006).

Chemical reactions of free radicals and ion radicals are involved in the physical processes of radiation and are jointly responsible for the biological outcome (O'Neill and Wardman, 2009). When radiation is absorbed in biological material, the atoms of the target may be ionized or excited. With this interaction a chain of events is started that leads to biological changes, like breaking the sugar phosphate backbone, or damage to the bases of the DNA. A direct action occurs when the DNA backbone is directly damaged by IR. In case of indirect action (Goodhead, 1994; Hall and Giaccia, 2006) free hydroxyl radicals are produced through the radiolysis of water

that are able to diffuse and damage the target. In this thesis ionizing radiation (IR) is applied as a means to induce DNA damage.

1.2.2 DNA damage induction

The distribution of DNA damage inducing events can differ depending on the damage inducing source as shown in figure 1.

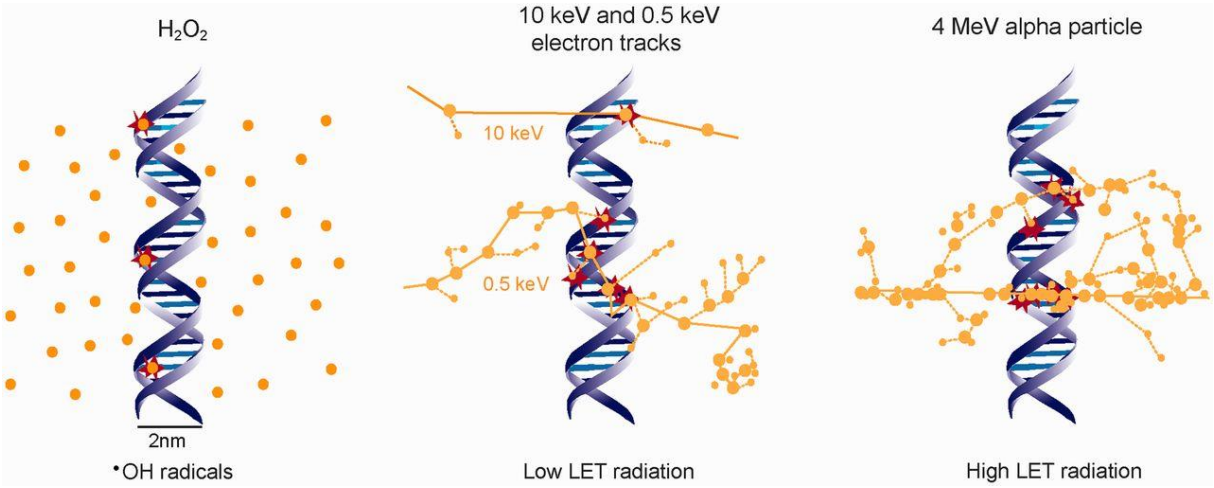

Figure 1: Distribution of DNA damage inducing events after exposure to H_2O_2 and IR of low and high LET. •OH radicals from H_2O_2 are evenly distributed in space and induce, therefore, also evenly distributed DNA damage. Large dots represent ionizations and small dots represent excitations along the radiation track (Schipler and Iliakis, 2013).

When cells are exposed to H_2O_2 the events of oxidation generated by the •OH radicals are evenly distributed within the cell, which is concentration dependent. In this case there are large amounts of SSBs generated (Iliakis et al., 1992; Schipler and Iliakis, 2013; Ward et al., 1985).

After IR exposure the ionizing events occur along the particle track and because of this, clustered damage can be induced. These clustering events increase with increasing LET (fig. 1) (Schipler and Iliakis, 2013). It is known that clustered DNA damage is the most biologically relevant damage, which is induced by IR (Goodhead, 1994; O'Neill and Wardman, 2009; Ward, 1988). Therefore IR generates a large spectrum of DNA damages, including modified bases (Sutherland et al., 2000), heat labile sites (Singh et al., 2009), DNA backbone breaks (Sancar et al., 2004) and backbone damage like single strand breaks (SSBs) or double strand breaks (DSBs), while the DSBs are the most genotoxic lesions.

With the use of more densely ionizing radiation the likelihood of residual unrepaired or misrepaired biological damage is increased, for a given absorbed dose. The particles, which have higher LET, are much more likely to induce direct DNA damage compared to particles with lower LET, which are more prone to induce indirect damage as shown in figure 2. Therefore the probability of residual damage is much less open to modifications, by i.e. chemicals or cellular factors, than after sparely ionizing radiation (Goodhead, 1994; Schipler and Iliakis, 2013).

Direct action

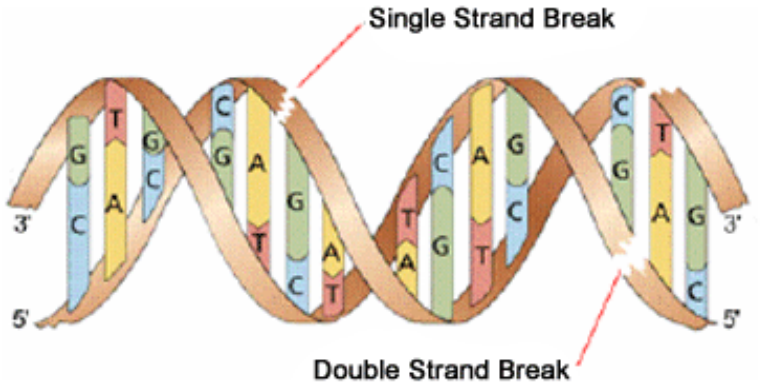

Indirect action

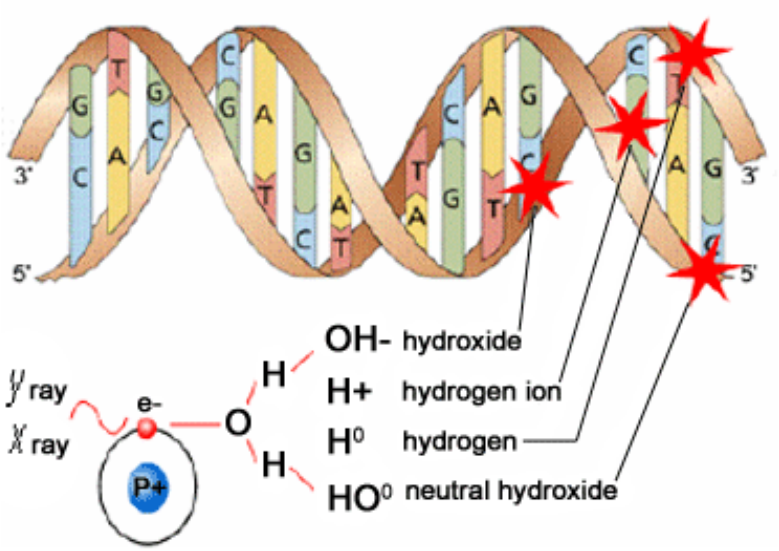

Figure 2: Two different actions, direct or indirect, of ionizing radiation to the DNA. Obtained from: http://teachnuclear.ca/contents/cna_bio_effects_rad/direct_indirect/.

The number of DNA DSBs per unit dose increases with dose. After exposure to low LET radiation, about 20 - 40 prompt DSBs per Gy, around 1000 SSBs and many base damages are induced by X-rays. (Ward, 1990).

1.2.3 Consequences of DNA DSBs in eukaryotic cells

There are many different types of DNA damage, each of 10^{13} cells gets tens of thousands DNA lesions per day. When lesions appear they may cause defects in genomic replication and transcription, when they are left unrepaired or misrepaired they can lead to mutations or genome aberrations. The most deleterious lesions are the DNA DSBs, which occur in each dividing cell at an estimated frequency of 10 breaks per day (Jackson and Bartek, 2009). They can occur for example through replication-fork collapse, during the processing of interstrand crosslinks or after exposure to IR (Ciccia and Elledge, 2010; Jackson and Bartek, 2009; Kennedy and D'Andrea, 2006).

1.2.3.1 DNA DSBs and chromosomal aberrations

When IR induced DNA DSBs are left unrepaired or misrepaired they can cause mutations and chromosomal aberrations, which can lead to the loss or gain of whole chromosomes or chromosome fragments, that can lead to genomic instability. The genomic instability can cause cell death or carcinogenesis (Jackson, 2002; Mladenov and Iliakis, 2011; Price and D'Andrea, 2013). Additional to the DSBs, which are induced, also programmed DSBs occur, which are critical for physiological processes, e.g. meiosis (Bohgaki et al., 2010).

DNA DSBs may be induced directly by i.e. IR, but for most mutagens they are more commonly the consequence of the operation of either the normal DNA synthetic process or the enzymatic repair mechanisms (Bender et al., 1974). The easiest way a DNA DSB can be formed is when two SSBs are induced nearby on opposite DNA strands (Mladenov and Iliakis, 2011). Although most of the SSBs are repaired, at least in repair proficient cells, a single-strand nuclease could convert a fraction of them to double-strand breaks (Bender et al., 1974; Natarajan and Obe, 1978). There is also the possibility of clustered DNA damage induction, which can be generated by ionization clusters from all types of IR. The cluster-complexity increases when LET is increased and an associated increase in the ratio of DSBs to SSBs is observed (Nikjoo et al., 1999).

The main target for damage induction is the DNA (Bender et al., 1974). It is believed that DSBs are involved in the formation of chromosome breaks and chromosomal

aberrations (Bryant, 1984; Natarajan and Obe, 1978). It is thought that chromosomal aberrations are lethal lesions, because about 1 aberration per cell corresponds to a survival of only 37% (Dewey et al., 1971). There are two general types of chromosomal aberrations induced by X-rays; one is a chromatid aberration and the other is a chromosome aberration. A general phenomenon found in repair proficient cells is that chromosome-type aberrations occur in cells, which were irradiated in G1- or G0- phase of the cell cycle, whereas cells exposed to X-rays in S- or G2-phase have almost all chromatid-type aberrations. Cells which were irradiated in early S-phase have most commonly chromatid-types of aberrations but they can also show some chromosome-type aberrations (Bailey and Bedford, 2006). This shows that the higher frequency of chromatid and chromosomal aberrations occurs as a result of conversion of SSBs to DSBs (Natarajan and Obe, 1978).

Chromatid and chromosomal aberrations can result in different genetic deficiencies like the loss of a terminal segment of a chromosome, the formation of a reciprocal interchange, the fusion between different chromosomes (fig. 3C), the fusion or exchange between the arms of the same chromosome. Additionally acentric ring fragments, acentric chromosomes or dicentric chromosomes can also form (fig.3A) (Gostissa et al., 2011; Sax, 1940). Examples of some of these deficiencies are shown in figure 3.

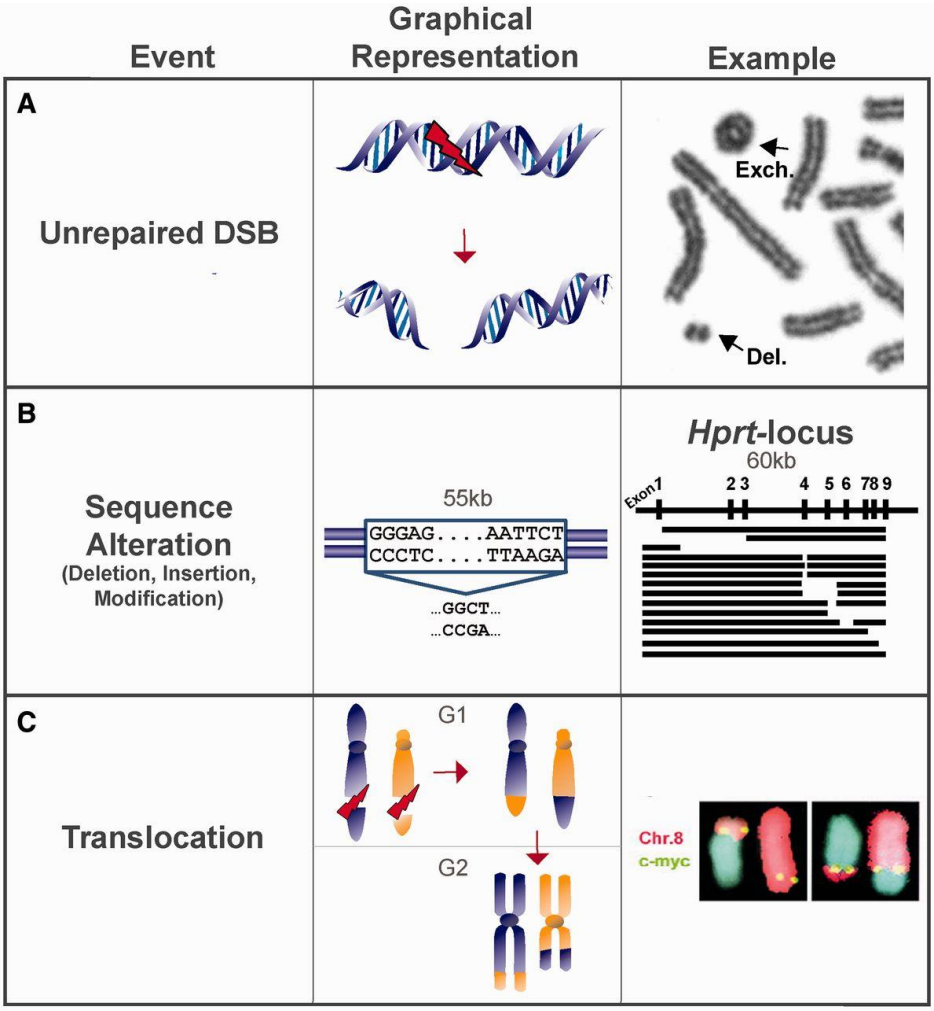

Figure 3: Different events of DNA DSB misrepair. (A) Unrepaired DSBs can result in an acentric fragment (Del). (B) Rejoining of the DSB occurs but the junction is altered, which can result in large deletions. (C) Joining of incongruent ends can lead to chromosomal translocations (Schipler and Iliakis, 2013).

1.2.3.2 Chromosomal exchanges and translocations

One of the DNA misrepair events is a chromosomal exchange (CE) and/or translocation (CT) (Lengauer et al., 1998). There is the possibility of inter and intra CTs formation. An inter-chromosomal translocation forms between two different chromosomes and an intra-chromosomal translocation forms within one chromosome. It can be distinguished between either balanced translocations, where the exchange of material is even and no genetic information is added or missing or unbalanced translocations that undergo unequal exchanges of chromosome material resulting in extra or missing genes (fig. 4).

Translocation formation requires the formation of paired DSBs on separate chromosomes (inter-chromosomal) or within a chromosome (intra-chromosomal), the two broken ends must be present at the same time and they must be in physical proximity for joining. Finally the joining of DNA DSBs in two separate chromosomal loci occurs. (Gostissa et al., 2011; Nussenzweig and Nussenzweig, 2010).

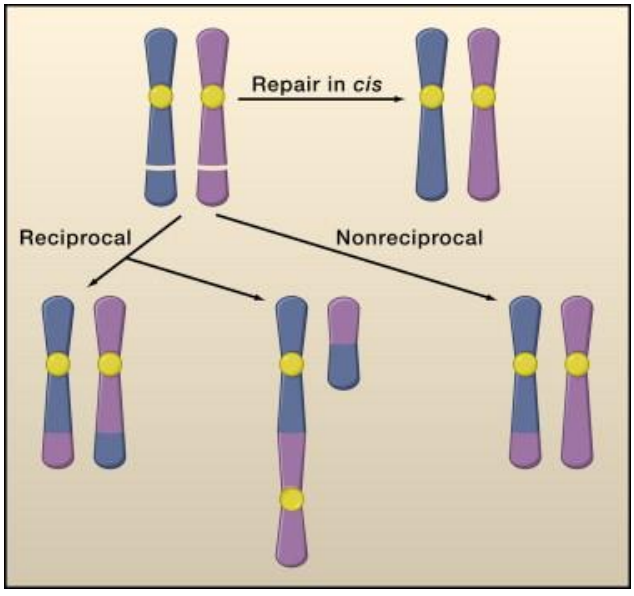

Figure 4: Chromosomal translocations (CTs) happen due to misrepair of DNA DSBs. A formation of paired DNA DSBs on different chromosomes or within a chromosome is required for the formation of a translocation. DSBs can either be repaired in cis or a rearrangement occurs between non-homologous chromosomes, which result in a translocation. (Nussenzweig and Nussenzweig, 2010).

CTs occur spontaneously in normal cells but more frequently in repair deficient cells. To maintain genomic stability and avoid CTs the cell has developed several repair pathways; D-NHEJ and HRR are the most prominent. In repair proficient cells the

translocations are suppressed by components, which mediate the repair by D-NHEJ and HR; when factors involved in these pathways are absent, a normal cell is more at risk for developing cancer phenotype (Gostissa et al., 2011; Nussenzweig and Nussenzweig, 2010).

When D-NHEJ is active, the formation of CTs is suppressed, because of the high speed end-joining of the correct DNA ends (Gostissa et al., 2011; Iliakis et al., 2007; Lieber, 2010). In principle there is a potential for CTs formation during D-NHEJ repair, but this appears to be happening infrequently (Schipler and Iliakis, 2013). If factors of the D-NHEJ e.g. DNA-PKcs or Ku are absent, there is no capturing of the DNA ends and they are processed by the DNA-PKcs independent non-homologous end joining pathway, B-NHEJ. It is a slow pathway and the broken DNA ends remain for a longer time unrepaired. During that time they may interact with other DNA ends in the vicinity, which can increase the formation of CTs (Iliakis et al., 2004; Lieber, 2010).

CTs are fundamental pathogenetic events in lymphomas and leukemia and also in many other types of cancer (Gostissa et al., 2011).

1.3 Repair pathways of DNA DSBs

To maintain genomic stability and prevent chromosomal aberrations cells have evolved at least six different mechanisms to repair different kinds of DNA damage (Kennedy and D'Andrea, 2006). In higher eukaryotes the two major repair pathways responsible for the repair of IR induced DNA DSB are D-NHEJ and HRR (Helleday et al., 2007; Nussenzweig and Nussenzweig, 2010; Wang et al., 2001). In addition, there exists an alternative pathway, which operates as backup (B-NHEJ).

In principle, D-NHEJ simply joins the broken DNA ends and ligates them after removing damaged nucleotides. Therefore it is possible that undamaged nucleotides are removed or new nucleotides added. Since the original DNA sequence cannot be always restored, D-NHEJ is termed to be error prone. The second main repair pathway is HRR, which is said to repair DNA DSBs error-free. Thereby a homologue template is used to restore the DNA sequence in the region of the DSB.

The contribution of D-NHEJ and HRR in the repair of DSBs is strongly cell cycle phase dependent (Essers et al., 2000). While HRR is known to be active in late S- and G2-phase because it needs a sister chromatid as a template for restoring the correct DNA sequence (Johnson and Jasin, 2000), D-NHEJ is active throughout the cell cycle since it does not need a template to repair DSBs. Furthermore, B-NHEJ is active throughout the cell cycle, although it shows an increased activity in G2-phase and a reduced one in G1-phase of the cell cycle (Iliakis, 2009; Singh et al., 2012; Wu et al., 2008a).

The correct repair of DNA DSBs is of great importance for the prevention of mutations or genomic rearrangements, as even a single unrepaired or misrepaired DSB can lead to cell death or even cancer (Wyman and Kanaar, 2006). Before the DSB repair machinery is initiated, the damage has to be detected by a DSB repair signaling system.

1.3.1 DSB repair signaling

The DNA damage response (DDR) is a well arranged process, which is needed to maintain genomic integrity (Hakem, 2008; Harper and Elledge, 2007). As soon as DNA damage in form of DSBs is detected within the cell, the cell is able to stop progression through the cell cycle by activation of cell cycle checkpoints. This gives the cell time to restore the damaged DNA. In mammalian cells there are three DNA damage checkpoints: the first is before the G1/S-boarder, the second is before the intra S-phase and the third comes before the G2/M-border. Through changes in the chromatin structure adjacent to DSBs, signaling and repair proteins are able to bind at the lesions (Bohgaki et al., 2010; Gospodinov and Herceg, 2013).
In mammalian cells the key DDR signaling components are the PIKK kinases ataxia-telangiectasia-mutated (ATM) and ataxia telangiectasia and Rad3-related protein (ATR), where ATM is the major kinase in the response to DSBs in S-phase.
The first factor that binds DSBs is the MRE11-RAD50-NBS1 (MRN) mediator complex, which then recruits ATM to the broken DNA ends. When ATR-interacting protein (ATRIP) binds to RPA-coated ssDNA, ATR is also recruited to the vicinity of the break (Zou and Elledge, 2003). After phosphorylation of PIKK kinases they subsequently phosphorylate central cell cycle regulators such as p53 and the

checkpoint kinases 1 and 2 (CHK1 and CHK2). Together with ATM and ATR they reduce the activity of cyclin-dependent kinase (CDK), which results in the activation of DNA damage checkpoints to give the cell more time for repair (Bartek and Lukas, 2007; Gospodinov and Herceg, 2013; Jackson and Bartek, 2009; Kastan and Bartek, 2004). If the repair of the damaged DNA is successful, the DDR is inactivated. But if the repair fails, chronic DDR signaling initiates cell death (Halazonetis et al., 2008). Furthermore a defect in DDR can cause different developmental, neurological and immunological disorders, and can lead to cancer (Schipler and Iliakis, 2013).

After the activation of DDR, DSB repair proceeds, this is described in the next paragraphs.

1.3.2 Homologous recombination repair (HRR)

The fundamental characteristic of HRR is that it needs a template for the repair of the broken chromosomes, which can in principle be either an homologous chromosome or the sister chromatid generated after DNA replication (Mladenov and Iliakis, 2011). Since sister chromatids are only available in late S-phase and G2-phase of the cell cycle HRR, is restricted to these two phases (Nussenzweig and Nussenzweig, 2010). Due to the fact HRR requires a template to restore the damaged DNA it is a slow but error free pathway (Schipler and Iliakis, 2013).

HRR can be subdivided into the presynaptic, synaptic and postsynaptic phases. The presynapsis starts after the damage is recognized and HRR is initiated when broken ends are processed to build long single-stranded DNA (ssDNA) regions. The ssDNA regions are covered by the replication protein A (RPA) complex. Additional proteins, which are involved in this step are the nucleases MRE11-RAD50-NBS1 (MRN), EXO1, DNA2, C-terminal binding interacting protein (CtIP) and the Bloom helicase BLM (Heyer et al., 2010). First MRE11 and CtIP remove terminal nucleotides from the 5´-ends to generate long 3'-ssDNA overhangs on both sides of the break, followed by resection through EXO1 and/or BLM and DNA2 (Mimitou and Symington, 2008; Povirk, 2012). The RPA complex covers the ssDNA overhangs to prevent formation of secondary structures, so that the RAD51 filaments are able to assemble. To allow timely RAD51 filament formation on ssDNA some mediator proteins are needed, where three classes exist. The proteins of the first class are the

RAD51 paralogs RAD51B, RAD51C, RAD51D, XRCC2 and XRCC3 (Thompson and Schild, 2001). They share the RecA core with RAD51 but they are not able to build filaments on DNA and fail to perform the range of DNA-pairing reactions catalyzed by RAD51. The second class is the RAD52 protein that has two independent roles, first it has mediator functions and second it acts in strand annealing of RPA-bound ssDNA. The last class of mediator proteins is typified by BRCA2, which is the human breast and ovarian cancer tumor suppressor protein. BRCA2 contains ssDNA binding motifs, a double stranded DNA (dsDNA) binding motif and a number of RAD51 binding sites. This suggest that it targets RAD51 filament nucleation to the dsDNA junction at the resected end (Heyer et al., 2010; Yang et al., 2005). All three mediators classes have been described, but their functions and the interplay between them is poorly understood (Heyer et al., 2010).

Then synapsis starts, where RAD51 filament performs the search of homology (West, 2003) in addition to strand invasion, whereby a displacement loop (D-loop) is generated so that the invading strand can prime DNA synthesis within it. The RAD51 filament is stabilized by the motor protein RAD54, which improves the D-loop formation by RAD51. Furthermore it supports the transition from DNA strand invasion to DNA synthesis by detaching RAD51 from heteroduplex DNA (Heyer et al., 2006; Nussenzweig and Nussenzweig, 2010).

The last step in HRR is the postsynapsis, where Holliday junctions become resolved, resulting in a crossover or non-crossover product (Dueva and Iliakis, 2013). There are three subpathways of HRR, consisting of break-induced replication (BIR), synthesis-dependent strand annealing (SDSA) and double Holliday junction (dHJ) formation. Each pathway has specific enzymatic requirements that have been only partially defined (West, 2003) and will not be described further in this thesis. The main players and their interactions in HRR are illustrated in figure 5.

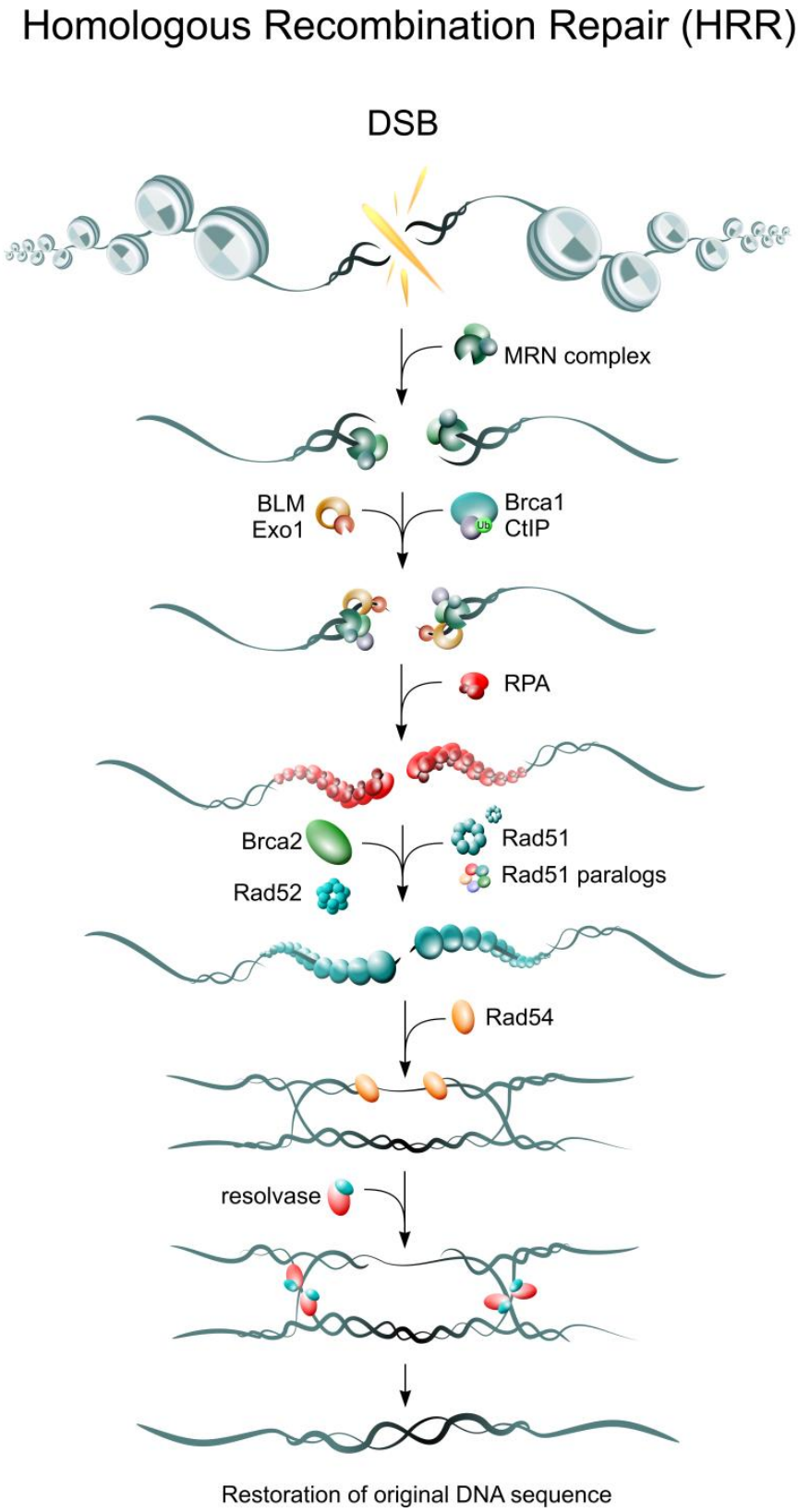

Figure 5: Overview about the interactions of the main players in Homologues recombination repair (Mladenov and Iliakis, 2011).

Nevertheless, if there are defects in HRR, they cause genomic instability, which can lead to aberrant expression or regulation of tumor suppressors, oncogenes and cell transformation, so that cancer may occur (Heyer et al., 2010; San Filippo et al., 2008).

1.3.3 DNA-PKcs dependent non-homologous end-joining (D-NHEJ)

D-NHEJ is known as the major repair mechanism in eukaryotic cells. It is a very fast process, which is active throughout the cell cycle because it does not require a homologous template. The mechanism of D-NHEJ tolerates limited or extensive additions or loss of nucleotides at the rejoining site, which can change the DNA sequence in the repaired molecule (Mladenov and Iliakis, 2011). Since D-NHEJ cannot ensure the ligation of the correct ends and can lead to chromosomal aberrations, the pathway is stated to be error prone (Iliakis et al., 2004; Lieber, 2008).

This repair pathway requires three enzymatic steps; first it needs a nuclease to remove the damaged DNA, second a polymerase to facilitate the repair, and last a ligase for reconstruction of the sugar-phosphate backbone (Lieber, 2008). The whole process is initiated by the recruitment of the Ku complex, which is known to interact with all other important repair components like the nuclease (Artemis/DNA-PKcs), the polymerases (μ and λ), and the ligase complex (XLF/XRCC4/DNA Ligase IV). Ku is a heterodimer, comprising of the components KU70 (73 kDa) and KU80 (86 kDa). Ku has an open ring-shaped structure, where both subunits form a ring that can slide over broken DNA ends, hence it has a high affinity for DNA termini (Weterings and Chen, 2008).This is followed by recruitment and binding of DNA-dependent protein kinase catalytic subunit (DNA-PKcs) and Artemis (Weterings and Chen, 2008). When the Ku-complex moves internally, DNA-PKcs can interact with the DNA and can activate in this way its serine/threonine kinase activity, which phosphorylates itself, as well as Artemis and several other proteins (Ma et al., 2002). This causes a change in the conformation of DNA-PKcs, and the active DNA-PK holoenzyme is formed (Meek et al., 2004), which promotes the end-processing by Artemis and subsequent ligation of the broken DNA via the Ligase IV/XRCC4/XLF-complex. DNA Ligase IV is able to ligate DNA ends with compatible overhangs or blunt ends

(Lieber, 2008; Mladenov and Iliakis, 2011). An overview of the interaction of the main players in D-NHEJ is shown in figure 6.

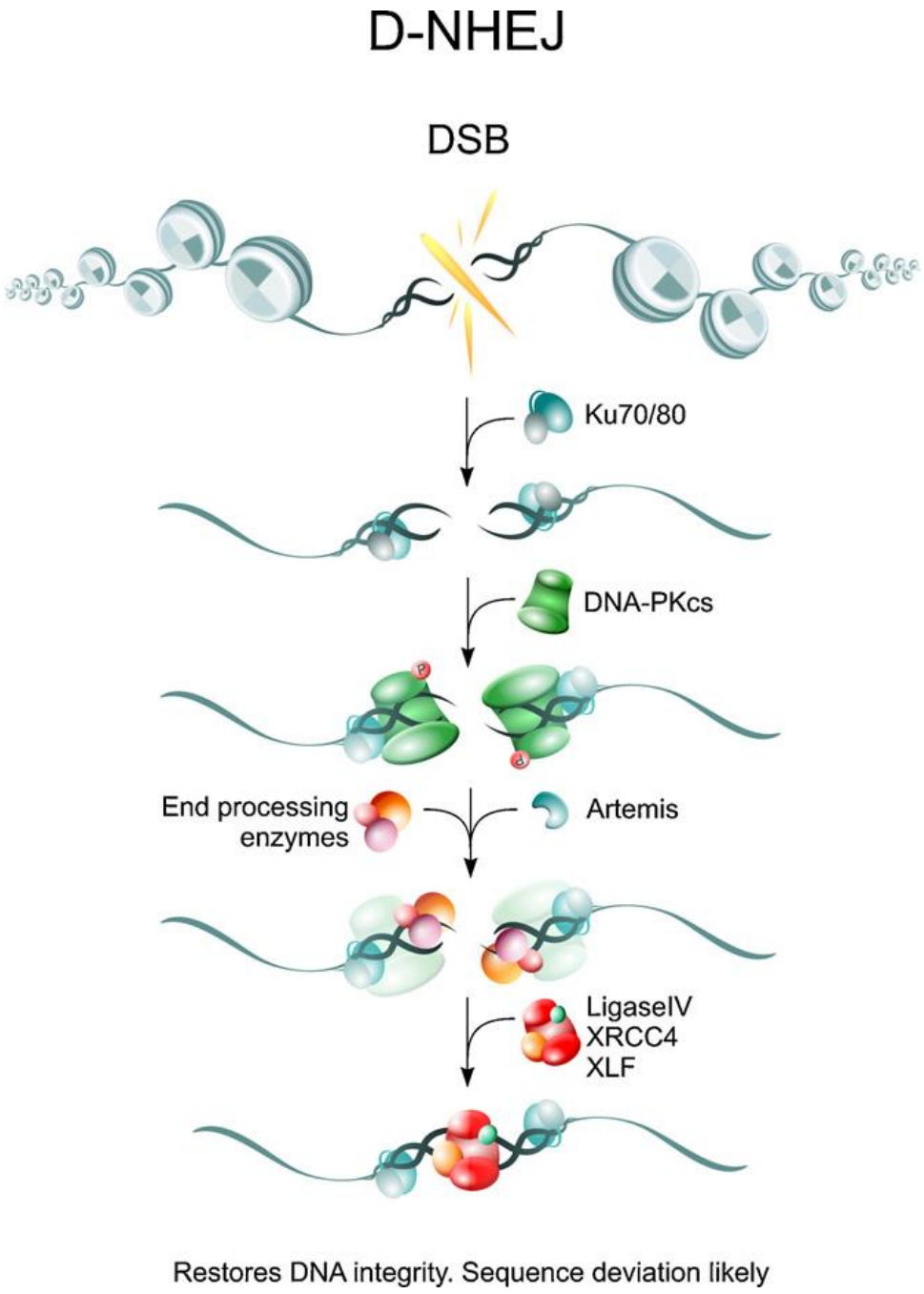

Figure 6: Overview of the interactions of the main players in DNA-PKcs dependent non-homologues end-joining repair (Mladenov and Iliakis, 2011).

D-NHEJ cannot ensure that the DNA sequence is restored but efficiently maintains genomic integrity. However, activation of D-NHEJ is known to suppress other repair pathways, because the active DNA-PKcs competes against some proteins involved in other DSB repair pathways, for example in B-NHEJ (Mladenov and Iliakis, 2011).

1.3.4 Backup pathway of non-homologues end-joining (B-NHEJ)

The third pathway is the backup pathway, or B-NHEJ. We prefer the term backup pathway, because it is active when the other pathways are compromised. This pathway was found in cells with defects in D-NHEJ components, which have slower DSB repair kinetics but still rejoin the majority of the breaks (DiBiase et al., 2000; Wang et al., 2001). Furthermore, defects of HRR components in D-NHEJ mutants did not cause an additional defect in repair capability of DSBs (Wang et al., 2001), which pointed to an alternative form of end joining (Wang et al., 2006).

B-NHEJ works with slower kinetics and is less efficient and more error-prone than D-NHEJ (Iliakis et al., 2004). After repair of B-NHEJ it has been shown that deletions and other modifications at the junctions are larger than after repair by D-NHEJ; there is also a strong increase in the joining of unrelated ends (Schipler and Iliakis, 2013). This is the reason why chromosomal aberrations are more likely to be formed by B-NHEJ than by D-NHEJ (Iliakis et al., 2004). Furthermore, B-NHEJ, in general, operates throughout the cell cycle (Iliakis, 2009; Wu et al., 2008a; Wu et al., 2008b), but its activity also shows cell cycle-dependent fluctuations with an increased activity in G2, a reduced one in G1 and appears nearly compromised in quiescent cells (Dueva and Iliakis, 2013; Singh et al., 2011; Windhofer et al., 2007b).
Until now not much is known about the biochemistry of B-NHEJ, as well as the mechanisms of regulation and how B-NHEJ is integrated into the cellular DNA DSB processing machinery. However, it was revealed that it frequently utilizes microhomologies, which is why this form of end-joining is often called microhomology-mediated end-joining (MMEJ) (Dueva and Iliakis, 2013; Verkaik et al., 2002). Since B-NHEJ can act as a backup to D-NHEJ, many of the early factors of D-NHEJ may be present at the junction, but this process must be abrogated prior to ligation by LIG4. In case of B-NHEJ the end ligation step can be done by either LIG3 or LIG1 (Arakawa et al., 2012; Della-Maria et al., 2011; Dueva and Iliakis, 2013; Paul et al., 2013; Wang et al., 2005; Windhofer et al., 2007a).
Usually PARP-1 acts in SSB repair and base excision repair (BER) where it works as a sensor for DNA damage (Caldecott, 2001), but recently it was shown to be also involved in B-NHEJ (Audebert et al., 2004; Mansour et al., 2010; Wang et al., 2006). There is evidence that D-NHEJ components like Ku suppress B-NHEJ by preventing

PARP-1 to bind to the end of the DNA (Cheng et al., 2011; Schipler and Iliakis, 2013; Wang et al., 2006), and in addition possibly it is suppressed by HRR (Dueva and Iliakis, 2013), because there are hints that B-NHEJ could also be a backup of HRR (Jeggo et al., 2011). Since it is shown that B-NHEJ is dependent on the MRN complex, as well as CtIP, it can operate on resected ends, which in turn inactivates D-NHEJ. (Lee-Theilen et al., 2011; Xie et al., 2009; Zhong et al., 2002). An overview of the B-NHEJ proteins and their interaction is shown in figure 7.

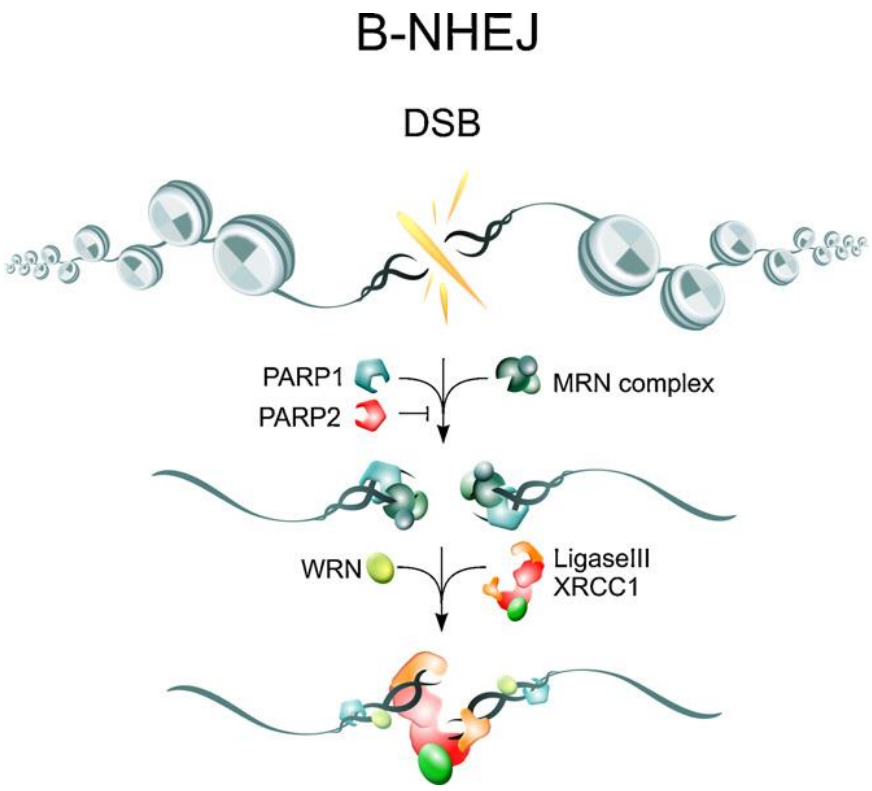

Figure 7: Overview of the interactions of the main players in DNA-PKcs independent non-homologous end-joining (B-NHEJ) (Mladenov and Iliakis, 2011).

It was also found, that there are more deletions and other modifications at the joined junctions when using B-NHEJ and that there is a strong increase in the joining of probably unrelated ends (Schipler and Iliakis, 2013). As a result, more chromosomal aberrations form after DSB processing by B-NHEJ, which can lead to cancer (Roukos et al., 2013). That is why in the field of cancer treatment and protection from carcinogenesis therapists want to combine B-NHEJ inhibitors with other treatment modalities to improve the therapy (Dueva and Iliakis, 2013).

1.3.4.1 Role of B-NHEJ in the formation of chromosomal translocations

It is now emerging that the alternative pathway B-NHEJ is responsible for the formation of chromosome translocations (CTs), which are the hallmark of cancer (Roukos et al., 2013). The critical factor for the creation of CTs is the extent of DNA end resection, since CTs do not often appear to be formed at homologous sequences (Stephens et al., 2011; Stephens et al., 2009). In HRR, CTs are inhibited by extensive DNA resection (Richardson et al., 1998), while in D-NHEJ the components of the pathway seem to suppress the formation of CTs (Ferguson et al., 2000; Weinstock et al., 2007). When a cell is deficient in KU80, LIG4 or KU80/LIG4 the frequency of CTs is higher (Boboila et al., 2010a; Boboila et al., 2010b; Simsek and Jasin, 2010). Some experiments revealed that Ku reduces the mobility of DNA ends, which inhibits the formation of CTs (Drouet et al., 2005). This is a direct evidence that the error-prone B-NHEJ plays a role in CT formation (Mladenov and Iliakis, 2011). In addition, it is suggested that other components of B-NHEJ like LIG3 and CtIP also take part in the formation of CTs generated by the error-prone processing of restriction endonuclease (RE)-caused DSBs (Simsek et al., 2011; Zhang and Jasin, 2011). Another important protein in alternative end-joining is PARP-1. It also seems to have a contribution in CT formation, since it was shown that inhibition of PARP-1 reduces the frequency of CTs in G1 cells from site-directed DSBs, as well as of DSBs in cells that were exposed to high doses of IR (Wray et al., 2013).

Overall, it is clear that the most important thing to prevent the formation of CTs is to have a proper balance of DNA resection. Since B-NHEJ is active throughout the cell cycle it could form CTs when HRR and/or D-NHEJ fail to be active. It is also possible for B-NHEJ to form CTs if there is an inhibition of long-range resection in S/G2-phase (EXO1/DNA2-dependent) and if there is a stimulation of short-range resection in G1, which is MRN/CtIP-dependent, respectively (Symington and Gautier, 2011).

Despite the potential consequences of B-NHEJ in the formation of CTs, not much is known about the underlying mechanisms either for site specific, programmed DSBs, or for randomly induced DSBs through exposure to IR (Greaves and Wiemels, 2003; Mladenov and Iliakis, 2011).

1.4 Cell cycle and repair pathway choice

The fact that eukaryotic cells evolved three different DSB repair pathways, D-NHEJ, HRR and B-NHEJ, which have all a different outcome and ability to faithfully restore the genome, implicates a kind of repair pathway choice. On the one hand there is D-NHEJ, which is very fast but potential error prone, because it can cause small sequence alterations or translocations. On the other hand there is HRR; which works slower but error-free. However, there is the third pathway, B-NHEJ, which has the highest probability to form translocations, as well as large deletions and other sequence alterations at the junction (Dueva and Iliakis, 2013).
Although there are many details on the mechanisms and much information about the proteins involved in repair pathway choice known, it is still unknown how cells decide to use a certain repair pathway (You and Bailis, 2010; Yun and Hiom, 2009; Zhang et al., 2009). This information would be from high importance.

Biochemical studies showed that in cells of higher eukaryotes the predominant pathway to repair DSBs is thought to be D-NHEJ (Heller and Marians, 2006), although this pathway is known to be error-prone, since it does not depend on extensive regions of homology (Jeggo, 1998). This hypothesis is based on the fact that none of the mutants deficient in important HRR genes displayed a DSB repair defect compared to wt in PFGE experiments. Therefore, it is believed that in higher eukaryotes DSB repair by HR plays only a minor role. In contrast, HRR mutant cells show the same radiosensitivity to killing as D-NHEJ mutants (Soni, 2010). Whereas B-NHEJ acts as a backup when D-NHEJ fails to complete end-processing, it could also be assumed that if HRR fails after the resection step it will be backed up by B-NHEJ as well (Dueva and Iliakis, 2013).

1.4.1 Cell cycle dependent repair pathway choice

Since HRR needs a template to faithfully restore the DNA sequence, the choice between HRR and D-NHEJ is cell cycle dependent. Therefore HRR is upregulated when sister chromatids are available, which is the case in late S-phase and G2-phase of the cell cycle (Kadyk and Hartwell, 1992; Nussenzweig and Nussenzweig, 2010). Another evidence for HRR getting involved in this phase of the cell cycle is the increase in RAD51 and RAD52 expression during S-phase (Chen et al., 1997;

Shrivastav et al., 2008). The amount of the HRR component CtIP is regulated throughout cell cycle as well, with a high level in S- and G2-phase and a low level in G1 (Gospodinov and Herceg, 2013; Limbo et al., 2007).
However, D-NHEJ is active throughout the cell cycle and is the predominant pathway during G1-phase, but remains also active in S- and G2-phase, where it could compete with HRR (Bohgaki et al., 2010; Takata et al., 1998). The idea of a possible competition between D-NHEJ and HRR arose after the finding that plasmid DNA transfected into mammalian cells could be repaired by both pathways (Roth and Wilson, 1985). It is likely that the critical step for pathway choice is the step of DNA end resection. When it is initiated it prevents D-NHEJ and promotes HRR and the other way round (Symington and Gautier, 2011).

Cyclin dependent kinases (CDKs) are the key regulators of cell cycle progression, they phosphorylate proteins, which are involved in resection (Jazayeri et al., 2006), like the MRN complex and BRCA2 (Huertas et al., 2008). There is evidence that an active suppression of D-NHEJ in G2 by inhibition of D-NHEJ factor binding to DSBs exists, but it can still be due to elevated end resection (Zhang et al., 2009). Furthermore CDK1 is essential in HR after strand invasion and before initiation of DNA synthesis (Ira et al., 2004). It is also needed for the expression and posttranslational modifications of CtIP, which also fluctuate throughout cell cycle (Limbo et al., 2007; Zhang et al., 2009).
Taken together, CDK1 is an important protein in cell cycle dependent repair pathway choice, because it controls this process through the activation of nucleolytic processing of DNA ends to produce ssDNA, which is needed for HRR and inhibits D-NHEJ at the same time (Aylon et al., 2004).
The fact that proteins like the MRN-complex, BRCA1, histone H2AX, PARP-1, DNA-PKcs and ATM are involved in both pathways, could be a hint that the choice between these two pathways is under active control and not really in competition (Kim et al., 2005; Shrivastav et al., 2008). Thereby DNA-PKcs seems to be another important protein, since some results suggested that after inhibition of DNA-PKcs it cannot dissociate from the DNA ends and thus access for the repair factors of other pathways is blocked (Convery et al., 2005; Kurimasa et al., 1999; Shrivastav et al., 2008).

In summary, there is indication that the repair pathway choice is regulated through the expression levels or post-translational modifications of repair proteins, as well as through CDK activity (Ira et al., 2004). However it is still unclear whether such responses reveal coordinating functions or are themselves the outcome of some overarching coordination (Mladenov and Iliakis, 2011).

1.4.2 The interplay between cell cycle and radiosensitivity in mammalian cells

There are cell cycle-dependent fluctuations in radiosensitivity to killing, which differ between cells of different species, shown in table 1.

Table 1: Cell cycle-dependent fluctuation in radiosensitivity in different species (Hall and Giaccia, 2006).

	Chinese hamster cells	Human cells
M-phase	most sensitive	most sensitive
G1-phase	intermediate sensitive	first resistant but getting sensitive towards the end
early S-phase	intermediate sensitive	intermediate sensitive
late S-phase	resistant	resistant
G2-phase	most sensitive	most sensitive

There is a difference between Chinese hamster and human cells in the radiosensitivity during the G1-phase of the cell cycle (tab. 1), due to differences in the times cells remain in G1-phase, which is 11 h in human cells and only 1 h in Chinese hamster cells (Hall and Giaccia, 2006).

It is known that Chinese hamster cells irradiated at the G1/S-border of the cell cycle are generally radiosensitive, whereas cells irradiated in mid or late S-phase are radioresistant. This advantage is lost in HRR mutant cells; they remain radiosensitive throughout the cell cycle, due to a lack of the radioresistance during S-phase, shown in figure 8 (Cheong et al., 1994; Tamulevicius et al., 2007).

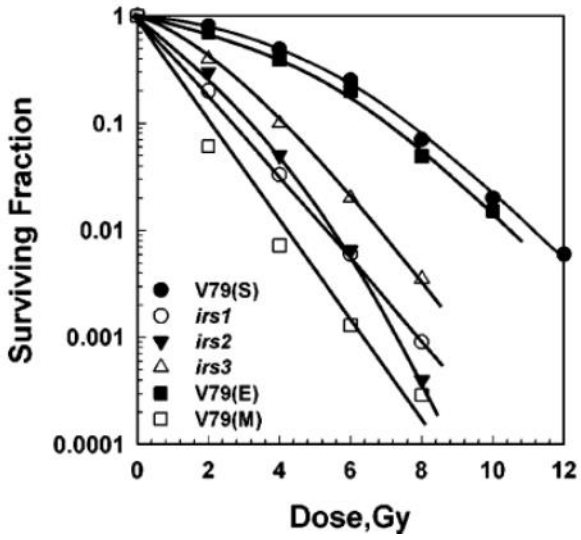

Figure 8: Comparison of the intrinsic radiosensitivity of different mutants with cells of the same origin, tested in late S- and M-phase. Survival curves for Chinese hamster wild type (V79) and HRR mutant cells (Irs1, Irs2 and Irs3) (Tamulevicius et al., 2007).

Figure 8 clearly demonstrates that for the radioresistance to killing in S- and G2-phase a functional HRR is needed. The radiosensitivity in the M-phase of the cell cycle is caused by the transition of chromatin into a state, which interrupts its capability to engage HRR due to the condensation process and the separation of the sister chromatids. Therefore, cells are in general radiosensitive in M-phase since they lack chromatid-dependent HRR (Tamulevicius et al., 2007).

1.5 Previous work

Prior to this thesis a lot of work was done in our lab. For the better understanding of the background of this thesis this chapter will give a short overview of the different results, which were obtained during the last years and led to the development of the aims of this thesis.

1.5.1 Role of HRR in the repair of DNA DSBs

In cells of higher eukaryotes it was assumed that HRR plays only a minor role in the repair of IR induced DSB and D-NHEJ completely undertakes this part (Heller and Marians, 2006).

Using the clonogenic survival assay the radiosensitivity of different cell lines can be analyzed. Here, the radiosensitivity to killing in wild type (wt), D-NHEJ and HRR deficient Chinese hamster cells was evaluated. The obtained results are shown in figure 9.

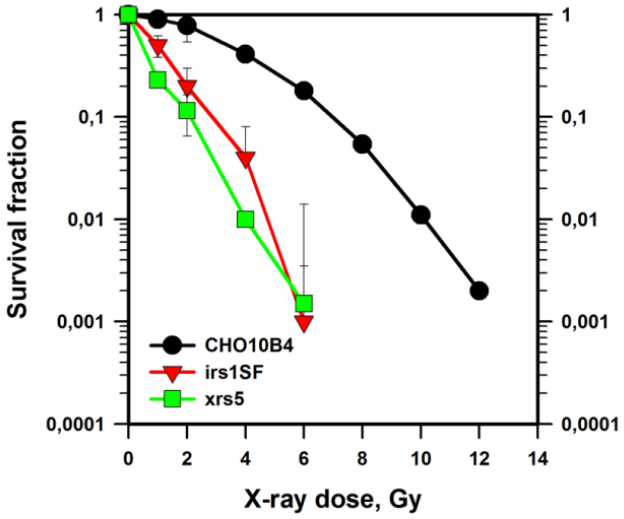

Figure 9: Clonogenic survival assay in wild type, D-NHEJ and HRR deficient Chinese hamster cells. Exponentially growing asynchronous cultures were irradiated with various doses of X-rays and allowed to form colonies. The cell survival is plotted as a function of radiation dose (Soni, 2010).

Both mutants, D-NHEJ (xrs5) and HRR deficient (irs1SF) cells show an increased radiosensitivity compared to the wt cells (CHO10B4) (fig. 9). The same result was found in another HRR deficient cell line, irs1tor, which is mutant in *XRCC2* (not shown). We concluded from the obtained results that D-NHEJ and HRR have the same contribution in protecting cells for IR induced cell killing.

In contrast to this, using PFGE to measure DSB repair, HRR seems to play no role in the repair of DSBs. The obtained PFGE data are pictured in figure 10.

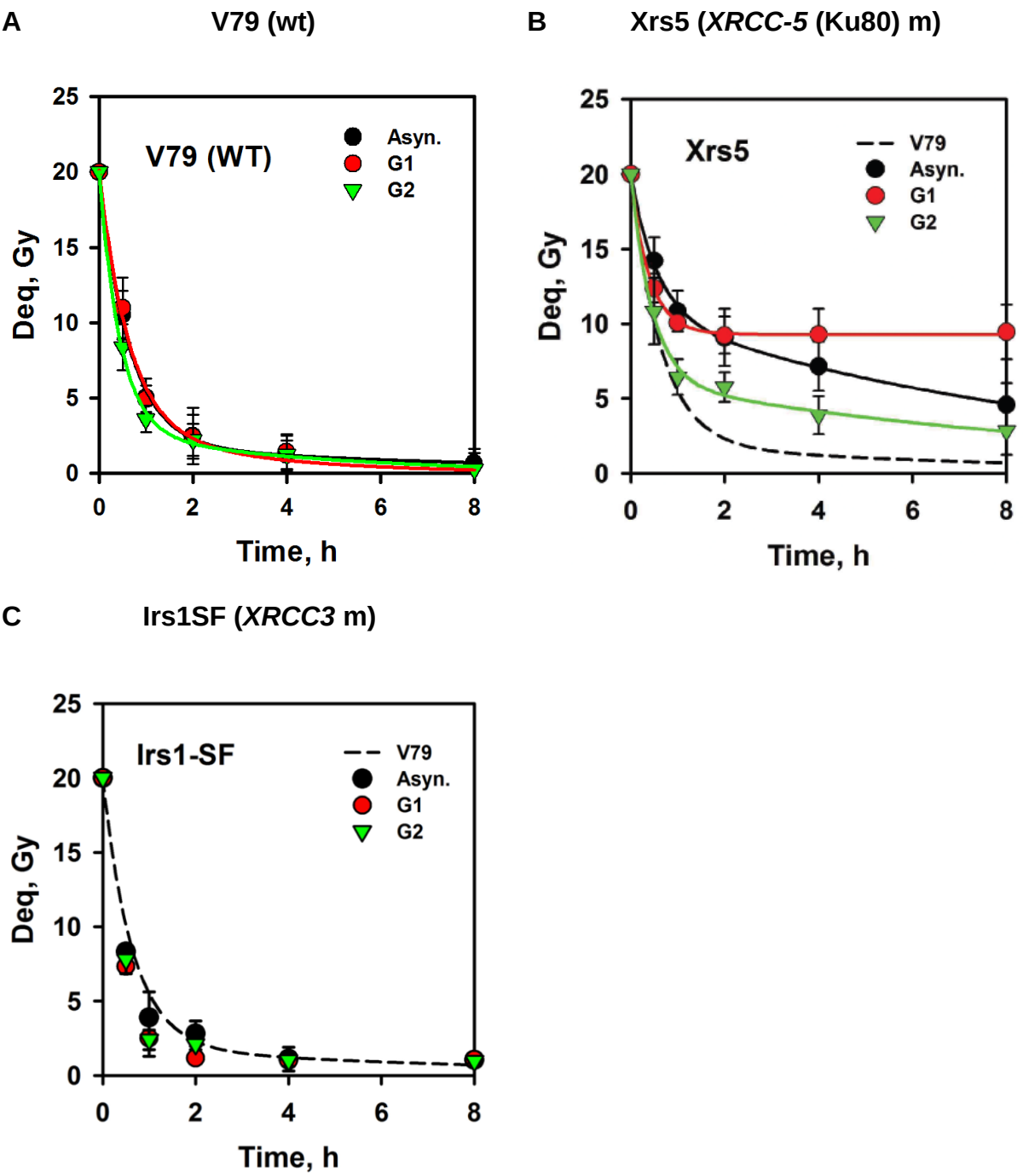

Figure 10: Rejoining of DSBs in wild type, D-NHEJ and HRR deficient Chinese hamster cells, measured with Pulsed field gel electrophoresis. Exponentially growing asynchronous cultures or synchronous cells enriched in G1- and G2-phase of the cell cycle, obtained by centrifugal elutriation, were irradiated with 20 Gy of X-rays and were allowed to repair up to 8 h. (A) Wild type cell line, (B) D-NHEJ deficient cell line and (C) HRR deficient cell line (Wu et al., 2008a).

These experiments revealed that in D-NHEJ mutant Chinese hamster cells, B-NHEJ is repairing the DSBs in G1-phase, since HRR is unlikely to function efficiently in G1-

phase. In addition all D-NHEJ mutants showed an enhanced DSB repair capability in G2-phase of the cell cycle (fig.10B). Surprisingly, cells with mutations in genes of HRR components, here *XRCC3*, did not show a compromised repair of IR induced DSBs (fig. 10C). After these and many other experiments it was evident that the increase of the DSB repair capability observed in G2-phase cells of D-NHEJ mutants is due to an enhanced function of B-NHEJ (Wu et al., 2008a).

Still the question remains open why no contribution of HRR was detected in the repair of randomly induced DSBs in higher eukaryotes measured by PFGE, even though we know that it contributes to cell survival and the repair of site-specific DSBs. There are different possibilities; first it could be that only a small fraction of DSBs is repaired by HRR, which cannot be detected with PFGE. Furthermore it could be due to an integrated DSB repair system, where D-NHEJ restores integrity in the DNA, while HRR handles sequence restoration in a subsequent step (Wu et al., 2008a).

Because of the inconsistent results in the experiments described above, the role of HRR in the repair of IR induced DSBs remains open. To investigate the apparent inconsistency between cell survival results and PFGE results another biological assay was used. We studied the repair of IR induced DSBs through their transformation to chromatid breaks. Using this method it is possible to investigate the contribution of HRR to the repair of chromosomal breaks.

1.5.2 HRR is required for the repair of chromosome breaks

With the help of this system we were able to investigate the repair of IR induced DSBs by means of their transformation to chromatid breaks. Thereby one specifically investigates the kinetics of chromatid breaks in the G2-phase of the cell cycle without synchronizing the cells, even after very low doses of IR, e.g. 1 to 2 Gy.

The G2-phase of Chinese hamster cells has duration of 4 to 5 h. Therefore we allowed cells to repair DSBs for 1 to 5 h at 37°C. Using this technique and time frame it is possible to assess only the response of cells, which are in G2-phase at the time of irradiation.

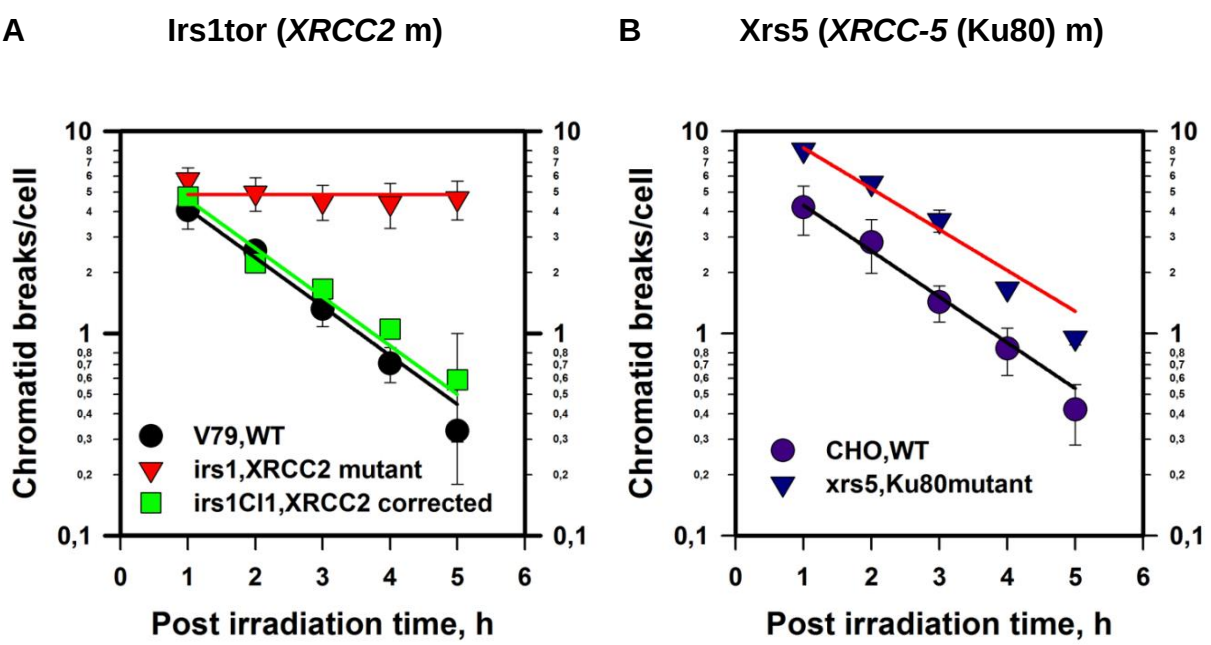

Figure 11: Kinetics of chromatid breaks in exponentially growing Chinese hamster cells, irradiated with 1 Gy X-rays and allowed to repair for up to 5 h after irradiation. The number of chromatid breaks per cell is plotted against time. (A) Repair kinetics in HRR deficient hamster cells and (B) repair kinetics in D-NHEJ deficient hamster cells (Soni, 2010).

When D-NHEJ fails to repair DNA DSBs, more DSBs are converted to chromatid breaks, e.g. a ~2- to 3-fold increase in comparison to wild type cells. But in D-NHEJ deficient cells there is no detectable defect in the repair kinetics of chromatid breaks and the number of breaks decreases with the same kinetics as in wt cells. This shows that D-NHEJ is not contributing to the repair of the subset of DSBs causing G2 chromosome breaks at low doses (fig.11B).

Surprisingly, there is almost no repair of G2-chromosome breaks in HRR deficient cells (fig.11A). HRR is known to be important for the genomic stability, but it still remains unclear, which role HRR has in the repair of IR induced DSBs. Our findings clearly show that HRR is absolutely necessary for the repair of G2-chromosomal breaks. Since D-NHEJ seems not to play a role in the repair of DSBs after low doses of IR, our results suggests that those few DSBs, which are the precursors of chromosome breaks, are specifically processed by HRR.

Since recently it was shown that HRR is not a minor DSB repair pathway and has a direct role in the repair of chromosomal breaks in G2-phase these findings could refute previous PFGE results (Soni, 2010).

To see if the G2-checkpoint has an influence on the repair of G2-chromosomal breaks a Calyculin-A induced premature chromosome condensation (PCC) assay was used, since the checkpoint could stop cell cycle progression and enable the DSB repair.

A **Irs1SF (*XRCC3* m)** **B** **Irs1tor (*XRCC2* m)**

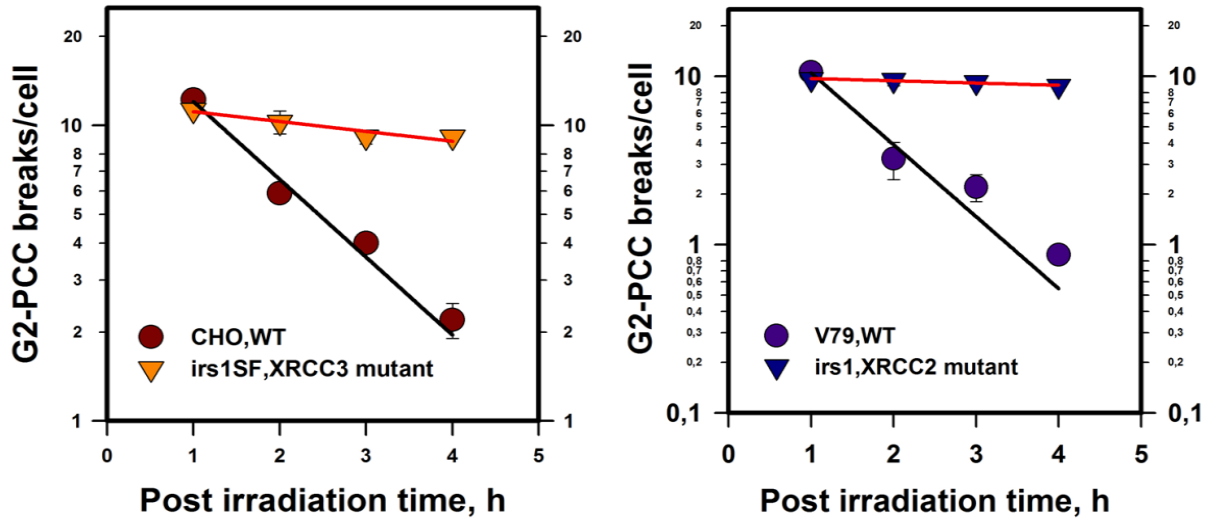

Figure 12: Kinetics of G2-PCC breaks in exponentially growing Chinese hamster cells irradiated with 1 Gy X-rays and allowed to repair for up to 5 h after irradiation. The number of G2-PCC breaks per cell is plotted against time. (A) and (B) Repair kinetics in HRR deficient hamster cells (Soni, 2010).

The initial number of G2-PCC breaks in wt and HRR deficient cells is similar, but in the latter most of the breaks remain unrepaired (fig. 12A and B). These graphs clearly show an influence on the repair of chromatid breaks by the G2-checkpoint. Combined, our findings suggest that the repair of chromosomal breaks in wt cells is facilitated by the G2-checkpoint, but it seems not to work properly in the absence of HRR (Soni, 2010).

In summary, these experiments demonstrate that HRR mutants show a complete inhibition in the repair of IR induced chromosomal breaks. This effect is clearly detectable at small doses (0.5 - 1 Gy) of IR, as shown before. In contrast, there is an almost normal repair of DSB quantified with PFGE after the induction with high doses of IR.

1.5.3 Saturation of RAD51 foci formation at higher doses

A third important finding from our lab indicates that in comparison to γH2AX foci, which increased linearly with increasing the applied radiation dose and are frequently used as a marker of the total number of DSBs generated after irradiation (Paull et al., 2000), RAD51 foci reached a plateau at higher irradiation doses. This clearly indicates that the two major DSBs repair pathways are not equivalent and could be differently regulated in a dose dependent manner.

At the stage of homology search RAD51 recombinase could be visualized as clearly distinct nuclear foci, which are an accepted marker for ongoing DSB repair by homologous recombination.

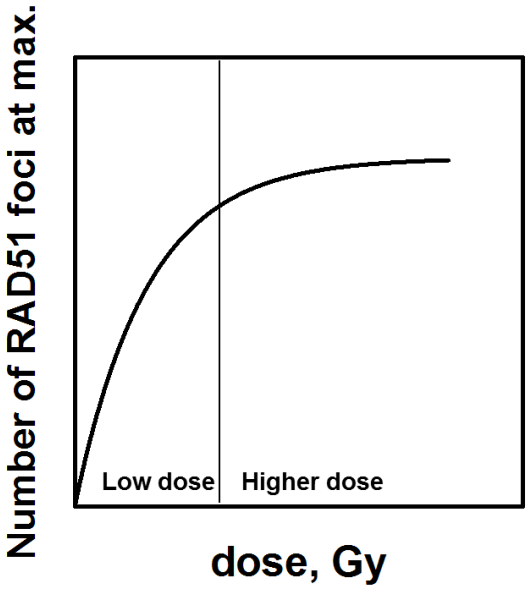

Figure 13: Schematic graph: Plateau of RAD51 foci formation at higher doses.

Therefore, the RAD51 foci formation was used to estimate the number of DSBs repaired by homologous recombination. It has been found that the maximum number of RAD51 foci appeared at different time points after irradiation with a strong correlation to the applied dose. When the maximums of RAD51 foci were plotted as a function of irradiation dose a clear saturation of RAD51 foci was observed at higher doses, which indicates that HRR might be actively regulated in a dose dependent fashion (fig. 13) (unpublished data).

These two findings, presented in the last 2 chapters (chapter 1.5.2 and 1.5.3) generate a contradiction to the assumption that HRR plays a minor role in the repair of DNA DSBs (chapter 1.5.1).

All these results could be somehow related to the size of dose applied; therefore it is interesting to find out more about the hypothesis that there might be a dose dependent switch for the repair pathway choice, which is the intention of this thesis.

1.6 Aims of the present thesis

The general aim of the present thesis is to find out the contributions and the interplay of the three repair pathways HRR, D-NHEJ and B-NHEJ in the processing of DNA DSBs and chromosomal breaks throughout the cell cycle and especially in G2-phase cells. Additionally we wished to find out if there is a dose depended switch between repair pathways.

Earlier findings revealed that there is a saturation of RAD51 foci formation after exposure to higher doses and that HRR mutants show an almost complete inhibition in the repair of IR induced chromosomal breaks at small doses of radiation (0.5 - 2 Gy). However normal repair of DNA DSBs, which are induced by higher doses of IR, can be measured with PFGE in HRR deficient cells. To understand this contradiction, experiments were performed with PFGE and the G2-PCC assay. A broad overlapping dose-spectrum was applied in order to analyze DSB repair with PFGE at lower doses and G2-PCCs at higher doses. The system used for G2-PCC allows the measurement of repair in the G2-phase of the cell cycle without the need for synchronization and at very low radiation doses. With these investigations we wished to find out if the contribution of HRR decreases with increasing doses of IR and/or if a different pathway is getting more involved in the repair of DNA damage by higher doses. For these investigations Chinese hamster cells are employed, which are wild type and D-NHEJ or HRR deficient.

Furthermore we wished to explore the involvement of B-NHEJ in the repair of DSBs. Until now, the contribution of B-NHEJ to the repair of chromosomal breaks could not be conclusively quantified. It is known that B-NHEJ is dependent on PARP-1, LIG3 or LIG1 and XRCC1. Based on this knowledge we wished to investigate the impact of a PARP inhibitor on the repair of chromosomal breaks in different D-NHEJ mutants, and specifically in the formation of chromosomal exchanges/translocations. There is evidence that B-NHEJ is responsible for the formation of chromosome translocations (CTs), which are the hallmark of cancer (Roukos et al., 2013). In addition we wished to apply fluorescence in situ hybridization (FISH) to get a real picture of the frequency of CT formation. Finally, we wished to investigate if there are interactions and/or mutual regulations between B-NHEJ and D-NHEJ, as well as between B-NHEJ and HRR.

2 Materials and methods

2.1 Materials

2.1.1 Laboratory Apparatus

Table 2: Laboratory Apparatus

Laboratory Apparatus	Provider
Aluminum filter	GE-Healthcare, Piscataway, NJ, USA
Axio imager.Z2	Carl Zeiss, Jena, Germany
Cell counter, Multisizer™ 3	Beckman Coulter, Krefeld, Germany
Centrifuge, BioFuge (Fresco)	BioFuge Fresco Heraeus, Magdeburg, Germany
Electrophoresis gel boxes, Horizon 20•25	Life TechnologiesTM, Carlsbad, CA, USA
Flow cytometer, Coulter Epics XL	Beckman Coulter, Krefeld, Germany
FluorImager, Typhoon 9400	Molecular Dynamics, Germany
Laminar flow hood, HeraSafe	Heraeus, Magdeburg, Germany
Magnetic stirrer	MR Hei-Mix L, Heidolph, Schwaback, Germany
MCO-18 O2/CO2 incubators	Sanyo, Munich, Germany
Metafer Slide Scanning Platform	MetaSystems, Altlussheim, Germany
Mini centrifuge	Biofuge fresco Heraeus, Magdeburg, Germany
Peristaltic pump	IDEX Health & Science GmbH, Wertheim-Mondfeld, Germany
pH-Meter	WTW, InoLab, Weinheim, Germany
Pipets	Mettler Toledo GmbH, Giessen, Germany
Pipet-aid	BD Falcon, Heidelberg, Germany
Power supply, PowerPacKTM HC	Bio-Rad, Munich, Germany

PTB dosimeter	Physikalisch-Technische Bundesanstalt, Braunschweig, Germany
SDS PAGE and blotting apparatus	Bio-Rad, Munich, Germany
Vortexer, Vortex-Genie 2	Scientific Industries, Bohemia, NY, USA
Water bath	GFL, Hannover, Germany
Weighing balance, BP 110 S	Sartorius, Goettingen, Germany
X-ray machine, “Isovolt 320HS”	Seifert/Pantak, General Electric-Pantak, USA

2.1.2 Disposable Elements

Table 3: Disposable Elements

Disposable Elements	Provider
3 mm diameter glass tubes	CM Scientific Ltd., Shipley, UK
0.5, 1.5 ml and 2 ml tubes	Greiner, Frickenhausen, Germany
12 ml non-cap tubes	Greiner, Frickenhausen, Germany
15 and 50 ml tubes	Greiner, Frickenhausen, Germany
2, 5, 10, 25 ml pipets	Greiner, Frickenhausen, Germany
18x18 mm^2 coverslips	Roth, Karlsruhe, Germany
24x32 mm^2 coverslips	Roth, Karlsruhe, Germany
24x60 mm^2 coverslips	Roth, Karlsruhe, Germany
Cell culture dishes/flasks	Greiner, Frickenhausen, Germany
Flasks, beakers, cylinders	Schott Duran, Wertheim, Germany
Gloves	Peha-soft® Satine, Hartmann, Heidenheim, Germany
Microscope slides	Roth, Karlsruhe, Germany
Para film	Lab Depot, Dawsonville, GA, USA
Pasteur pipettes	BD Falcon, Heidelberg, Germany

Pipettes	Greiner, Frickenhausen, Germany
Pipet tips	Greiner, Frickenhausen, Germany

2.1.3 Chemical Reagents

Table 4: Chemical Reagents

Chemical Reagents	Provider
5-bromo-2´-deoxyuridine (BrdU)	Sigma-Aldrich, Steinheim, Germany
2-Mercaptoethanol	Sigma-Aldrich, Steinheim, Germany
Acetic acid	Roth, Karlsruhe, Germany
Agarose	Bio-Rad, Munich, Germany
Boric acid	Roth, Karlsruhe, Germany
Bovine serum albumin fraction IV	Roth, Karlsruhe, Germany
Buffer Tablets „GURR“	Gibco™, Invitrogen, Karlsruhe, Germany
Chicken serum	Gibco™, Invitrogen, Karlsruhe, Germany
Crystal violet	Merck, Darmstadt, Germany
DAPI	Sigma-Aldrich, Steinheim, Germany
Dimethyl sulfoxide	Sigma-Aldrich, Steinheim, Germany
Dulbecco's Modified Eagle Medium	Gibco™, Invitrogen, Karlsruhe, Germany
Entellan	Merck, Darmstadt, Germany
Ethanol	Sigma-Aldrich, Steinheim, Germany
Ethidium bromide	Roth, Karlsruhe, Germany
Ethylenediaminetetraacetic acid	Roth, Karlsruhe, Germany
Fetal bovine serum	Biochrom, Berlin, Germany; PAA, Coelbe, Germany; Gibco™, Invitrogen, Karlsruhe, Germany

Fixogum, Rubber cement	Marabu GmbH & Co. KG, Tamm, Germany
Giemsa	Roth, Karlsruhe, Germany
Glycerol	Roth, Karlsruhe, Germany
Glycine	Roth, Karlsruhe, Germany
HCl	Roth, Karlsruhe, Germany
Isopropanol	Sigma-Aldrich, Steinheim, Germany
KCl	Roth, Karlsruhe, Germany
KH_2PO_4	Roth, Karlsruhe, Germany
KOH	Roth, Karlsruhe, Germany
Low melting agarose	Roth, Karlsruhe, Germany
Mc Coy's 5A medium	Sigma-Aldrich, Steinheim, Germany
Methanol	Sigma-Aldrich, Steinheim, Germany
$MgCl_2$	Merck, Darmstadt, Germany
Minimal Essential Medium	Gibco™, Invitrogen, Karlsruhe, Germany
NaCl	Roth, Karlsruhe, Germany
$NaHCO^3$	Roth, Karlsruhe, Germany
NaOH	Roth, Karlsruhe, Germany
N-lauryl sarcosine	Merck, Heidelberg, Germany
Nocodazole	Sigma-Aldrich, Steinheim, Germany
NU7441	Tocris Bioscience, Ellisville, MO, USA
Paraformaldehyde	Honeywell Specialty Chemicals GmbH, Seelze, Germany
Penicillin	Sigma-Aldrich, Steinheim, Germany
ProLong® Gold antifade reagent	Invitrogen, Karlsruhe, Germany

Protease inhibitor cocktail	Sigma-Aldrich, Steinheim, Germany
RNase A	Sigma-Aldrich, Steinheim, Germany
RPMI medium	Sigma-Aldrich, Steinheim, Germany
Sodium dodecyl sulfate	Roth, Karlsruhe, Germany
Streptomycin	Calbiochem, Invitrogen, Karlsruhe, Germany
Tris base	Roth, Karlsruhe, Germany
Tris-HCl	Roth, Karlsruhe, Germany
TritonX-100	Sigma-Aldrich, Steinheim, Germany
Trypsin	Biochrom , Berlin, Germany
Tween^{TM}20	Roth, Karlsruhe, Germany

2.1.4 Antibodies

Table 5: Antibodies

Antibody	Provider
Anti-BrdU mouse monoclonal antibody	Beckson-Dickinson
FITC-conjugated rabbit anti-mouse IgG	Sigma-Aldrich, Steinheim, Germany
XCP1 Green (chromosome 1)	MetaSystems, Altlussheim, Germany
XCP2 Orange (chromosome 2)	MetaSystems, Altlussheim, Germany

2.1.5 Buffer and solutions

Carnoy's fixative

1:3 of acidic acid:Methanol

DAPI solution

(2 µg/ml DAPI, 0.1 M Tris, 0.1 M NaCl, 5 mM $MgCl_2$, 0.05% TritonX-100)

HEPES buffer

(20 mM HEPES, 5 mM $NaHCO_3$ resuspended in serum free media)

High Temperature Lysis Buffer

(10 mM Tris-HCl, 50 mM NaCl, 100 mM EDTA, 2% N-lauryl sarcosine (NLS), pH 7.6, and 0.2 mg/ml Protease just before use)

Hypotonic solution

(0.075 M: 0.56 g potassium chloride in 100 ml of MilliQ water)

PBS

(137 mM NaCl, 2.7 mM KCl, 10 mM Na_2HPO_4, 1.76 mM KH_2PO_4, pH 7.4)

PI-staining-buffer

(0.1 M Tris, 0.1 M NaCl, 5 mM $MgCl_2$, 0.05% Triton X-100 in MilliQ water)

RNase Buffer

(10 mM Tris-HCl, 50 mM NaCl, 100 mM EDTA, pH 7.6, and 0.1 mg/ml RNase A added just before use)

PI-RNaseA-staining solution

(PI: 4 mg/ml MilliQ water; RNaseA: 6.2 mg/ml buffer, buffer for RNaseA: 10mM TRIS, 100 mM EDTA, 50 mM NaCl, pH 7.6)

Saline-sodium Citrate Buffer (SSC)

(Saline-sodium Citrate Buffer: 3.0 M NaCl and 0.3 M $C_6H_5Na_3O_7*2H_2O$)

SSCT

(Saline-sodium Citrate Buffer: 3.0 M NaCl and 0.3 M $C_6H_5Na_3O_7*2H_2O$ containing 0.05% Tween20)

Sorensons buffer

One Buffer tablet (GURR) dissolved in 1 liter of MilliQ water

TBE buffer (0.5x)

(45 mM Tris, 45 mM Boric Acid, and 1 mM EDTA)

Washing Buffer (Western blot)

(10 mM Tris-HCl, 50 mM NaCl, 100 mM EDTA, pH 7.6)

2.1.6 Softwares

Table 6: Softwares

Software	Provider
Adobe® Creative Suite® 5.5	Adobe Systems Inc., USA
Ikaros (Version 3.5)	MetaSystems, Altlussheim, Germany
Isis (Version 3.5)	MetaSystems, Altlussheim, Germany
ImageQuant™ 5.0	GE Healthcare Life Sciences, USA
Metafer	MetaSystems, Altlussheim, Germany
Microsoft Office 2010®	Microsoft, USA
SigmaPlot® 11.0	Systat Software, USA
WincycleTM	Phoenix Flow Systems, USA

2.1.7 Cell lines

Table 7: List of cell lines used for the experiments

No.	Species	Cell line name	Cell type	Mutation(m)/ Knockout (KO)
1	Human	A549	lung carcinoma	Wild type
2	Human	HCT116 wt	Colorectal tumor	Wild type
3	Human	HCT116 DNA-PKcs$^{-/-}$	Colorectal tumor	DNA-PKcs KO
4	human	HCT116 Lig4$^{-/-}$	Colorectal tumor	Ligase 4 KO
5	Chinese hamster	V79	Fibroblast	Wild type
6	Chinese hamster	Xrs6	Ovarian	XRCC-5 (Ku80) m
7	Chinese hamster	Irs1tor	Fibroblast	XRCC2 m

8	Chinese hamster	Irs2tor	Fibroblast	Rad51B m
9	Chinese hamster	Irs3tor	Fibroblast	Rad51C m
10	Mouse	PK34N	embryonic fibroblasts	Wild type
11	Mouse	PK33N	embryonic fibroblasts	DNA-PKcs KO
12	Mouse	PK80-193A	embryonic fibroblasts	DNA-PKcs and KU80 KO
13	Mouse	Mef Ku80$^{-/-}$	embryonic fibroblasts	KU80 KO
14	Chicken	DT40 wt	B cell lymphoblasts	Wild type
15	Chicken	DT40 Lig4$^{-/-}$	B cell lymphoblasts	Ligase 4 KO

2.2 Methods

2.2.1 Cell culture and growth conditions

The mouse, Chinese hamster and human cells were maintained at 37°C in a humidified atmosphere with 5% CO_2 and 95% air. The optimal temperature for DT40 cells was 39.5°C.

A549 and HCT116 colorectal tumor cells were maintained in McCoy's 5A medium supplemented with 10% FBS. Chinese hamster cells were grown in McCoy's 5A or MEM supplemented with 10% FBS. Mouse embryo fibroblasts (MEF) were grown in DMEM supplemented with 10% FBS. DT40 cells were grown in DMEM/ F12 or RPMI supplemented with 10% FBS, 1% chicken serum and 10 µl/100 ml β-Mercaptoethanol.

100 mm cell culture dishes with 15 ml suitable medium supplemented with FBS were used to grow the adherent cells. The cells were passaged every 2 days avoiding confluence levels above 80%. For routine passage, media was removed and cells were washed with 10 ml PBS. After this the cells were rinsed with 2 ml trypsin solution (0.05% trypsin in EDTA) and incubated for 5 min at 37°C. Detached cells were resuspended in 10 ml media supplemented with 10% FBS. By passing cells through a Pasteur pipette single cell suspensions were obtained and counted (Multisizer™ 3, Beckman Coulter), and appropriate number of cells was further seeded and incubated.

Suspension cells were grown in 100 mm bacteria dishes with 10 ml of the appropriate growth medium. Cells were subcultured every 3 days without exceeding a cell number of 2 million cells per ml of medium. For the subculture the cell suspension was pipetted through a Pasteur pipette to break the clumps and the cell number was counted. After calculating the desired cell number cells were re-seeded into a new dish and incubated. The cells were passaged at least two times before being used in experiments in case of newly thawed cells. After about 40 passages cells were discarded, since their genomic stability could not be guaranteed.

2.2.2 Inhibitor treatment

Table 8: **Inhibitors used before irradiation**

Inhibitor	Mechanism of action	Working concentration
Aphidicolin	Potent inhibitor of DNA polymerase α and δ.	5 µmol/ L
NU7441	Potent inhibitor of DNAPKcs	5 µmol/ L
PJ34	Potent inhibitor of poly(ADP-ribose) polymerase (PARP)	5 µmol/ L
VE821	Potent inhibitor of the DNA damage response (DDR) kinase ATR.	5 µmol/ L

The inhibitors indicated in the table 8 were applied to culture medium 1 h before the cells were exposed to ionizing radiation and remained in the cell culture medium during whole experimental procedure. All these inhibitors are soluble in DMSO.

Table 9: Inhibitors used after irradiation

Drug	Mechanism of action	Working concentration
Calyculin A	Serine/Threonine Phosphatase Inhibitor, which induces PCCs in interphase cells	100 nmol/ L (Stock: 10 µM in DMSO).
Colcemid	Prevents spindle formation during mitosis, arresting cells in metaphase	0.1 µg/ ml (Stock: 10 µg/ ml in PBS w/o Ca^{++}, Mg^{++}).

The inhibitors indicated in table 9 were used after irradiation at specific post-irradiation times. Calyculin A was added for 30 min and Colcemid for 1 h before harvesting the cells at specific time points.

2.2.3 X-ray irradiation

Cells were exposed to different doses of X-ray. Irradiation was carried out with an X-ray machine (“Isovolt 320HS”, General Electric) with an effective photon energy of approximately 90 keV. This machine operated at 320 kV and 10 mA using a 1.65 mm aluminum filter (GE-Healthcare) at a distance of 750 mm for 100 mm dishes and 500 mm for 60 mm dishes and a dose rate of approximately 1.3 Gy/ min.

The dosimetry was performed with a PTB dosimeter (Physikalisch-Technische Bundesanstalt, Braunschweig, Germany) and Frick`s chemical dosimetry, which was used to calibrate an in-field ionization monitor. An even distribution of dose was ensured by rotating the radiation table. Cells were returned to the incubator immediately after exposure to IR.

2.2.4 Cytogenetic assays

2.2.4.1 Assay to measure the kinetics of G2-chromosome breaks at Metaphase

The protocol, which is used here is the modified protocol used by Bryant et al., 2008 (Bryant et al., 2008).
To measure the kinetics of G2-chromosome breaks exponentially growing cells were irradiated with 1 Gy X-rays. After this the irradiated cells were allowed to repair 1 to 5 h at 37°C; within this time frame it is possible to detect mainly the response of the cells, which were irradiated in G2-phase.
Colcemid was added 1h before the respective time point to arrest the cells in metaphase with an exception of 1 h time point where Colcemid was added 30 min after IR to allow the migration of cells, which were at mitosis during irradiation.
At time of harvesting, cells were washed with 10 ml of PBS, trypsinized and incubated for 5 min at 37°C. The detached cells were resuspended in 5 ml medium and a single cell suspension was obtained by pipetting up and down using a 5 ml glass pipette. Then cells were centrifuged at 1200 rpm for 7 min at 4°C. After removing the supernatant 10 ml hypotonic solution was added drop wise following incubation at room temperature (RT) for 10 min. After 10 min cells were again centrifuged at 1200 rpm for 7 min at 4°C and hypotonic solution was removed. The cells were resuspended in Carnoy’s fixative added drop wise up to 10 ml. Both hypotonic solution and Carnoy’s fixative were prepared fresh on the day of

experiment. Cells were washed for 2 to 3 times with Carnoy's fixative before spreading on a clean Microscope slide, 76x26 mm^2, with a thin water film. The slides were allowed to dry overnight stained afterwards for 15 min in 5% Giemsa solution. After staining the slides were allowed to dry for 2 to 3 h before mounting with Entellan.

Slides were scanned using a 10x and a 60x (oil) objective with a bright field microscopy facilitated by an automated analysis station (Axio Imager.Z2, Zeiss) and controlled by Metafer software (MetaSystems).
For each time point about 50 to 100 metaphases were scanned using the Metafer software. Chromatid breaks and exchanges were scored using Ikaros software Version 3.5 (Metasystems). One chromatid exchange was scored as two chromatid breaks. Figure 14 and 15 show the metaphase spreads as well chromatid exchanges.

Figure 14: Example of metaphases from Human Colorectal tumor cells. Colcemid completely inhibits the formation of spindle microtubule (MTs). The result is that during nuclear envelope breakdown (NEB) the chromosomes are released into cytoplasm where they remain randomly dispersed (Rieder and Cole, 1998). Chromatid strands become during this incubation more and more condensed. Metaphase chromosomes have a classical four arm structure, shown in the circle, a pair of sister chromatids attach to each other at the centromere (shown with an arrow).

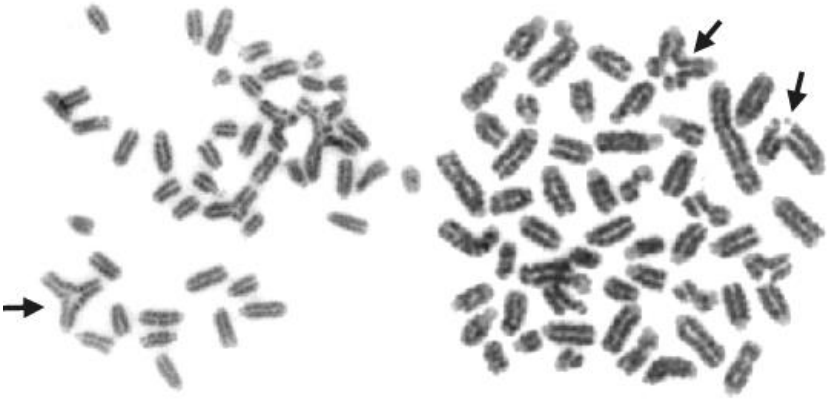

Figure 15: Example of metaphases from mouse embryonic fibroblasts. After irradiation with 1 Gy X-rays cells repair the breaks. In some cases they show chromosomal crossover, which is the exchange of genetic material between chromosomes, they are marked with black arrows. For analysis one chromosomal crossover is counted as 2 breaks.

2.2.4.2 Premature chromosome condensation (PCCs)

100 nmol/ L Calyculin A was added 30 min before harvesting the particular time point to induce PCCs. The detached cells were harvested in a 15 ml tube and processed for cytogenetics. The procedure for cytogenetic preparation and analysis is the same as described above (chapter 2.2.4.1). The main difference of the G2-PCCs compared to G2-Metaphases is that PCCs lack the centromeric constriction (fig. 16).

Figure 16: Example of G2-Premature chromosome condensation (PCC) spreading in Chinese hamster cells. To achieve G2-PCC Calyculin A, a potent phosphatase inhibitor, is used. This inhibitor condenses chromosomes in G2 without the need for cells to progress to mitosis. A typical characteristic of PCCs is the lack of the centromere. Calyculin A induced PCC provides a method of examining the kinetics of G2-phase chromatid breaks after irradiation without the complication of G2-cell cycle checkpoint arrest (Bryant et al., 2008). The black arrows shows a chromatid break.

2.2.4.3 Fluorescence in situ hybridization (FISH)

The slide preparation for FISH is the same as described in chapter 2.2.4.1. The slides were prepared shortly before starting the hybridization. The probes for human chromosome 1 and 2 were employed.

Table 10: Stock solutions for FISH

Solution	Concentration
Water	MilliQ
Ethanol, denatured	100%
NaOH	1 N
Tween^{TM}20	0.05%
Saline-sodium Citrate Buffer (SSC),	20x

Sample denaturation

Table 11: Solutions required for slide denaturation

Concentration/ Solution	pH	Temperature
0.1x SSC	pH 7.0 - 7.5	room temperature
0.1x SSC	pH 7.0 - 7.5	4°C
2x SSC	pH 7.0 - 7.5	70°C (+/- 1°C)
2x SSC	pH 7.0 - 7.5	4°C
0.07 mol/ L NaOH	-	room temperature
70% Ethanol	-	room temperature
95% Ethanol	-	room temperature
100% Ethanol	-	room temperature

One coplin jar of each with 0.1x SSC and 2x SSC was put into the refrigerator and one coplin jar with 2x SSC was pre-warmed at 70°C (+/- 1°C) in a water bath before starting the slide denaturation.
Freshly prepared slides were put into 2x SSC at 70°C (+/- 1°C) and incubated for 30 min. Then the coplin jar was removed from the water bath and allowed to cool down for 20 min at RT. The slides were then transferred to 0.1x SSC at RT for 1 min. After this DNA was denatured in 0.07 N NaOH at RT for 1 min followed by an incubation in 0.1x SSC at 4 °C for 1 min and afterwards in 2x SSC at 4 °C for 1 min. For fixation of the cells, slides were merged into a coplin jar with 70% ethanol for 1 min followed by incubation in 95% and 100% ethanol for 1 min each. Slides were then air dried.

Probe Amplification, Denaturation and Hybridization

Note: The probe denaturation was performed using a PCR machine while the slides were processed as mentioned above. This facilitates the hybridization process as soon as slides are dried after denaturation.

The probe cocktail was prepared according to the intended hybridization area: 7 µl for a 18x18 mm^2 cover slip, 10 µl for a 22x22 mm^2 coverslip, or 12 µl for a 24x24 mm^2 coverslip.
Probes were amplified and denatured by incubating at 75°C (+/- °C) for 5 min; after this they were put briefly on ice for cooling following incubation at 37°C (+/- 1 °C) for 30 min. This procedure can be done with the PCR machine.
After the PCR was finished, tubes were briefly spun down to collect the probe cocktail. Denatured and pre-amplified probe cocktail was then pipetted onto the denatured chromosome preparation and overlaid with a coverslip. The coverslip was sealed with rubber cement (Fixogum, Marabu GmbH & Co. KG, Tamm, Germany) and slides were incubated for 1 to 2 days in a humidified chamber at 37°C (+/- 1 °C).

Post-hybridization Washing

Table 12: Solutions required for post-hybridization washing

Concentration/ Solution	pH	Temperature
0.4x SSC	pH 7.0 - 7.5	72°C (+/- 1°C)
2x SSCT	pH 7.0 - 7.5, containing 0.05% Tween20	room temperature

After incubation, rubber cement and cover slips were removed carefully. The slides were placed in prewarmed (72°C, +/- 1°C) 0.4x SSC for 2 min following incubation in 2x SSCT for 30 seconds (sec). Immediately thereafter, slides were stained with DAPI (Sigma-Aldrich, Steinheim, Germany) for 30 min and were washed briefly in MilliQ water to avoid crystal formation, and were air dried.

Next the slides were covered with 20 µl of the antifade solution and overlaid with a 24x60 mm^2 cover slip. After a penetration of 10 min it is possible to proceed with microscopy (Metasystems) and analysis. Slides were then scanned using 10x and 60x (oil) objective respectively with a fluorescent microscope, which has an automated analysis station (Axio Imager.Z2, Zeiss) and controlled by Metafer software (MetaSystems).

About 100 metaphases were scanned using the Metafer software. Translocations (fig. 17) and exchanges were scored using Isis (Version 3.5) (Metasystems).

The slides need to be stored at -20°C.

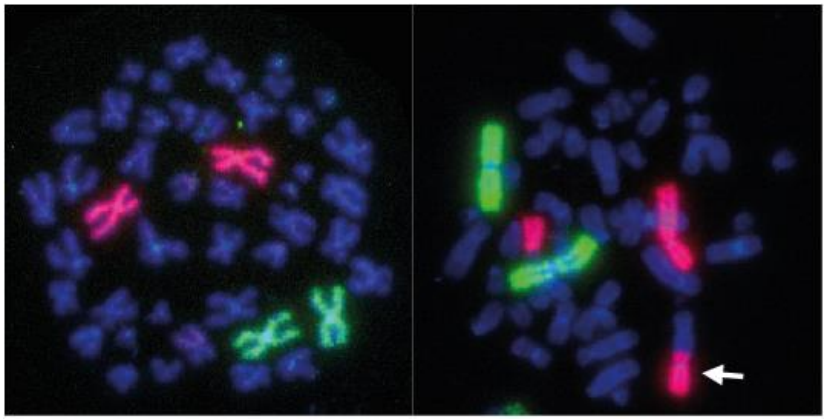

Figure 17: Examples of metaphases from Human Colorectal tumor cells stained with Fluorescence in situ hybridization (FISH) probes. Chromosome 1 is green and chromosome 2 is red colored. With FISH it is possible to score these translocations (white arrow), which are not visible when cells are stained with Giemsa.

2.2.5 Pulsed field gel electrophoresis - PFGE (Asymmetric field inversion gel electrophoresis (AFIGE))

PFGE is a specific technique to evaluate induction and repair of DSBs. The advantage of this method is the fact that fragmentation of chromosomal DNA with radiation leads to a linear dose-dependent increase in the fraction of DNA that enters the gel, whereas intact mammalian chromosomes are unable to migrate into the gel. PFGE resolves DNA fragments ranging in size from 0.2 - 6 Mbp, whereas gel electrophoresis with a constant electric field cannot resolve DNA fragments above 50 kbp.

After collecting on ice the cells were resuspended in cold serum-free medium (prepared in 20 mM HEPES, 5 mM $NaHCO_3$) at a concentration of $6x10^6$ cells/ ml. Cells were then mixed with an equal volume of pre-warmed (50°C) HEPES-buffered serum-free medium containing 1% low melting agarose to reach a concentration of $3x10^6$ cells/ml. This cell-agarose suspension was pipetted into 3 mm diameter glass tubes and placed in ice for several minutes to allow solidification. The solidified agarose-embedded cell suspension was extruded from glass tube and cut into 5 mm long blocks containing approximately $2x10^5$ cells/ plug (for each time point at least 3 plugs were prepared). For dose response the plugs were placed in a 60 mm Petri dish with 5 ml cold serum-free medium and placed on ice and exposed to different X-ray doses. To estimate the dose response, cells were exposed to 0, 1, 2, 3, 4, 5, 10, 15 and 20 Gy. Due to technical difficulties in determining the 0 h repair time point, the initial value of the repair kinetics was obtained from the dose response curve. The plugs were placed in lysis buffer (10 mM Tris-HCl, 50 mM NaCl, 100 mM EDTA, 2% N-lauryl sarcosine (NLS), pH 7.6 and freshly added 0.2 mg/ ml protease), and incubated at 4°C for 1 h before at 50°C for 16 - 18 h. For repair kinetics of IR-induced DSBs, irradiated cells were returned to the incubator for the indicated repair times. After completing the repair time interval, cells were embedded into agarose and lysed as described above. After lysis, plugs were washed in washing buffer (10 mM Tris-HCl, 50 mM NaCl, 100 mM EDTA, pH 7.6) while gently shaking at 37°C for 1 h. Afterwards plugs were treated for 1 h at 37°C in the same buffer with 0.1 mg/ ml freshly added RNase A. Because of the lysis step at 50°C we named this protocol as High Temperature Lysis (HTL).

Asymmetric field inversion gel electrophoresis was used for quantification of IR induced DSBs (Denko et al., 1989), this was carried out in 0.5% agarose gels containing 0.5 µg/ ml ethidium bromide (stock solution 10 mg/ ml in ddH_2O) in 0.5x TBE buffer (45 mM Tris, 45 mM boric acid, and 1 mM EDTA). Agarose plugs were loaded into the wells, which were sealed with 1% agarose. 1 - 2 h before starting electrophoresis, the buffer (0.5x TBE) was pre-cooled to 8°C. AFIGE was carried out for 40 h at 8°C using alternating cycles of 50 V (1.25 V/ cm) for 900 sec in the forward direction of DNA migration and 200 V (5 V/ cm) for 75 sec in the reverse direction. During this time the temperature of TBE buffer was maintained at 8°C by circulation through an external cooling unit. After completion of electrophoresis, the gel was scanned in a FluorImager (Typhoon 9400; Molecular Dynamics).

Table 13: Parameters for FluorImager, Typhoon™ 9410

Mode	Setting
Acquisition mode	Fluorescence
Laser	Green (532)
PMT gain	470 V
Sensitivity	Normal
Emission filter	610 BP SPYRO RyPy EtBr
Pixel size	200 microns
Focal plane	+3 mm

Under these electrophoresis conditions smaller DNA fragment migrate out of the well into lane, while intact chromosomal DNA remains in the well. To estimate DSBs, the fraction of DNA released (FDR) was measured using ImageQuant™ 5.0. The parameter of FDR is defined as the fraction of DNA found in the lane and is calculated by dividing the signal in the lane with the total signal of the sample. It is equivalent to the fraction of unrepaired DNA DSBs in the sample. Measured FDR in non-irradiated cells is termed background and was subtracted from the values of FDR measured in irradiated cells. When induction of DSBs was measured at different doses of irradiation, FDR was plotted against radiation dose to obtain dose

response curves. In order to facilitate the inter comparison of results obtained and to account for differences in the dose response curves between different cell lines and experiments, repair kinetics are not presented as FDR versus time but rather as dose equivalent (DEQ) versus time. We used dose response curves to estimate DEQ values from each FDR value. This way of analysis has an advantage as it corrects for non-linear dose response curves. Repair kinetics curves were fitted using non-linear regression analysis to calculate repair half times. In general, two components were assumed to exist in the repair curves and fitting algorithms were selected accordingly. For all graphs and curve fitting analyses SigmaPlot® 11.0 was used.

2.2.6 Flow cytometry

2.2.6.1 Cell cycle analysis by flow cytometry

Propidium iodide (PI) binds to DNA proportional to its mass. Cell cycle distribution was assessed by measuring PI fluorescence in a flow cytometer. Cells were washed with cold PBS and trypsinized at 37°C for 5 min. Single cell suspensions were prepared in 5 ml cold fresh media. About 1 million cells were collected and centrifuged at 1500 rpm, 4°C for 5 min. The cell pellets were washed with cold PBS and fixed in 70% ethanol at -20°C overnight. Supernatant was removed by centrifugation at 1500 rpm for 5 min. Pellets were washed with ice cold PBS and incubated in PBS containing PI (40 ug/ ml), and RNase (62 µg/ ml) at 37°C for 30 min in the dark. Samples were measured on a flow cytometer (COULTER EPICS XL, BECKMAN COULTER) according to pre-established protocols. 20,000 cells per sample were measured and the single cell population was gated to obtain standard histograms. Histogram files (*.HST) were generated by counting the frequency of cells with same PI signal intensity. The fractions of cells in the different phases of the cell cycle were calculated using the Wincycle® software. HST files were loaded into the Wincycle®. The parameter “S-phase growing order” was carefully chosen between 0.1 to 2, until the prediction model fitted the histogram shape. Cell cycle distributions were automatically calculated. G2 arrest kinetics was obtained by plotting the G2 fraction as a function of time after IR.

2.2.6.2 BrdU incorporation and detection

For the BrdU incorporation exponential growing cells were used. The S-phase cells were pulse-labeled by adding 10 µM of 5-bromo-2´-deoxyuridine (BrdU) for 30 min before irradiation. After this cells were washed two times with pre-warmed PBS and supplied with pre-warmed fresh growth medium.

About 0.8 - 1x10^6 cells were collected and fixed in 70% ethanol after different post IR times. After incubation in 2 ml 1 M HCl for 10 min at RT the cellular DNA was denatured. Cells were washed three times with PBS to remove the acid.

Primary anti-BrdU antibody (1:200 dilution) (Beckton-Dickinson), and a secondary, FITC-conjugated rabbit anti-mouse IgG (Sigma-Aldrich) (1:300) diluted in blocking buffer were sequentially applied. Finally, cells were stained with PI-RNaseA staining solution. Totally 20,000 cells per sample were analyzed in a flow cytometer. Proper gating was applied to estimate the fractions of BrdU positive cells in different phases of the cell cycle.

3 Results

3.1 DNHEJ, a fast DNA DSB repair pathway even after exposure to high IR doses

DNA DSBs are by at least three repair pathways; D-NHEJ, B-NHEJ, also named as alternative NHEJ (aNHEJ), and homology dependent HRR (Helleday et al., 2007; Iliakis, 2009; Lieber, 2010; Nussenzweig and Nussenzweig, 2010).

The most prominent differences in these three pathways are the speed and the accuracy. HRR is a slow, rather complex, but error-free repair pathway; B-NHEJ is also a slow pathway but its repair is error-prone, whereas D-NHEJ is fast but error-prone, which enables the repair of many DSBs in a short time. But the repair of IR induced DSBs show no detectable competition between HRR and D-NHEJ (Iliakis et al., 2004).

The repair of DNA DSBs can be measured using physical methods of detection i.e. PFGE, where the delivered dose was 20 Gy, as explained in “Materials and Methods”. In PFGE results, we cannot see a detectable defect in the removal of DSBs in HRR mutants, but cells with defects in D-NHEJ show clear repair defects and the DSBs are rejoined with slower kinetics (DiBiase et al., 2000; Mladenov and Iliakis, 2011; Wu et al., 2008a). We wanted to check how effective the D-NHEJ pathway is, even when the cells are irradiated with much higher doses, in this experiment additional doses of 40 and 80 Gy were delivered. Time points were taken 15 min up to 8 h post IR.

For PFGE experiments cells from Chinese hamster origin were used due to availability of many relevant mutants. Exponentially growing wild type cells (V79) and a D-NHEJ deficient cell line (Xrs6) were irradiated with the indicated IR doses and DSB repair kinetics were followed.

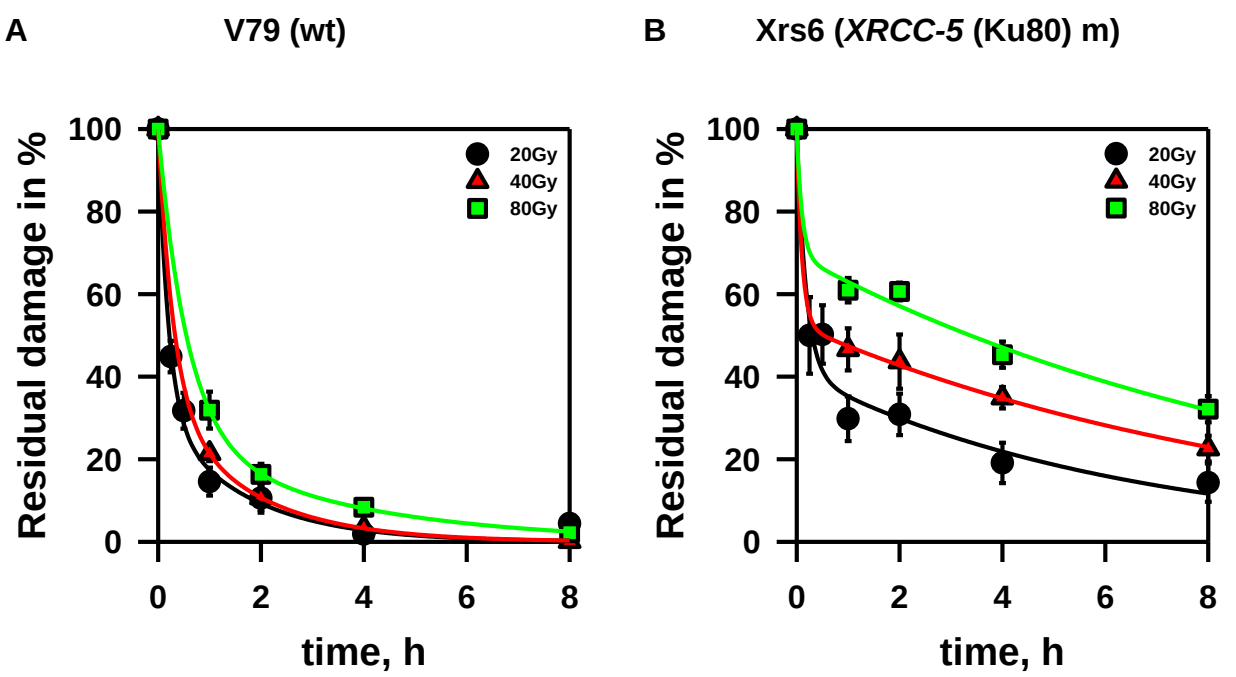

Figure 18: Kinetics of DNA DSB repair in exponentially growing Chinese hamster cells irradiated with various doses of X-rays. Cells were allowed to repair for up to 8 h after irradiation. Residual damage in % is plotted against time. (A) Repair kinetics in wild type cells and (B) repair kinetics in D-NHEJ deficient hamster cells. In both cases cells were exposed to 20, 40 and 80 Gy. The data points represent mean and standard errors from 2 or 3 independent experiments.

In figure 18 the repair kinetics is shown. We observed that the wild type cells exhibit fast repair kinetics irrespective of dose employed (fig 18A). Only 30% of the initial DSBs remained unrepaired after 30 min and at 8 h almost all DSBs are repaired.

Figure 18B shows the repair of the D-NHEJ deficient cell line after exposure to the same radiation doses. Clear repair defects are observed after 20 Gy of IR; after 30 min only 50% of the DSB breaks are repaired and at the last time point we have still 14% of the breaks left unrepaired. Increasing the dose decreases the speed of the repair kinetics; after a dose of 40 Gy 23% of the damage remains and after 80 Gy the cells have 32% residual damage at the last point measured.

This experiment reveals that D-NHEJ is an extremely effective repair pathway. Even after exposure to very high doses of IR there is no change in the repair of DSBs in wt cells. This shows that in the most important pathway for DSB repair is D-NHEJ, which is also demonstrated in figure 18B were the repair by B-NHEJ is slowing down with increasing radiation dose. This finding suggests that different DSB repair

pathways (D-NHEJ and B-NHEJ in this case) can have different responses to increasing radiation dose.

3.2 Is repair pathway choice dose-dependent?

We have observed previously in PFGE experiments that cells with mutations in HR proteins do not show any DSB repair defect when compared to wild type cells (Wu et al., 2008a). On the other hand it was found that HRR is absolutely necessary for the repair of G2-chromosomal breaks (Soni, 2010). This could mean that HRR is responsible at a minimum for these few DSBs, which are the precursors of chromosome breaks; because of their low numbers they remain undetected by PFGE. It was revealed in our lab that D-NHEJ does not appear to take part to the repair of G2-chromosome breaks in HRR deficient cells at low doses, this means that these few DSBs are processed exclusively by HRR (Soni, 2010). In addition it was found in late S- and G2-cells that with increasing IR doses RAD51 foci show saturation. On the basis of these results the laboratory investigates the working hypothesis that there is a saturation of HRR as the load of DSBs rises, which means that the ratio of DSBs reaching the strand invasion step in the HRR pathway decreases with increasing radiation dose (unpublished data).

These observations challenge the assumption that HRR plays a minor role in the repair of DNA DSB (Wu et al., 2008a), although its importance seems to be limited to low IR doses. Therefore, in the present work we wished to investigate whether there is a dose dependent switch between repair pathways. It is likely that HRR is active at low radiation doses and that at higher radiation doses e.g. 5 Gy, D-NHEJ and/or B-NHEJ are more preferred.

3.2.1 Repair of DSBs in wt and D-NHEJ deficient cells after exposure to doses lower than 20Gy

We obtained different results in different methods; one does not display a contribution of HRR (chapter 1.5.1) whereas the other shows it (chapter 1.5.2). Because of this the role of HRR to the repair of IR induced DSBs remains unclear.

To better understand this discrepancy, we first performed experiments with PFGE using lower doses than usually employed (20Gy). With these investigations we

wanted to check if the contribution of HRR to the repair of DNA DSBs decreases with increasing doses of IR. The doses chosen were 5, 10 and 20 Gy. If HRR becomes more prominent at low IR doses, we argue that we may see it as a change in the repair kinetics in wild type cells. For this investigation Chinese hamster cells were used, wild type (V79) and D-NHEJ deficient (Xrs6), which have a mutation in the *XRCC-5* gene. After irradiation the cells were allowed to repair from 15 min up to 8 h.

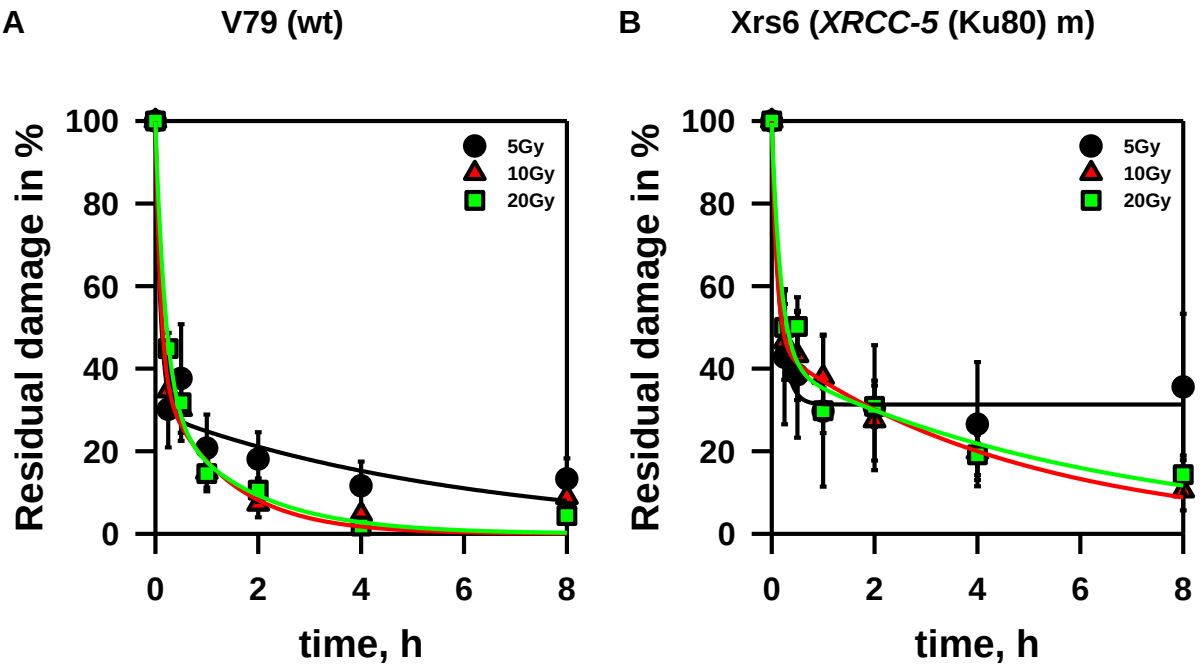

Figure 19: Rejoining of IR induced DSBs in exponentially growing Chinese hamster cells irradiated with 5, 10 and 20 Gy. After irradiation cells were allowed to repair for up to 8 h. The residual damage shown in % is plotted against the time. (A) Repair kinetics in wild type cells and (B) repair kinetics in D-NHEJ deficient hamster cells. Data points represent the mean and standard error from 4 to 6 independent experiments.

In the wild type cell line (V79) there is no difference in the repair kinetics after irradiation with 10 and 20 Gy (figure 19A), within 30 min only 30% of the initial DNA damage is left and after 4 h almost all damage is repaired. Looking at the curve of the cells, which were irradiated with 5 Gy, it is noticeable that in the first 30 min the kinetics of repair is similar to the kinetics of the cells, which were exposed to higher doses, but after 30 min it appears that the kinetics slows down. At 2 to 8 h cells irradiated with 5 Gy have 6 to 12% more residual damage left then those irradiated with 10 and 20 Gy.

In figure 19B the DSB kinetics of D-NHEJ deficient cells (Xrs6) also show trends of slowing down after exposure to 5 Gy. The kinetics of cells exposed to 10 and 20 Gy is similar, but the repair is much slower compared to V79; in this case there is 45% of the DNA damage left after 30 min repair.

3.2.2 Repair of DNA DSBs in HRR deficient cells after lower doses of IR

A change in the repair kinetics of wt cells exposed to 5 Gy could be demonstrated.
To see if there is also a change in the repair kinetics of HRR deficient cells we chose three Chinese hamster cell lines, irs1tor with a mutation in *XRCC2* gene, irs2tor mutated in *RAD51B* gene and irs3tor with a *RAD51C* mutation. In all these mutants HRR is not active, if HRR is responsible for the slower repair in the wild type cells, after 5 Gy, we would not expect a slower repair in these cases.

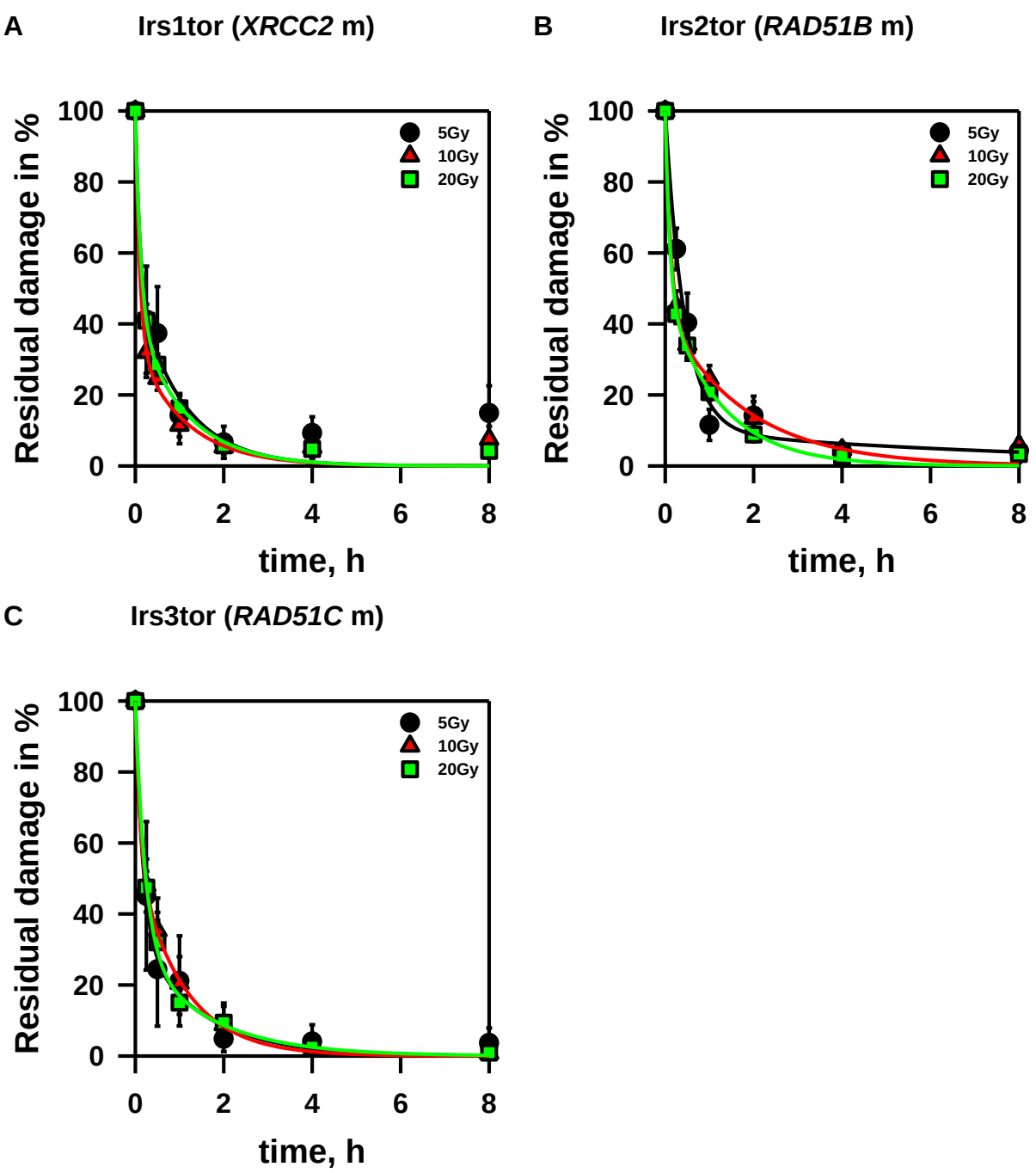

Figure 20: Kinetics of DNA DSB repair in exponentially growing Chinese hamster cells, which have mutations in HRR genes, after exposure to 5, 10 and 20 Gy. After irradiation cells were allowed to repair for up to 8 h. The residual damage shown in % is plotted against the time. (A) Repair kinetics of Irs1tor with a mutation in the *XRCC2* gene, (B) repair kinetics of Irs2tor mutated in the *RAD51B* gene and (C) repair kinetics of Irs3tor with a mutation in *RAD51C*. The data points represent mean and standard error from 3 independent experiments.

The repair kinetics curves after 5, 10 and 20 Gy from all three HRR deficient cells are comparable to V79 irradiated with 10 and 20 Gy. In every cell line there is only about 30% of DNA damage left at 30 min and after 4 h all the DNA DSBs are repaired (fig. 20), like in wild type cells (fig. 19A).

We assume that in the absence of HRR only B-NHEJ and D-NHEJ operate and thus DSBs are removed with fast kinetics. This can be seen as additional evidence that in wild type cells the contribution of HRR decreases with increasing doses of IR.

3.2.3 Which pathway is active in the repair of DNA DSBs?

We wished to investigate further if HRR and/or B-NHEJ get involved in the repair of DSBs when doses lower than 10 Gy are used. For this purpose we performed PFGE experiments, where inhibitors for HRR or B-NHEJ were used.

VE821 was used to inhibit HRR. VE821 is a highly selective and potent inhibitor of the DNA damage response kinase ATR, which sensitizes tumor cells to DNA damage induced by IR or chemotherapeutic drugs. VE821 is disrupting DNA damage checkpoints and is inhibiting DNA damage repair by HRR (Prevo et al., 2012).

B-NHEJ is inhibited by PARP-1 inhibitor PJ34 (Conrad et al., 2006).

Both inhibitors, VE821 and PJ34, were used at a concentration of 5 µM and were added 1 h before irradiation. In the experiments we used again the wild type cell line V79 and the D-NHEJ deficient cell line Xrs6, the cells were irradiated with doses of 5 and 20 Gy.

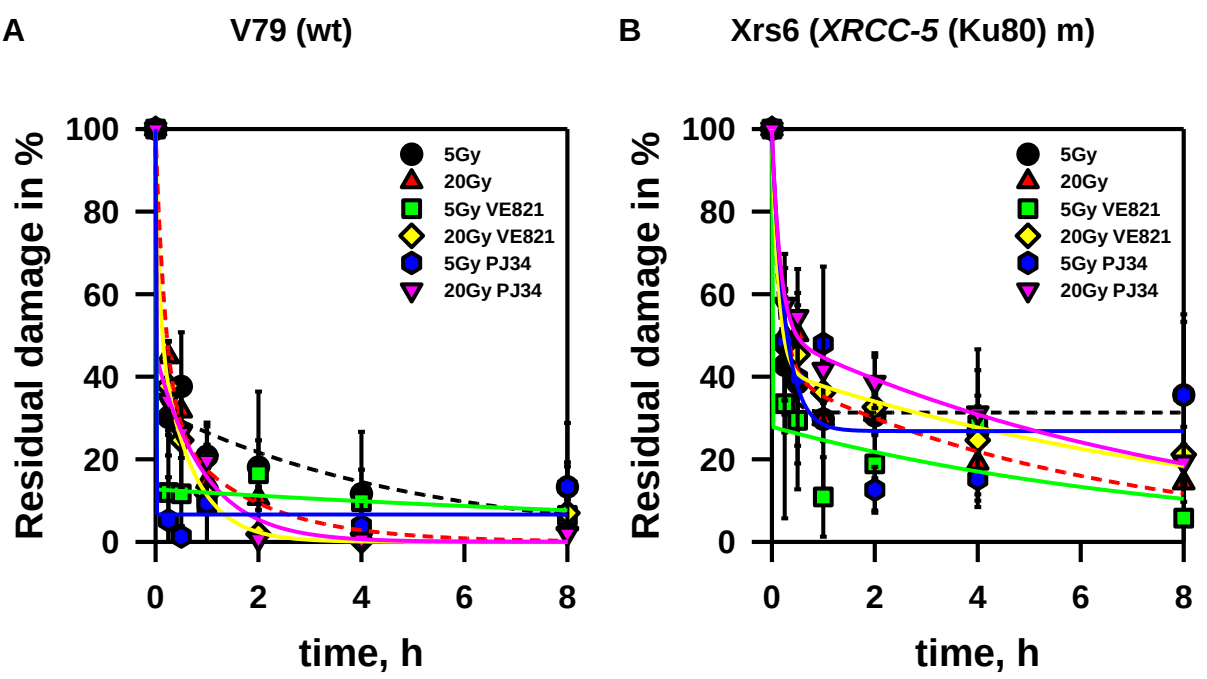

Figure 21: Rejoining of IR induced DSBs in exponentially growing Chinese hamster cells irradiated with 5 and 20 Gy. After irradiation cells were allowed to repair for up to 8 h. Residual damage in % is plotted against time. (A) Repair kinetics in wild type cells and (B) repair kinetics in D-NHEJ deficient hamster cells. In both cases the cell lines were treated with VE821 and PJ34 1 h prior exposure to IR, the untreated controls are shown in dashed lines.

When HRR and B-NHEJ were inhibited in wild type cells there is no effect on the repair kinetics after 20 Gy. In untreated wild type cells, irradiated with 20 Gy, only about 30% of DNA damage is left after 30 min of repair and after 4 h all DNA DSBs are rejoined (fig. 21A).

Figure 21B shows that also when the Xrs6 cells are treated with VE821 or PJ34 it does not change the repair kinetics compared to untreated cells (fig. 21B).

Looking in both cell lines, for cells exposed to 5 Gy, it is not possible to create clear curves; this can be due to the low sensitivity of the PFGE method. As described under “Material and Methods”, it is advisable to use doses higher than 10 Gy. Because of this limitation we decided to do the same experiment with V79 cells but using 10 Gy instead of 5 Gy.

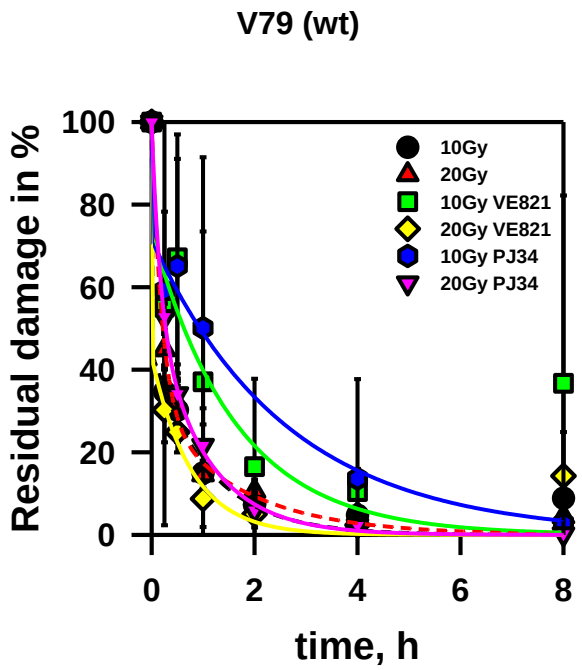

Figure 22: Kinetics of DNA DSB repair in exponentially growing Chinese hamster cells irradiated with 10 and 20 Gy. After irradiation cells were allowed to repair for up to 8 h. Residual damage in % is plotted against time. Repair kinetics in wild type cells, which were treated with VE821 and PJ34 1 h before irradiation, the untreated controls are shown in dashed lines.

Wild type cells that were treated with the PARP inhibitor and irradiated with 10 Gy seem to have slower repair kinetics than cells, which were treated with the ATR inhibitor (fig. 22). This could suggest the involvement of B-NHEJ in the repair of DSBs after a 10 Gy exposure.

Figure 23 shows DSB repair kinetics of V79 (fig. 23A) and Xrs6 (fig. 23B) cells, which were incubated with VE821 and PJ34 prior to 20 Gy of IR.

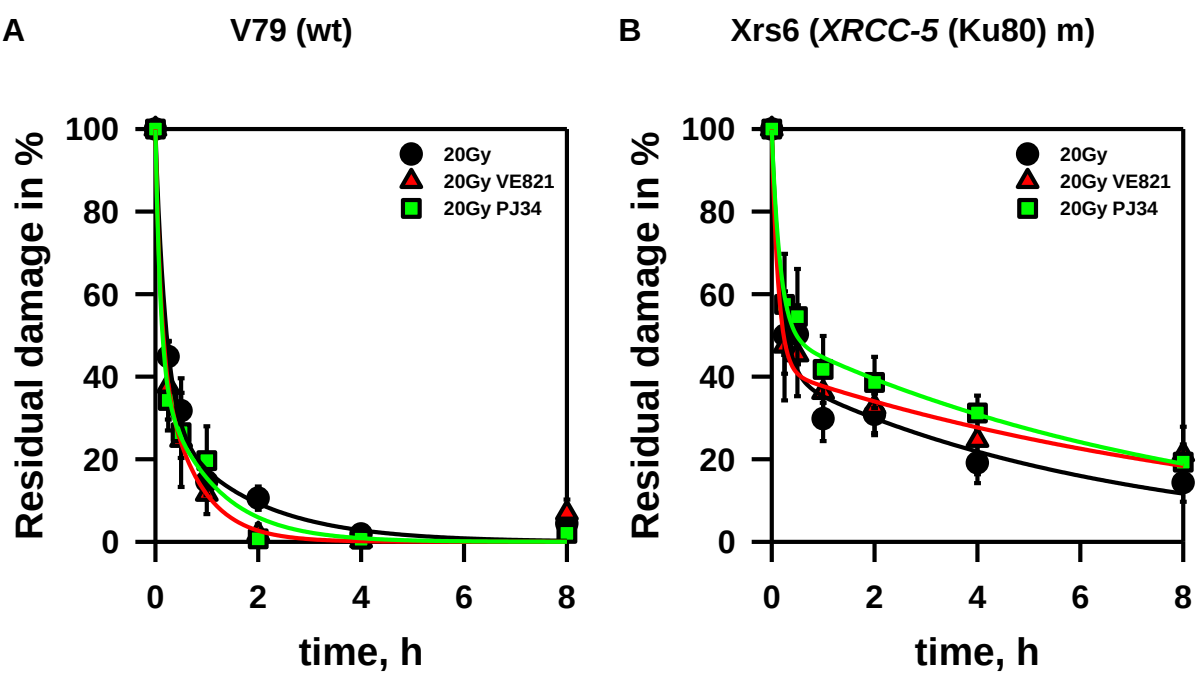

Figure 23: Rejoining of IR induced DSBs in exponentially growing Chinese hamster cells irradiated with 20 Gy. After irradiation cells were allowed to repair for up to 8 h. Residual damage in % is plotted against time. (A) Repair kinetics in wild type cells and (B) repair kinetics in D-NHEJ deficient hamster cells. Both cell lines were treated with VE821 and PJ34 1 h prior to IR.

After inhibition of HRR or B-NHEJ no difference in repair of DNA DSBs is detected in wild type cells (fig. 23A) because D-NHEJ is active. However D-NHEJ deficient cells show in both cases a slight reduction in the repair of DSBs (fig. 23B). In figure 23B it seems that HRR and B-NHEJ have an equal contribution in the repair of the DNA DSBs when D-NHEJ is inhibited.

Thus, at the DNA level it could not be demonstrated that there is a dose dependent switch between DSB repair pathways. But the results obtained after exposure to 10 Gy hint to an involvement of B-NHEJ. On the other hand, results obtained after 5 Gy exposures are more or less not correctly interpretable. Because of this limitation we started examining repair at the chromosomal level.

3.3 Repair of G2-PCC breaks in wt and HRR deficient cells after exposure to doses higher than 1 Gy

As reported before it was found that HRR is absolutely necessary for the repair of G2-chromosomal breaks, because HRR is responsible for the few DSBs, which are the precursors of chromosome breaks. D-NHEJ does not appear to take part in the repair of G2-chromosome breaks in HRR deficient cells at lower doses (Soni, 2010). In the current study, Calyculin A induced G2-PCC was employed in V79 cells (wt) and the HRR deficient mutants, irs1tor (*XRCC2* m), irs2tor (*RAD51B* m) and irs3tor (*RAD51C* m). Doses of 1, 2, 5 and 7 Gy were given. This approach allows the study of chromosomal damage and repair in irradiated G2 cells. Cells were allowed to repair for 2 to 8 h post IR.

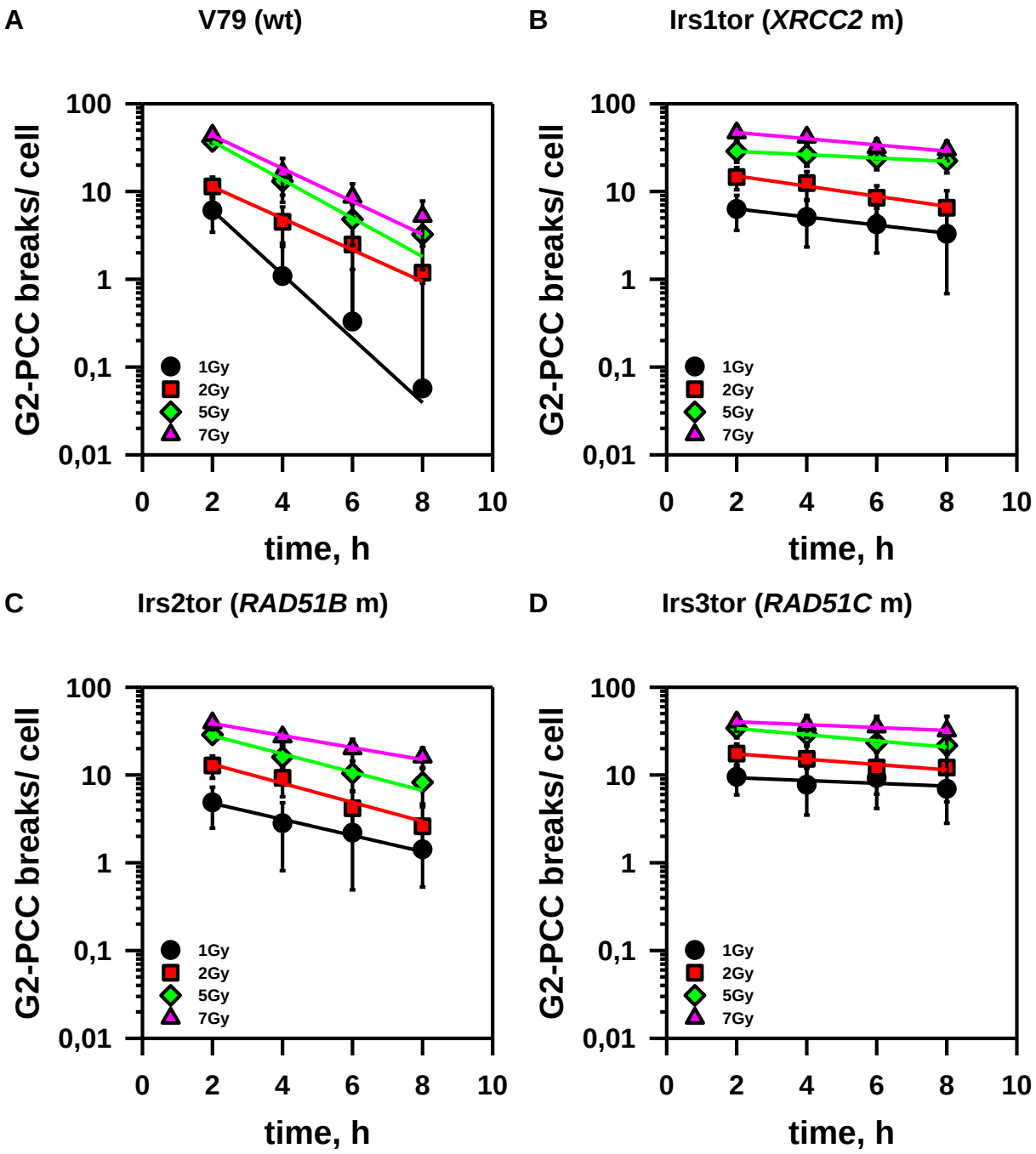

Figure 24: Kinetics of repair of G2-PCC breaks in exponentially growing Chinese hamster cells exposed to 1, 2, 5 and 7 Gy X-rays and allowed to repair for up to 8 h after irradiation. The number of G2-PCC breaks/ cell is plotted against time. (A) Wild type cells, (B) *XRCC2* m cells, (C) *RAD51B* m cells and (D) *RAD51C* m cells.

The results show that wild type cells repair PCC breaks with very fast repair kinetics, even after 5 and 7 Gy (fig. 24A). The first time point was 2 h post irradiation, after 1Gy of IR V79 has a damage of 6 G2-PCC breaks per cell, followed by 11 G2-PCC breaks per cells after 2 Gy of IR, 37 breaks after 5 Gy of IR and 43 G2-PCC breaks after 7 Gy of IR. This linear increase with dose was expected in the wild type cells. 8

h after irradiation with any dose the repair of chromosome damage is almost completed.

In Figure 24B the cell line with a mutation in *XRCC2* shows almost no repair after irradiation with 1 Gy, which was suspected because it was shown earlier that HRR deficient cells do not repair chromatid, as well G2-PCC breaks at low doses (Soni, 2010). This is also true for two additional HRR mutants irs2tor (fig. 24C) and irs3tor (fig. 24D). All three HRR mutants tested (fig. 24B, C and D) fail to show significant repair of G2-PCC breaks at all doses examined. If there was a dose dependent switch between repair pathways (from HRR at low doses to D-NHEJ or B-NHEJ at higher doses), we would expect an increase of repair in HRR mutants with increasing radiation dose. While analyzing these experiments it was noticed, that there is strong fluctuation in the numbers of breaks per cell in the different time points from about 15 to 40 G2-PCC breaks after 5 Gy. A reason for this could be that highly damaged late S-phase cells enter G2-phase at later time points and mask the response possibly due to their HRR defect that causes a loss in S-dependent radiosensitivity to killing.

Aphidicolin is a reversible inhibitor of eukaryotic nuclear DNA replication. It specifically inhibits the DNA polymerase alpha and delta in eukaryotic cells (Iliakis et al., 1982). Because it inhibits the DNA replication incubated cells can be blocked in the S-phase facilitating analysis of only irradiated G2-cells in our PCC experiments. Aphidicolin was used at a final concentration of 5 µM and was added 1 h prior to IR. The inhibitor was maintained during the entire experiment.

We first wished to check the effect of aphidicolin in our experimental conditions by flow cytometry. Cells were pulsed labeled with 10 µM BrdU before exposure to the indicated IR doses and collected at different post IR times matching the kinetics of G2-PCC breaks.

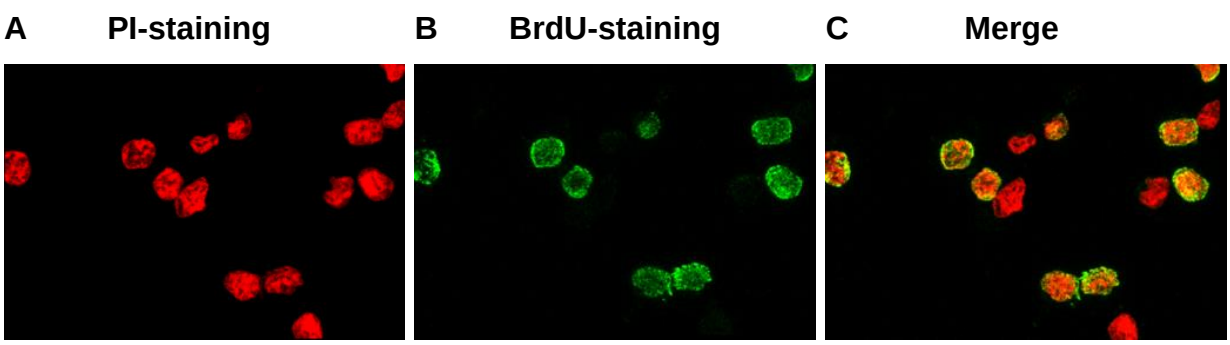

Figure 25: Confocal images of BrdU stained cells. (A) Images of cells, which are stained with Propidium iodide (PI), (B) Images of cells pulse-labeled with BrdU and (C) Merge of PI- and BrdU-staining.

The selected FACS histograms are shown in figure 26 and show clearly that aphidicolin treatment blocks cells for up to 8 h in S-phase. The histograms of the entire experiment are listed in appendix 1 (chapter 7). Representative confocal images are shown in Figure 25.

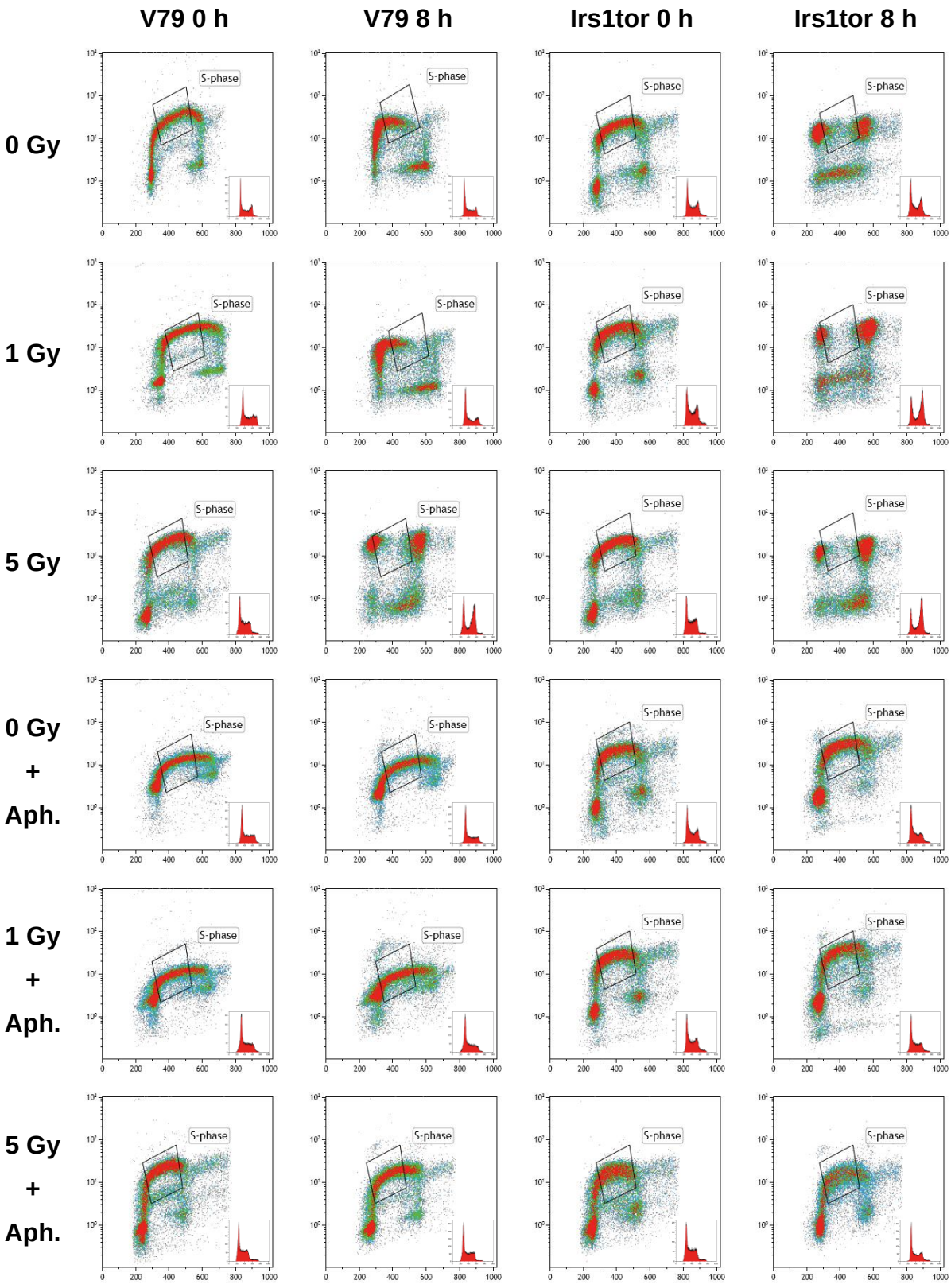

Figure 26: S-phase block by aphidicolin in Chinese hamster wild type and HRR mutants analyzed by flow cytometry. Two sets of exponentially growing cells were analyzed. The first set was untreated and the second was treated with aphidicolin (Aph.). In every set there are cells, which were irradiated with 0, 1 and 5 Gy X-rays. Flow cytometry was run at 0 and 8 h post-irradiation. BrdU-positive S-phase cells were estimated by gating in the density plots shown.

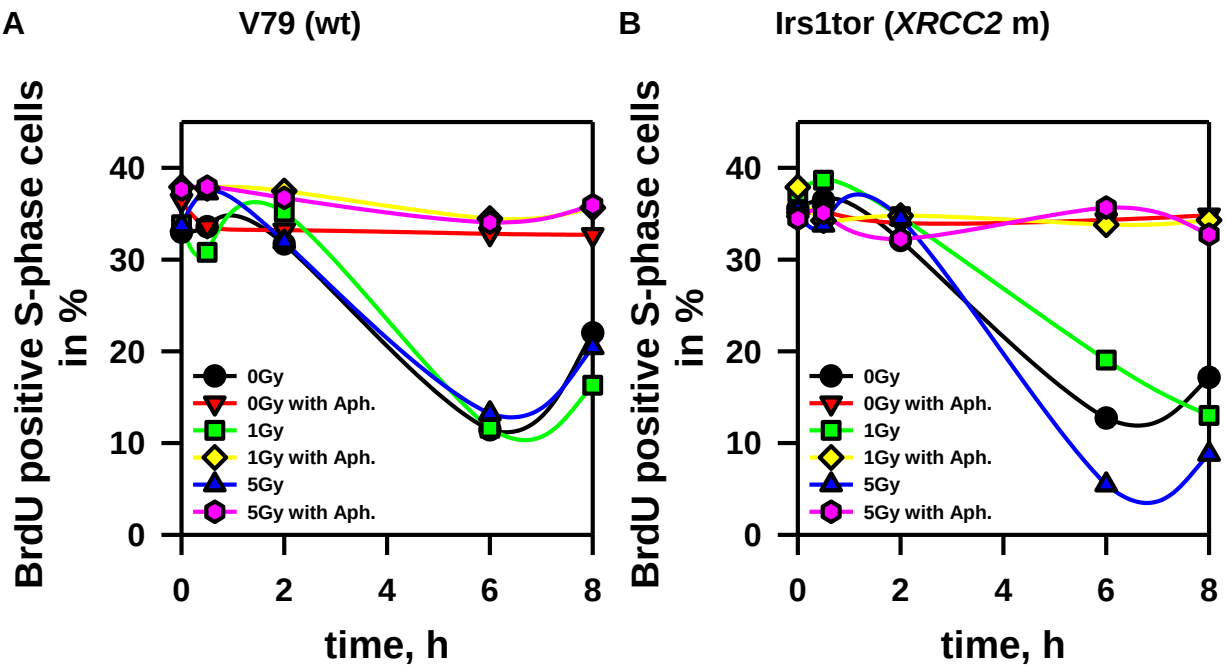

Figure 27: Study of S-phase block in wild type and HRR mutants of Chinese hamster cells by flow cytometry. Two sets of exponentially growing cells were analyzed. The first set is untreated while the cells of the second set are block in S-phase by treating with aphidicolin. In every set there are cells, irradiated with 0, 1 and 5 Gy X-rays. We analyzed the experiment by flow cytometry at 0 and 8 h post-irradiation and followed BrdU-positive S-phase cells. The % of BrdU positive S-phase cells is plotted against time. (A) Wild type cells and (B) XRCC2 m cells.

In figure 27 it is clearly shown that in both cell lines, V79 and Irs1tor, cells are blocked in S-phase after treatment with aphidicolin. In both cell lines the fraction of S-phase cells remains constant at about 35%. Untreated cells move through the cell cycle after 6 h and there are less than 20% S-phase cells left.

3.4 Repair pathway switch can be detected at the chromosomal level in G2-phase cells

With the help of aphidicolin we can be sure that we only analyze these cells, which were in G2 at IR exposure. For the experiment we used wild type (V79) and XRCC2 mutant cells (Irs1tor). Two different doses i.e. 1 Gy (low dose) and 5 Gy (higher dose) were chosen for the experiment. Aphidicolin was added 1 h before irradiation and cells were harvested at 1, 2, 4, 6 and 8 h post IR. Before harvesting the respective time point, cells were treated with 100 nM Calyculin A for 30 min to induce PCCs (aphidicolin treated G1-, S- and G2-phase cells after Calyculin A induced G2-PCC are shown in appendix 2; shown also are G2-PCC breaks and exchanges in appendix 3 in chapter 7).

A V79 (wt) with aphidicolin

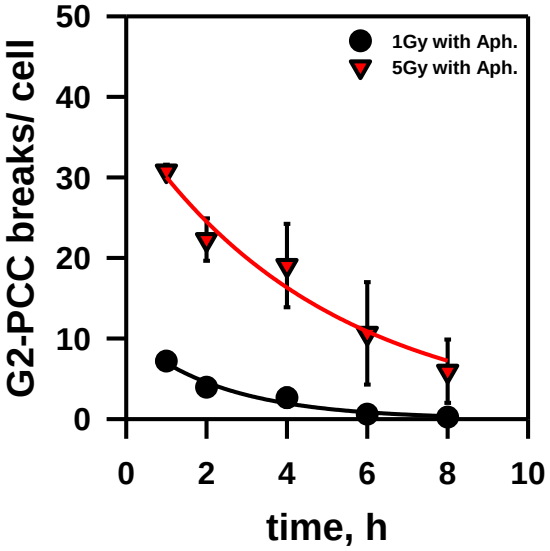

B Irs1Clone1 (corr.) with aphidicolin

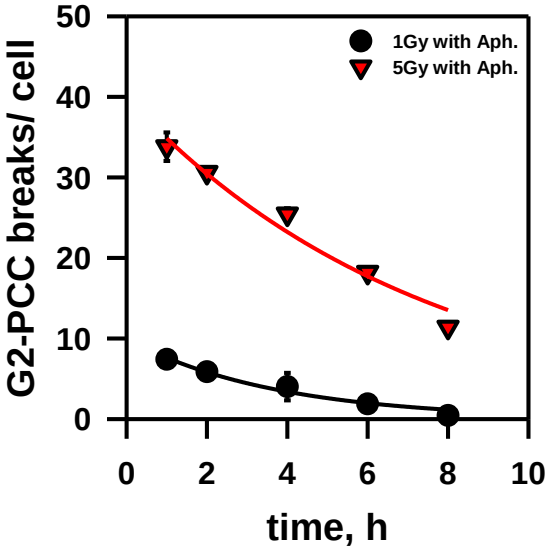

C Irs1tor (*XRCC2* m) with aphidicolin

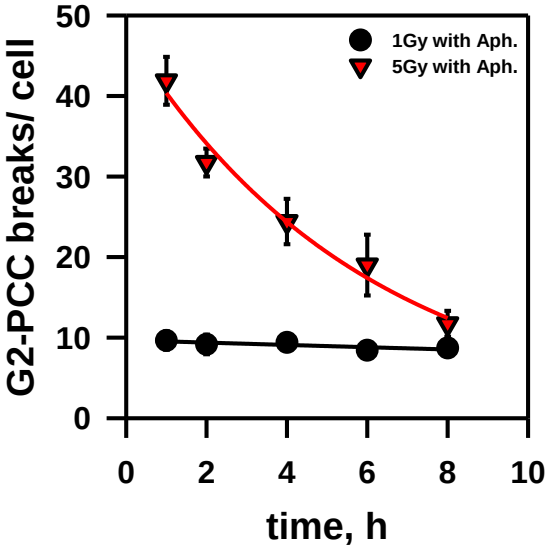

Figure 28: Kinetics of G2-PCC breaks in exponentially growing Chinese hamster cells irradiated with 1 and 5 Gy and allowed to repair for up to 8 h. Before irradiation cells were treated with aphidicolin to block S-phase cells from entering G2 during analysis. The number of G2-PCC breaks/ cell is plotted against time. (A) Wild type cells, (B) Irs1Clone1 cells, which are corrected for the mutation in *XRCC2* and (C) Irs1tor cells, which are mutated in *XRCC2*.

The wild type cells repair G2-PCC breaks with fast repair kinetics independent of the dose, after 8 h only 19% of the breaks remain unrepaired (fig. 28A). In figure 28C the HRR mutant cell line shows almost no repair after exposure to 1 Gy (90% of damage is left unrepaired), which support the results shown earlier (Soni, 2010). Surprisingly after 5 Gy of IR, fast repair kinetics are shown. This contrasts the results obtained without aphidicolin (fig. 24B). This kinetics now more resembles wild type cells, since only 27% of the initial DNA damage is left at 8h. In addition to wild type cells (V79) and the HRR deficient cells (Irs1tor), we also checked the kinetics of G2-PCC repair in the corrected cell line of Irs1tor (Irs1Clone1). The results are summarized in figure 28B and are similar to those obtained with the wt cells.

The repair of G2-PCC breaks in HRR deficient cells after irradiation with 5 Gy may indicate a dose dependent switch of DSB repair from HRR to B-NHEJ at high radiation doses. To find out more about the contribution of D-NHEJ and B-NHEJ in the repair of DSBs in Irs1tor after increasing dose, we use some inhibitors of the repair pathways.

3.4.1 Inhibition of B-NHEJ and D-NHEJ as a means to reveal their contribution to DSB repair at high radiation doses

It seems that there is a dose dependent switch of repair pathways. To find out, which pathway is active in Irs1tor after exposure to 5 Gy, specific inhibitors were used. For inhibition of D-NHEJ, a DNA-PK inhibitor (NU7441) was used. To inhibit B-NHEJ a PARP inhibitor, PJ34, was used.

3.4.1.1 Effect of B-NHEJ Inhibition

To see if B-NHEJ is active in Irs1tor, PARP-1 was inhibited with PJ34; the inhibitor was used in a working concentration of 5 µM and was added 1 h before irradiation.

A **V79 (wt) with PJ34** **B** **Irs1tor (*XRCC2* m) with PJ34**

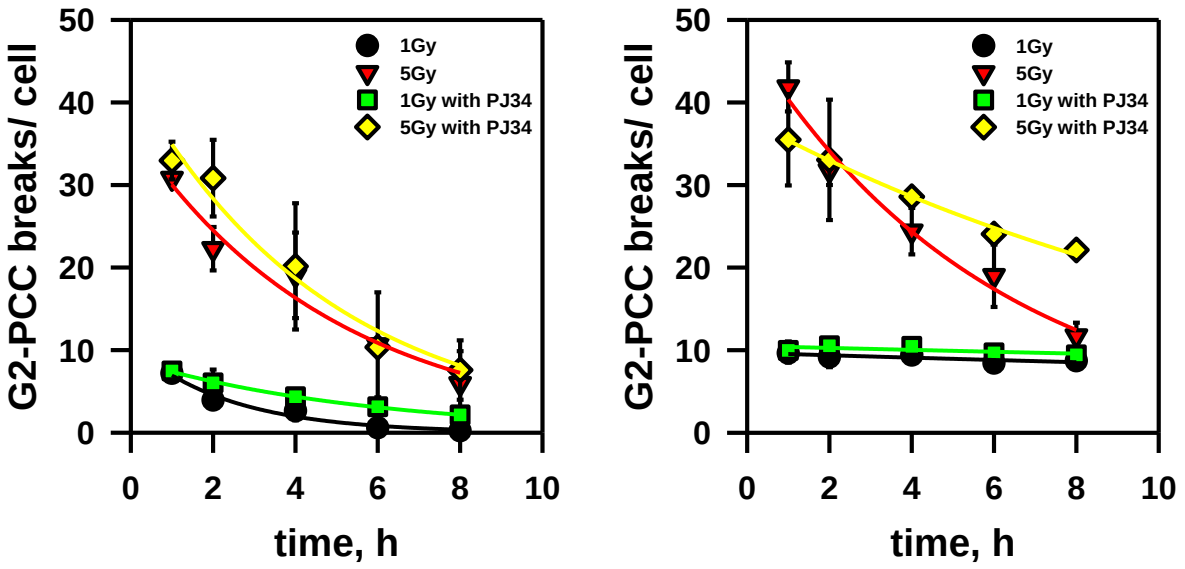

Figure 29: Effect of B-NHEJ inhibitor PJ34 on the kinetics of G2-PCC breaks in exponentially growing Chinese hamster cells irradiated with 1 and 5 Gy X-rays. Cells were treated with the indicated concentration of aphidicolin and PJ34 for 1 h before irradiation and allowed to repair for 8 h. Aphidicolin and PJ34 were maintained in the culture medium during the entire experiment. (A) Effect of 5 µM PJ34 on wild type and (B) HRR deficient cells.

When B-NHEJ is inhibited we see no significant change in the repair kinetic in wild type cells only after 1 Gy of IR, figure 29A. There is no change in initial damage with or without inhibitor, but after 8 h of repair there are still 28% residual breaks. After exposure to 5 Gy, the repair kinetics is the same as in untreated wild type cells (fig. 29A). In the HRR deficient cell line the result is different (fig. 29B) with no change in the repair kinetics after irradiation with 1 Gy, but relatively strong reduction in the

repair after exposure to 5 Gy. After inhibition of B-NHEJ there is 62% residual damage left - double that of untreated cells (27% residual damage). Since D-NHEJ is supposed to work here, it shows that D-NHEJ is not able to repair the DSB with the same kinetic as the untreated Irs1tor cells. This reveals that B-NHEJ must be involved in the repair of the G2-PCC breaks in HRR deficient cells after exposure to 5 Gy.

3.4.1.2 Effect of D-NHEJ inhibition

To explore more about the activity of D-NHEJ in Irs1tor cells, we employed DNA-PK inhibitor NU7441 at a working concentration of 5 µM and added it 1 h before irradiation.

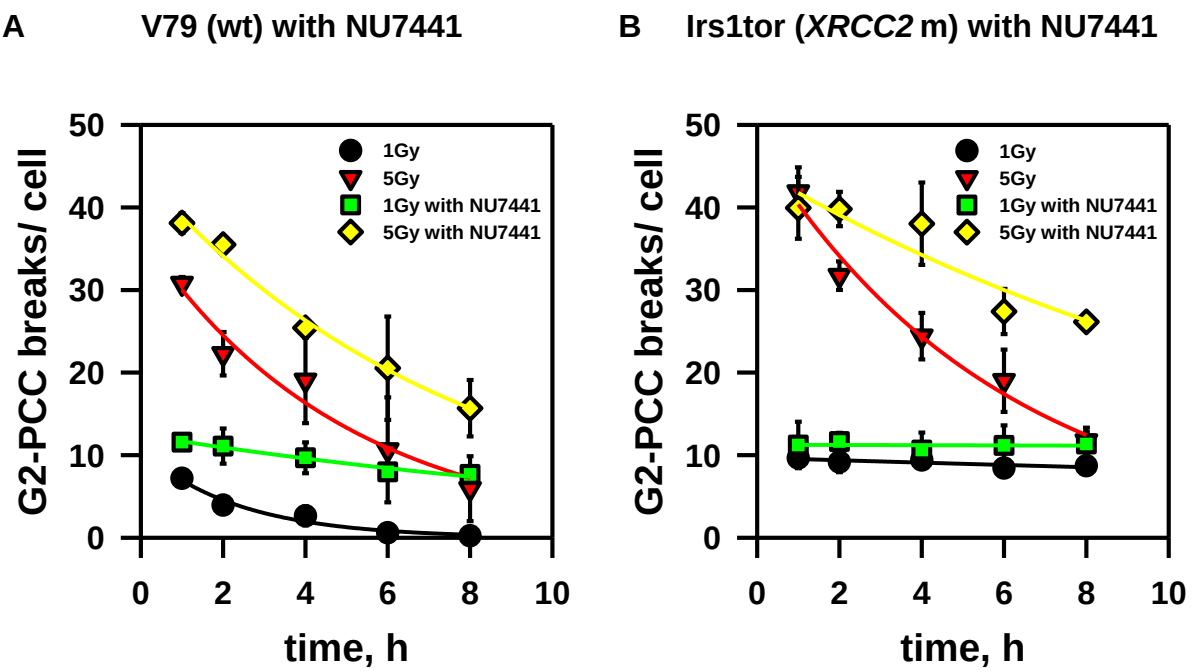

Figure 30: Effect of D-NHEJ inhibitor NU7441 on the kinetics of G2-PCC breaks in exponentially growing Chinese hamster cells irradiated with 1 and 5 Gy X-rays. Cells were treated with the indicated concentration of aphidicolin and NU7441 for 1 h before irradiation and allowed to repair for 8 h. Aphidicolin and NU7441 were maintained in the culture medium during the entire experiment. (A) Effect of 5 µM NU7441 on wild type and (B) HRR deficient cells.

In wild type cells the initial number of breaks is higher after inhibition of D-NHEJ (fig. 30A). Following 1 Gy IR the initial number of breaks is 11 breaks/ cell and after 8 h hours 66% residual damage is measured. When irradiated with 5 Gy we have 38 initial breaks and 41% of the damage is remaining at 8 h. In case of V79 the inhibition of D-NHEJ makes a bigger difference than inhibition of B-NHEJ.

Almost no repair was observed in HRR deficient cells treated with NU7441 when irradiated with 1 Gy IR (fig. 30B). After 5 Gy of IR the repair is impaired, there is more initial damage by about 10 breaks in untreated cells and after 8 h 65% residual damage is registered.

3.4.1.3 Comparison of repair kinetics in terms of residual damage

Three different sets of experiments in the 2 different cell lines, V79 and Irs1tor, were performed as outlined above. In the first set the cells were only treated with aphidicolin, in the second set B-NHEJ was additionally inhibited with PJ34 and in the third D-NHEJ was additionally inhibited with NU7441 and analysis was carried out at low and high doses of IR. The results of these experiments are combined in figure 31A for 1 Gy and figure 31B for 5 Gy. Because of the different initial numbers of G2-PCC breaks the residual damage of repair was calculated to facilitate comparison.

A Comparison V79 (wt) and Irs1tor (*XRCC2* m): 1 Gy

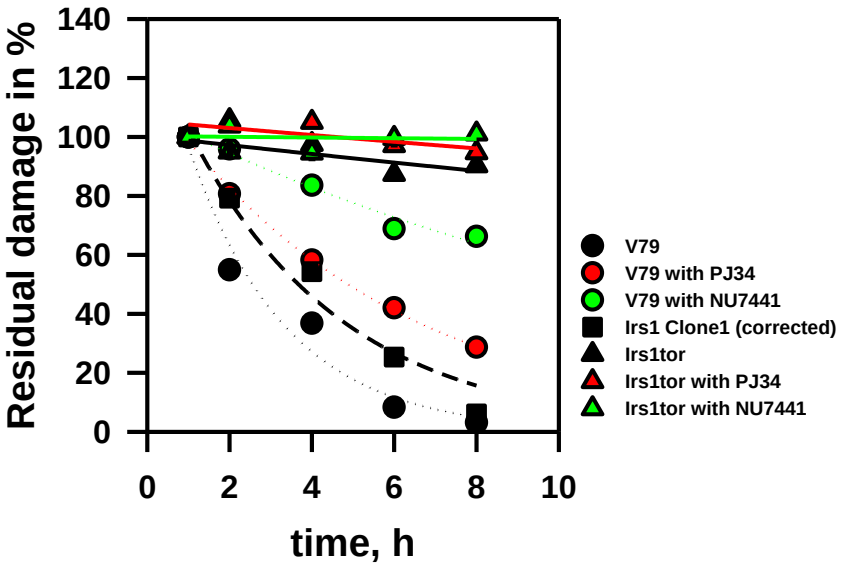

B Comparison V79 (wt) and Irs1tor (*XRCC2* m): 5 Gy

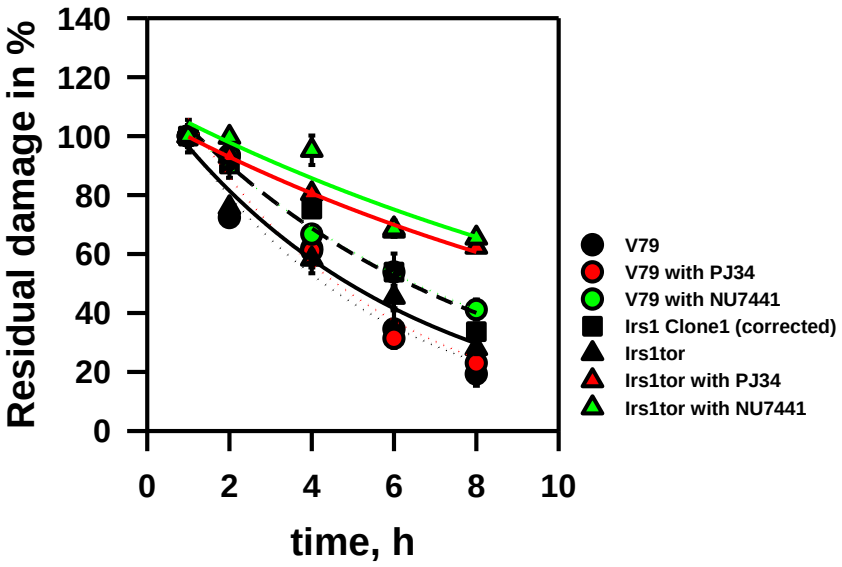

Figure 31: Effect of inhibitors on the kinetics of G2-PCC breaks in exponentially growing Chinese hamster cells. Cells were treated with the indicated concentration of aphidicolin and inhibitors for 1 h before irradiation and allowed to repair for 8 h. Aphidicolin and the inhibitors were present in the culture medium during the entire period of incubation. (A) Comparison of repair after 1 Gy of IR and (B) after 5 Gy of IR.

Figure 31A shows repair kinetics after 1 Gy of IR. Noticeably, there is almost no G2-PCC break repair in the HRR deficient cells even after inhibiting DNA-PK and PARP-1, which shows the importance of HRR in DSB repair after exposure to low radiation doses. In wild type cells the effect of the inhibitors is detectable. In untreated cells all breaks are repaired after 8 h, but when B-NHEJ is inhibited 28% of damage remains after 8 h, and after inhibition of D-NHEJ 66% PCC breaks remain unrepaired.

After exposure to 5 Gy (fig 31B) the HRR deficient cells start to repair; there is only about 27% of damage left unrepaired at 8h. Inhibition of B-NHEJ or D-NHEJ in this HRR deficient mutant, compromises DSB rejoining and about 62 - 65% of the damage remains unrepaired at 8 h (fig 31B). This suggest an about equal contribution of B-NHEJ and D-NHEJ in the repair of G2-PCC breaks after 5Gy of IR. In wild type cells there is no significant change in the repair of PCC breaks after inhibition of NHEJ pathways at 5 Gy (fig. 31A).
At 1 Gy there is a strong decrease in wt cells in DSB repair after inhibiting D-NHEJ and a small decrease after treatment with PJ34 (fig. 31A), which was not expected, since HRR was shown to be essential in chromosomal breaks repair after low dose exposure. These apparent contradictions make the results difficult to interpret.

With these results we could show that there is a dose dependency on DSB repair pathway switch.

3.5 Chromatid Exchange formation during G2-PCC break repair in HRR deficient cells

Most of IR-induced DSBs are repaired but if they remain unrepaired they could rejoin with other DNA ends, which results in misrepair (Natarajan and Palitti, 2008). Misrepaired chromosome breaks lead to the formation of chromosome aberrations. Depending on the cell cycle phase in which cells were irradiated different types of chromosome aberrations can occur i.e. chromosomal exchanges (CEs) (Hada et al., 2011).

CEs are known to be a hallmark of cancer and are likely to be formed by B-NHEJ and less likely by D-NHEJ. Cells which are deficient in D-NHEJ have a higher amount of CEs, which shows that D-NHEJ is not needed to form CEs (Simsek and Jasin, 2010; Weinstock et al., 2007).

DNA ends remain open and are processed by B-NHEJ, because this processing is slow the DNA ends might interact with other DNA ends nearby forming CEs (Iliakis et al., 2004). The proteins involved in B-NHEJ are PARP-1, LIG3 or LIG1 and its interacting partner XRCC1. While analyzing the G2-PCC breaks, it was striking that the HRR deficient cells display an increase in the frequency of CEs after exposure to 5 Gy.

3.5.1 HRR deficient cells have an increase in CEs after exposure to higher doses

The observation of increased CE frequency in Irs1tor could be a hint for a switch to B-NHEJ after 5 Gy of IR.

A V79 (wt) with aphidicolin

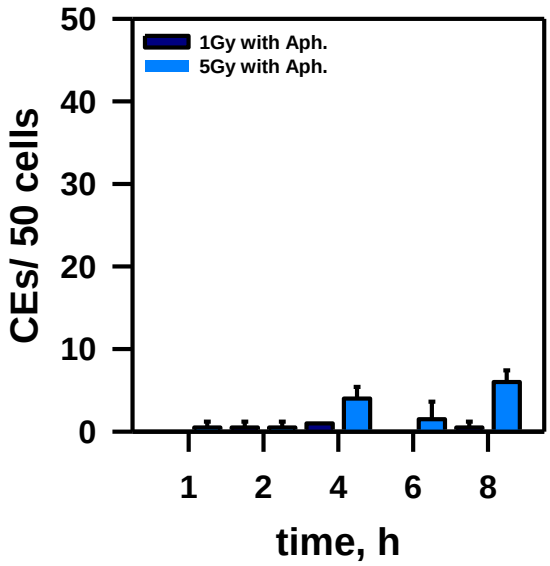

B Irs1Clone1 (corr.) with aphidicolin

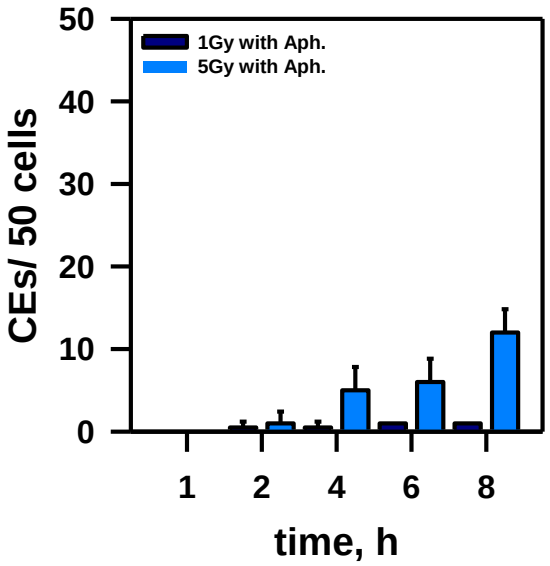

C Irs1tor (*XRCC2* m) with aphidicolin

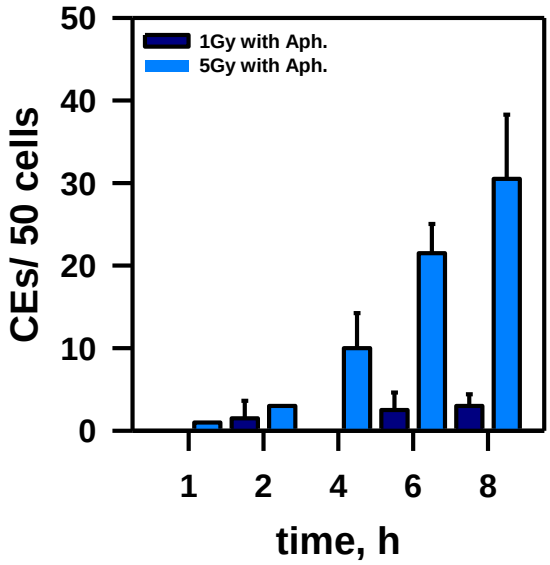

Figure 32: Kinetics of CEs in exponentially growing Chinese hamster cells irradiated with 1 and 5 Gy X-rays and allowed to repair for up to 8 h. The number of exchanges/ 50 cells is plotted against time. (A) Wild type cells, (B) Irs1Clone1 cells, which are corrected for the mutation of *XRCC2* and (C) Irs1tor cells, which are mutated in *XRCC2*.

There is almost no formation of CEs in wild type cells even after 5 Gy of IR as shown in figure 32A. Similar results are obtained with the corrected cell line Irs1Clone1; only at 8 h after 5 Gy radiation exposure there is a slight increase up to 12 CEs in 50 cells (fig. 32B), which is the double that scored in wild type cells at that time point. But the HRR deficient cell line showed dramatic increase in the number of CEs after 5 Gy of IR, starting from 4 h after irradiation and ending with 30 CEs in 50 cells 8 h post irradiation (fig. 32C). This increase we do not see in cells irradiated with 1 Gy, which is another proof for a pathway switch at higher doses. CEs are a characteristic for B-NHEJ, which could be a hint for a switch to the backup pathway.

3.5.2 What is the effect of different inhibitors on the formation of CEs?

It is known that CEs are more likely to be formed by B-NHEJ and less by D-NHEJ (Weinstock et al., 2007). We wished to examine how the frequency of CEs formation changes when B-NHEJ or D-NHEJ are chemically inhibited.

3.5.2.1 Effect of PARP-1 inhibition on the formation of CEs

One component of B-NHEJ, PARP-1, is involved in CEs formation. Indeed, inhibition of PARP reduces the frequency of translocations on IR induced DSBs in G1 cells (Wray et al., 2013), but this has not been examined in G2-phase. To examine whether B-NHEJ is responsible for CEs in the Irs1tor mutant, we treated cells with the PARP inhibitor PJ34. The inhibitor was used at a working concentration of 5 µM and was added 1 h prior to irradiation.

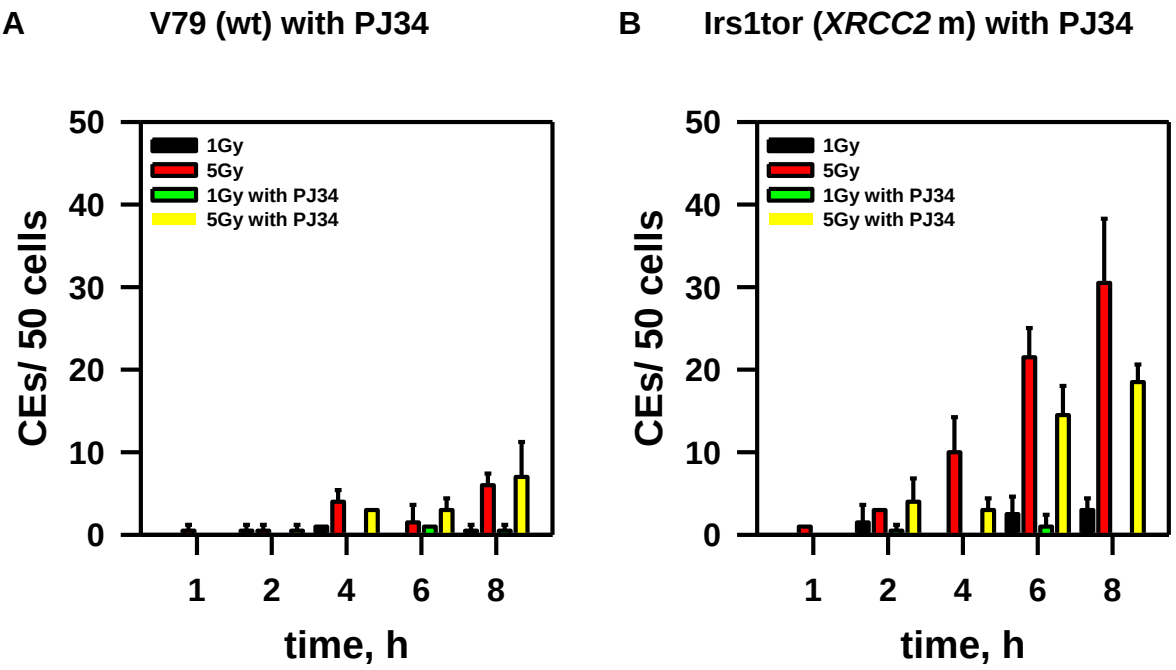

Figure 33: Effect of PARP-1 inhibition on the kinetics of CEs in exponentially growing Chinese hamster cells irradiated with 1 and 5 Gy X-rays. Cells were treated with the indicated concentration of PJ34 for 1 h before irradiation and allowed to repair for 8 h. PJ34 was maintained in the culture medium during the entire experiment. (A) Effect of 5 µM PJ34 on CEs formation in wild type and (B) HRR deficient cells.

As expected a remarkable decrease of CEs was found in Irs1tor after 5 Gy of IR; without PARP inhibitor there were 30 CEs per 50 cells at 8 h post IR but the number is reduced to 18 CEs when PARP was inhibited (fig. 33B). In wild type cells there is no significant effect of the PARP inhibitor on CEs formation, shown in figure 33A.

3.5.2.2 Effect of DNA-PK inhibitor on CEs formation

D-NHEJ has shown to be dispensable for CE formation (Weinstock et al., 2007), as increased frequencies of CEs were reported in case of D-NHEJ defect (Simsek and Jasin, 2010). We wished to study the effect of DNA-PK inhibition on CEs. The inhibitor NU7441 was used in a working concentration of 5 µM and was added 1 h prior to irradiation.

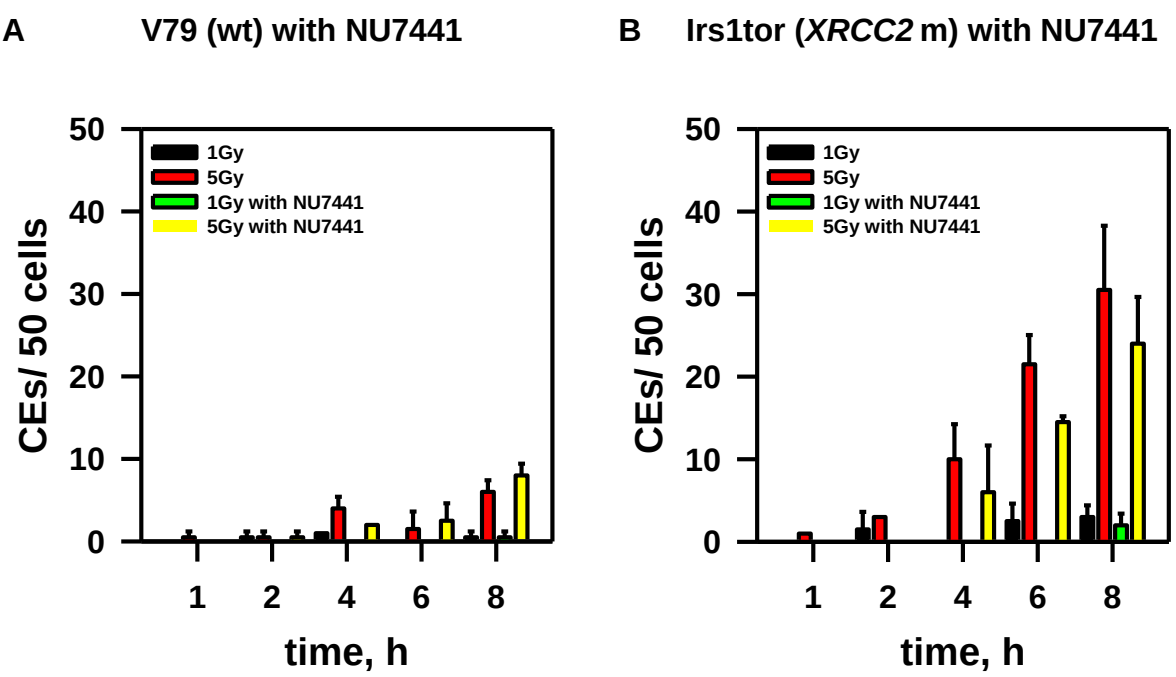

Figure 34: Effect of D-NHEJ inhibitor NU7441 on the kinetics of chromatid exchanges in exponentially growing Chinese hamster cells irradiated with 1 and 5 Gy X-rays. Cells were treated with the indicated concentration of NU7441 for 1 h before irradiation and allowed to repair for 8 h. NU7441 was maintained in the culture medium during the entire experiment. (A) Effect of 5 µM NU7441 on CEs formation in wild type and (B) HRR deficient cells.

In figure 34A it is illustrated that the inhibition of D-NHEJ does not affect the frequency of CE formation in wild type cells. Surprisingly we see a slight decrease in the formation of CEs from 30 to 24 CEs per 50 cells in the HRR deficient cell line (Irs1tor) (fig. 34B), it was expected to be a higher frequency of CEs formation, since D-NHEJ is known to inhibit formation of CEs due to B-NHEJ (Wang et al., 2006). There is almost no formation of CEs after exposure to 1 Gy.

3.5.2.3 Comparison of the frequency of CEs in the presence or absence of inhibitors

We have shown 3 different sets of experiments in V79 and Irs1tor cells. In the first set the cells were only irradiated in the presence of aphidicolin, in second set PARP was inhibited and in third set DNA-PK was inhibited – radiation and aphidicolin was always applied. All these results are combined for comparison in figure 35A for 1 Gy and figure 35B for 5 Gy.

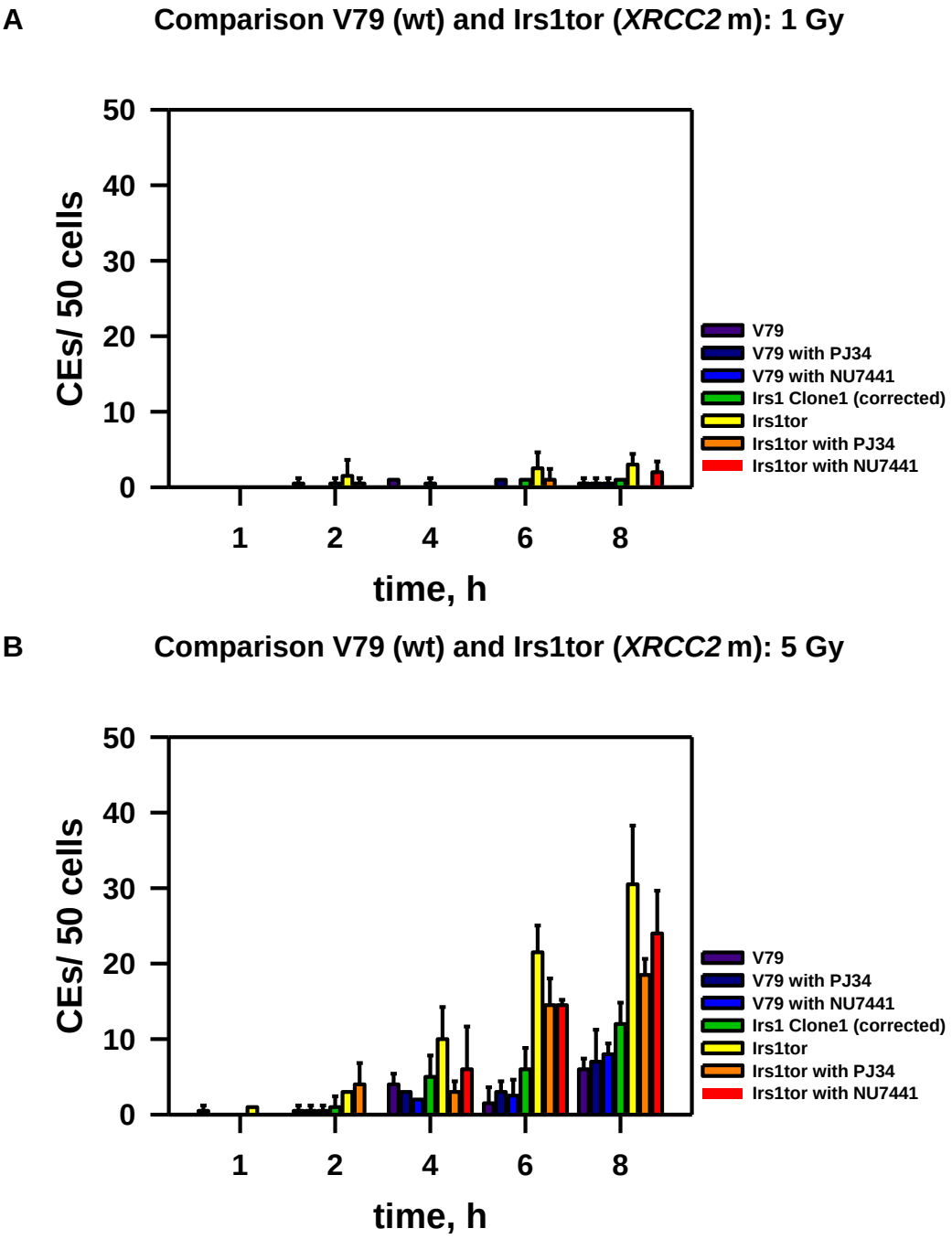

Figure 35: Effect of inhibitors on the kinetics of CEs formation in exponentially growing Chinese hamster cells. Cells were treated with the indicated concentration of aphidicolin and the inhibitors for 1 h before irradiation and allowed to repair up to 8 h. Aphidicolin and the inhibitors were maintained in the culture medium during the entire experimental procedure. (A) Comparison of effect on CEs formation after 1 Gy of IR with or without inhibitors and (B) after 5 Gy of IR with or without inhibitors.

The formation of CEs is a hint for an active B-NHEJ pathway. In figure 35A it is shown that after 1 Gy of IR there is almost no formation of CEs, but it starts after an exposure of a dose of 5 Gy (fig. 35B).

In figure 35B it is clearly shown that only in the HRR deficient cell line there is a strong increase in the frequency of CEs after exposure to 5 Gy. CEs were also increased in wild type cells after 5Gy of IR but much less than in Irs1tor cells. The inhibition of PARP-1 clearly resulted in decreased CEs in HRR deficient cells. These results show that in HRR deficient cells B-NHEJ is active when the cells are exposed to 5 Gy, which means that B-NHEJ backups HRR to the similar extent as for D-NHEJ.

3.5.3 CE formation in different species

We could show that in G2-PCCs of wild type and HRR deficient cells the formation of CEs is decreased when B-NHEJ is inhibited through PJ34. This shows an interaction between HRR and B-NHEJ in chromosomal break repair. Now we wished to investigate the impact of PJ34 on the formation of CEs in different D-NHEJ mutants and also on conditional LIG3 DT40 mutants aiming to find potential interactions and mutual regulation between B-NHEJ and D-NHEJ.

3.5.3.1 Effect of PARP-1 inhibition on the formation of CEs in D-NHEJ deficient Mouse embryonic fibroblasts (MEFs)

To investigate the effect of PARP-1 inhibition in MEFs, 4 different cell lines PK34N (wild type), PK33N (*DNA-PKcs*$^{-/-}$), *Ku80*$^{-/-}$ and double mutant PK80-193A (*DNA-PKcs*$^{-/-}$/ *Ku80*$^{-/-}$) were chosen.

The experiments with these cells were done with and without PARP inhibitor (PJ34) introduced 1 h before irradiation. The cells were irradiated with 1 Gy and allowed to repair for up to 5 h (examples of CEs are shown in appendix 4 in chapter 7).

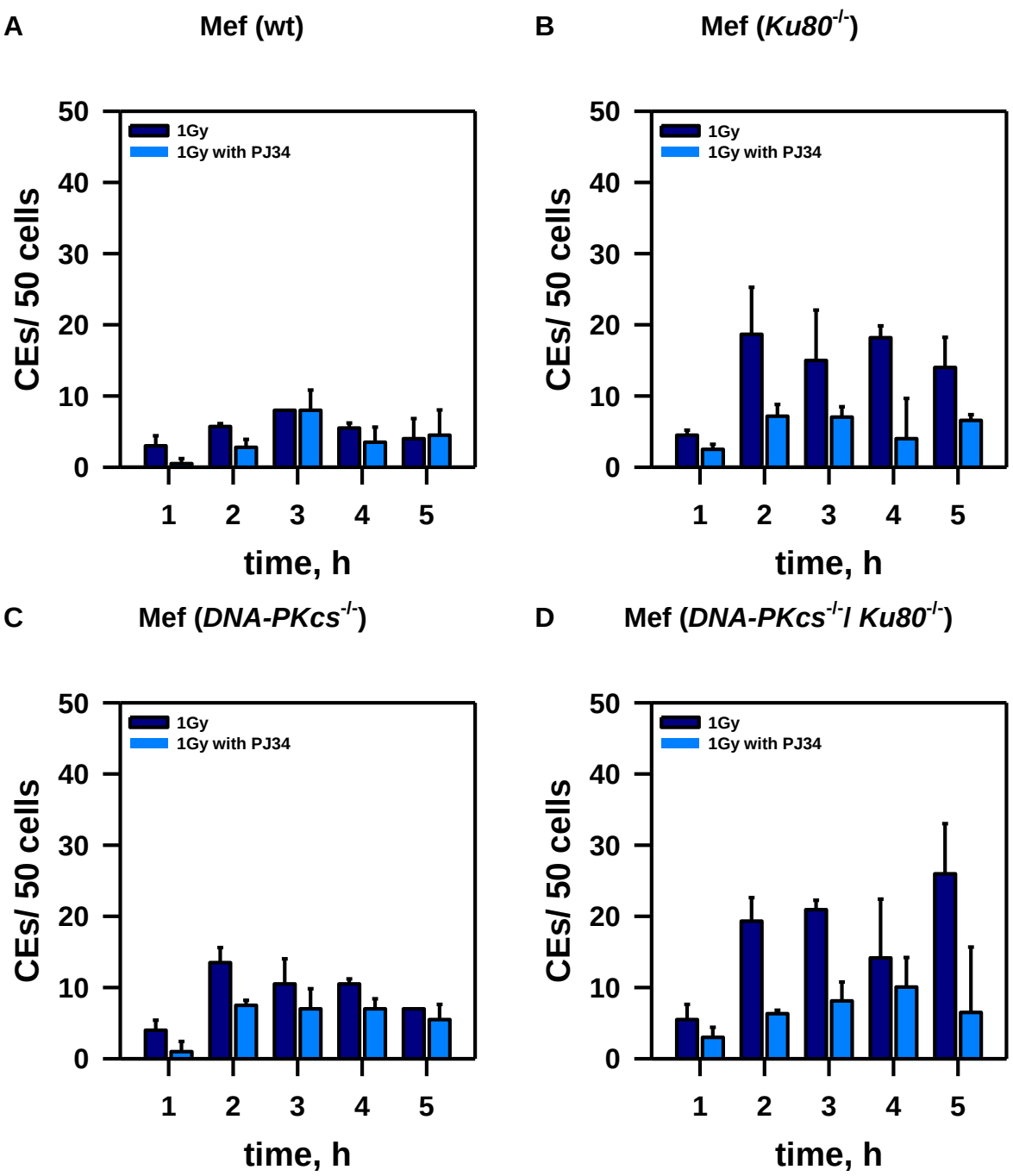

Figure 36: Effect of PARP-1 inhibition on the formation of CEs in exponentially growing MEFs irradiated with 1 Gy X-rays. Cells were treated with or without the indicated concentration of PJ34 1 h before irradiation and allowed to repair up to 5 h. PJ34 was maintained in the culture medium during the entire experiment. (A) Effect of 5 µM PJ34 on CEs formation in wild type, (B) in *Ku80*$^{-/-}$, (C) in *DNA-PKcs*$^{-/-}$ and (D) double knock out (*DNA-PKcs*$^{-/-}$/ *Ku80*$^{-/-}$) cells.

In MEF cell lines tested, PARP-1 inhibition resulted in reduced CEs. The extent of the decrease in wild type cells (fig. 36A) is smaller than in deficient in D-NHEJ, (figure 36B, C and D). One reason for this could be that wild type cells have functional D-NHEJ, which suppresses the formation of CEs, because of the high

speed and local changes in chromatin structure that facilitate joining of the correct ends (Wang et al., 2003).
Comparison of all 3 D-NHEJ deficient cell lines shows that the frequency of CEs formation after inhibition of B-NHEJ is strongly decreased. But despite inhibition of B-NHEJ there are still some CEs formed in all cases (in a range of 7 - 9 in 50 cells), these formations must be due to a different pathway like HRR.
This observation suggests the involvement of PARP-1 in CEs formation in G2 cells, in agreement with earlier findings on IR induced DSBs, here it was shown that PARP inhibitors reduce the frequency of translocations in G1 cells (Wray et al., 2013).

Another interesting observation is that the *Ku80*$^{-/-}$ cells (fig. 36B) show relatively more CEs than cells, which have a knock out in *DNA-PKcs* (fig. 36C). This is due to the more efficient binding of PARP-1 to DNA ends in the absence of Ku, which is a key determinant of pathway selection. When Ku80 is absent, PARP-1 can bind DNA ends more efficiently and this may result in increased CEs, as shown earlier (Wang et al., 2006). Double knock out cells displayed high frequency of CEs when compared to single mutants.

3.5.3.2 Effect of PARP-1 inhibition on the formation of CEs in D-NHEJ deficient Human colorectal tumor cells

We did further experiments with Human colorectal carcinoma (HCT116) cells to investigate CE formation after inhibition of B-NHEJ. A wild type, a *DNA-PKcs*$^{-/-}$ and a *Lig4*$^{-/-}$ cell lines were used in this set of experiments. The experiments were performed with or without PARP inhibitor (PJ34) in combination with IR. The cells were treated 1 h before exposure to IR, with a concentration of 5 µM. Then the cells were irradiated with 1 Gy and allowed to repair for up to 5 h (examples of CEs are shown in appendix 4 in chapter 7).

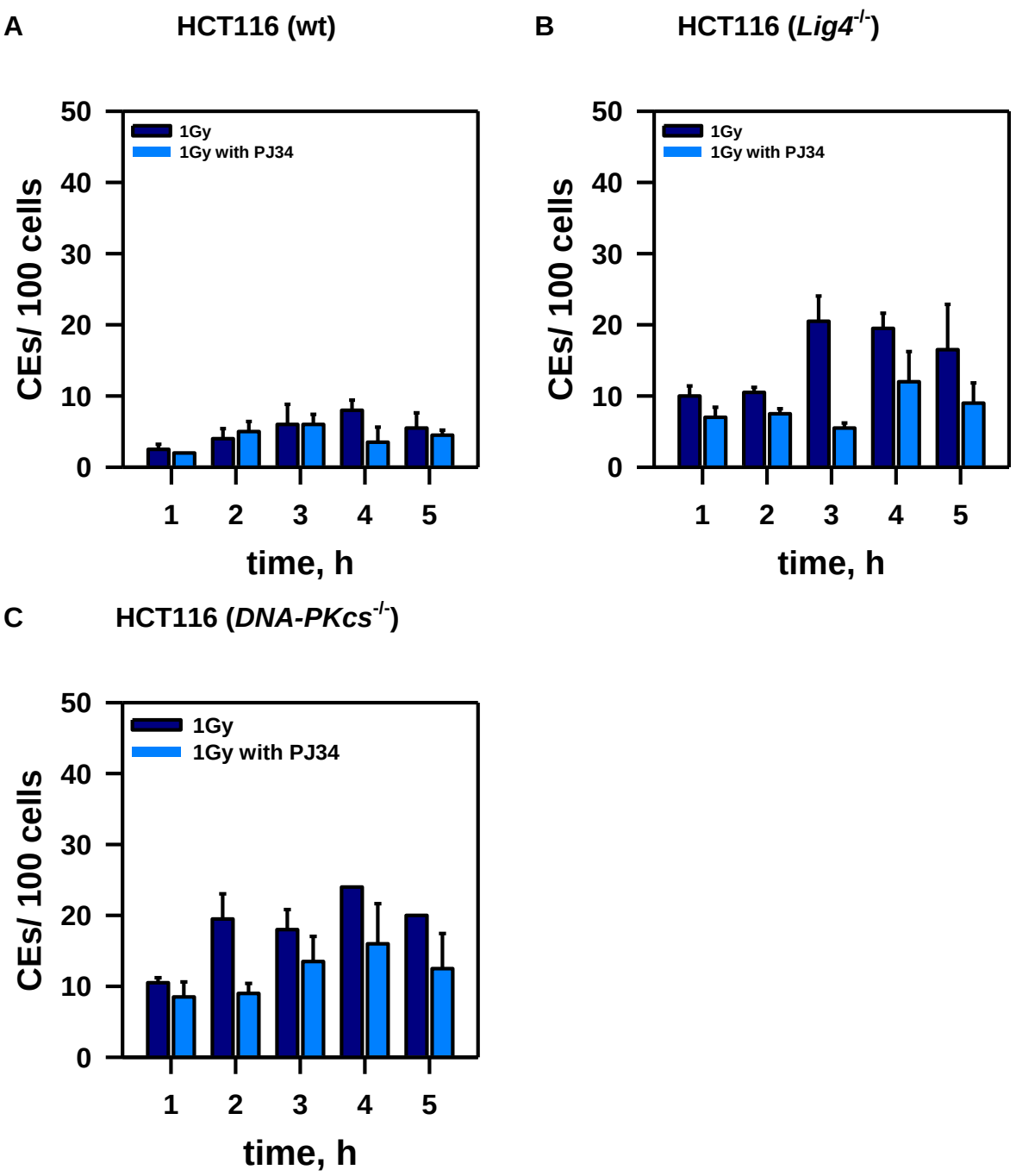

Figure 37: Effect of PARP-1 inhibition on the formation of CEs in exponentially growing Human colorectal tumor cells irradiated with 1 Gy X-rays. One set of cells is untreated and the other set was treated with the indicated concentration of PJ34 for 1 h before irradiation and allowed to repair for up to 5 h. PJ34 was maintained in the culture medium during the entire experiment. (A) Effect of 5 µM PJ34 on CEs formation in wild type, (B) in *Lig4*$^{-/-}$ and (C) in *DNA-PKcs*$^{-/-}$ cells.

Figure 37 shows that PARP-1 inhibition resulted in the same decrease in CE formation in HCT116 mutants as in MEFs (fig. 36). Additionally both D-NHEJ deficient cell lines (fig. 37B, C) display an increase in CEs formation, because the fast repair pathway is not active (Wang et al., 2003).

3.5.3.3 Effect of PARP-1 inhibition on the formation of CEs in DT40 (chicken) cells

We carried out additional experiments using DT40 cells, which are Chicken B-lymphocytes that have a 1000-fold up regulation in HR (Wang et al., 2001). Despite this the wild type cells do not show a difference in DNA DSB repair kinetics and when there is a defect in D-NHEJ on top of a HRR deficiency, the cells do not show an extra defect in DSB repair (Perrault et al., 2004). This shows that there is active B-NHEJ pathway. Because of the B-NHEJ activity we considered interesting to do some experiments in CEs formation using this cell system. For these investigations we chose a wild type and a D-NHEJ deficient cell line, which has a knock out in *Lig4*. The experiments were done with or without PARP inhibitor in combination with IR. Cells were allowed to repair for 5 h post IR.

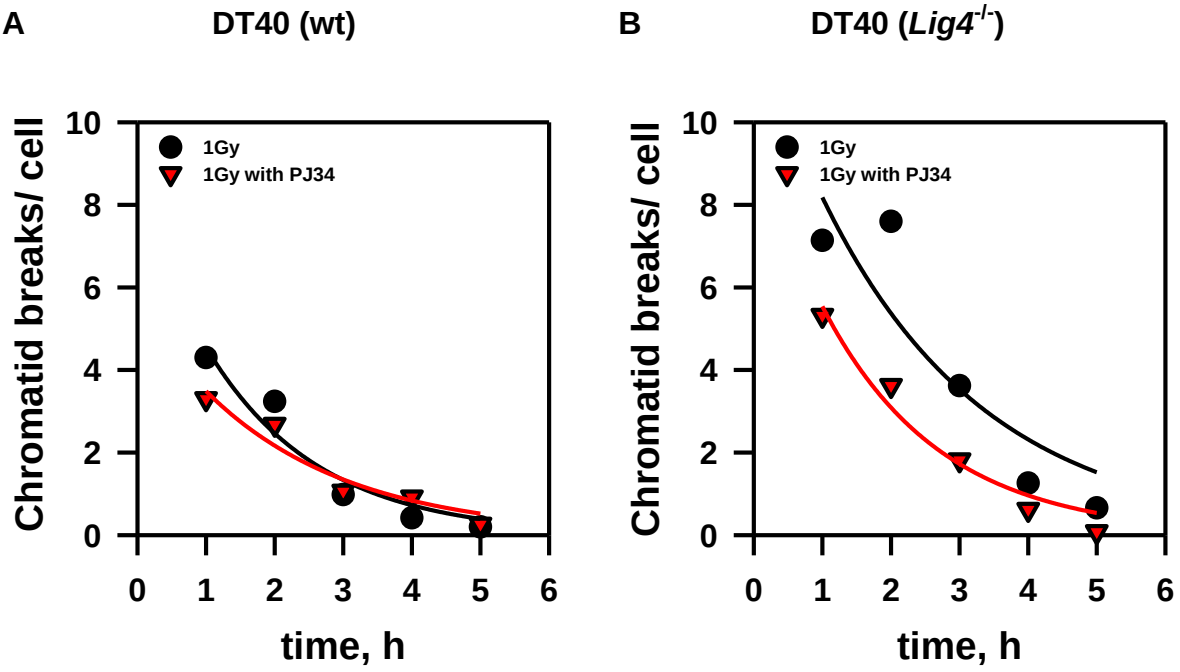

Figure 38: Effect of PARP-1 inhibition on the formation of chromatid breaks in exponentially growing Chicken B-lymphocytes irradiated with 1 Gy X-rays. One set of cells is untreated and the other set was treated with the indicated concentration of PJ34 for 1 h before irradiation and allowed to repair up to 5 h. PJ34 was maintained in the culture medium during the entire experiment. (A) Effect of 5 µM PJ34 on chromatid breaks kinetics in wild type and (B) in *Lig4*$^{-/-}$ cells.

In DT40 cells no CEs were observed in the large chromosomes. So it was not possible to analyze the CEs in this set of cell lines.

But in figure 38 it is shown that the PARP inhibitor has no effect on the repair of chromatid breaks. In wild type cells the damage induction is the same in both experiments, with or without PJ34 (fig 38A). In *Lig4*$^{-/-}$ cells the initial damage is higher, when the cells are treated with PJ34 but the kinetics is the same compared to untreated cells (fig. 38B). These experiments show that treatment of wild type and D-NHEJ deficient cells with PJ34 do not have an effect on the repair kinetics in these cells.

3.5.4 Multi-color FISH (M-FISH)

In all experiments where we investigated the CEs formation metaphases were stained conventionally using Giemsa staining. With this approach only asymmetric exchanges are possible to analyze, but to get a more complete picture of the CEs including symmetrical CEs, we introduced Fluorescence in situ hybridization (FISH) that facilitates scoring symmetric exchanges.

We standardized this method in Human colorectal carcinoma (HCT116) cells and analyzed it using the Metasystems analysis software.

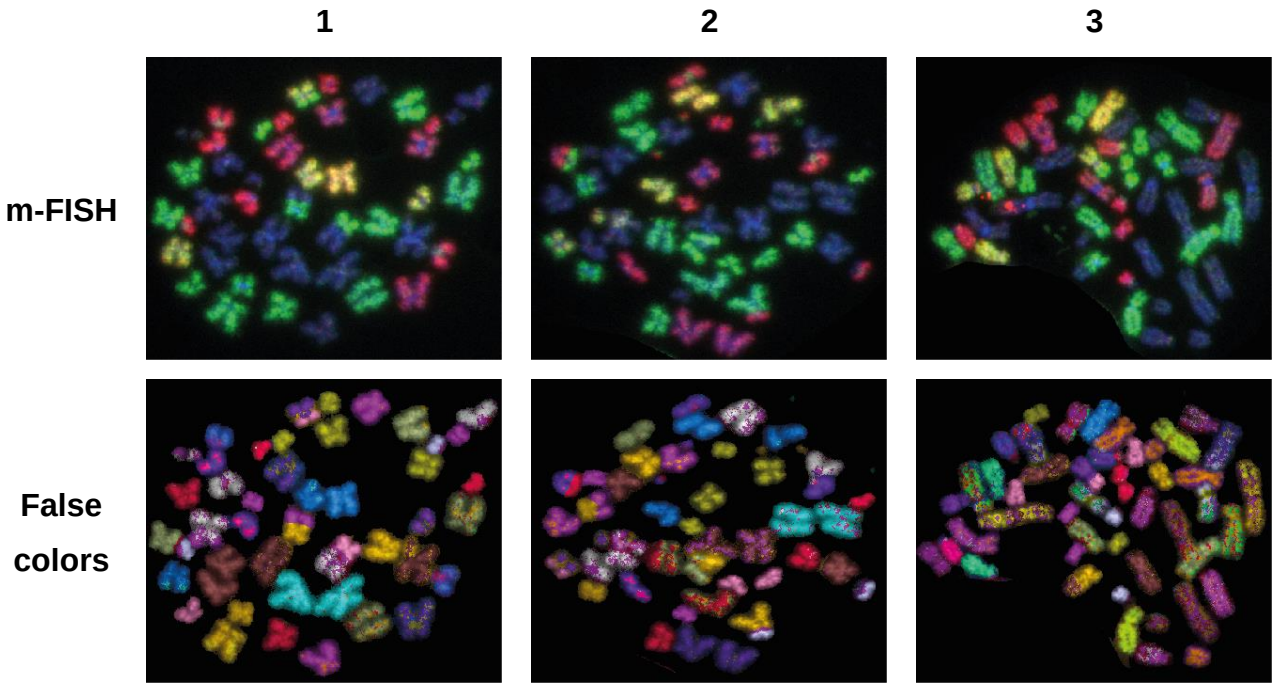

Figure 39: Multi-color Fluorescence in situ hybridization (FISH) pictures in exponentially growing Human colorectal carcinoma cells irradiated with 2 Gy X-rays. The upper row shows picture of m-FISH and in the lower the modified picture, by Isis, which shows the chromosomes in false colors.

After the modification of the chromosome pictures in the program Isis, we have the pictures illustrated in false colors (fig. 39). For further experiments we used two-color FISH instead of M-FISH.

3.5.5 Two-color FISH

When only 2 chromosomes are stained it is relatively easy to achieve comparable staining for chromosome analysis. We chose the 2 biggest chromosomes for these experiments chromosome 1, which is stained in green and chromosome 2, which is stained in red.

For the experiments we used HCT116 cells irradiated with 2 Gy IR.

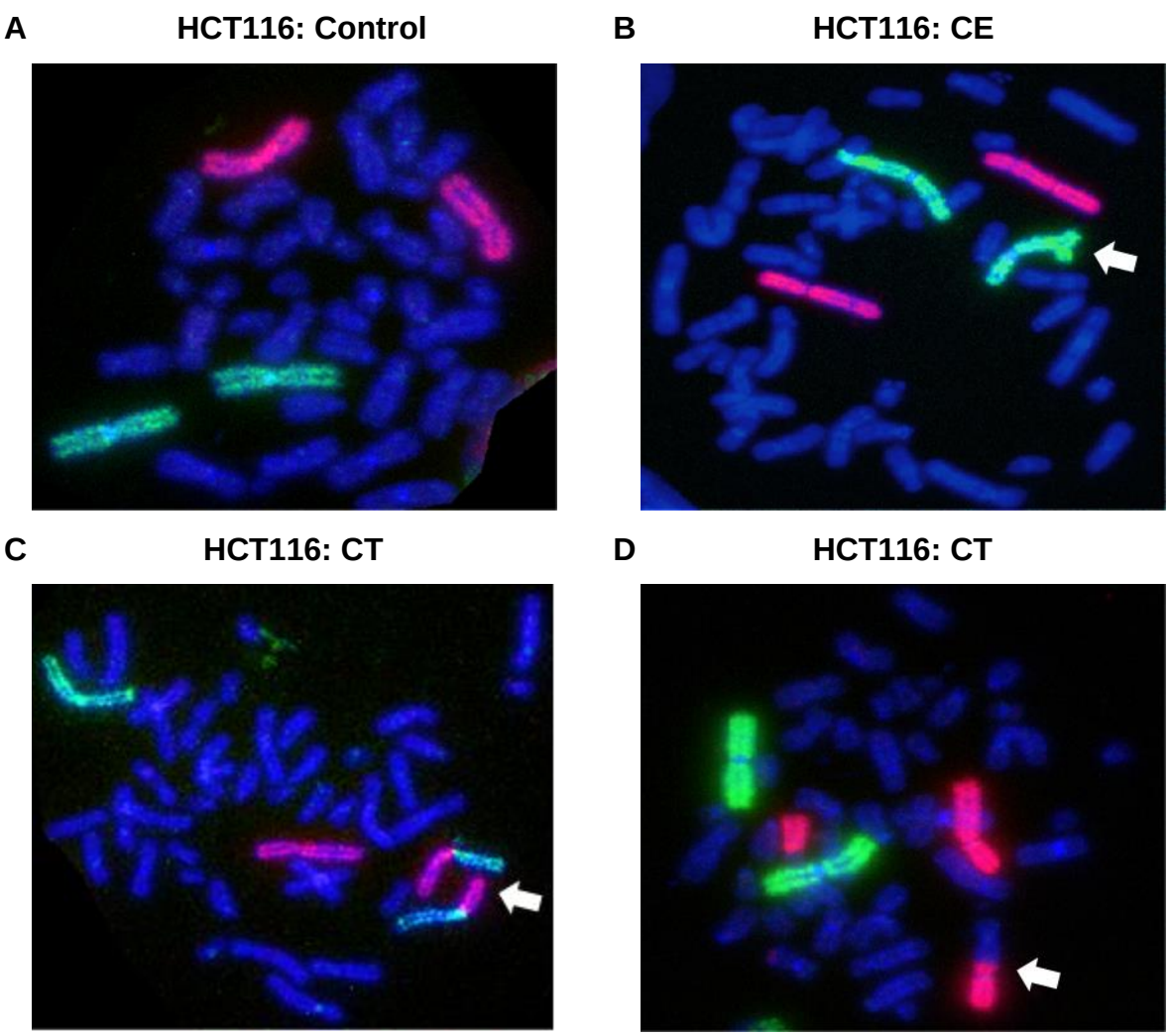

Figure 40: Two-color Fluorescence in situ hybridization (FISH) images of exponentially growing Human colorectal carcinoma cells irradiated with 2 Gy X-rays. Chromosome 1 is stained in green and chromosome 2 is stained in red. (A) Example of non-irradiated control cell, (B) example for an CE, (C) example for a CT between chromosome 1 and 2 and (D) example for CT of chromosome 2 with a DAPI stained chromosome (more CTs and CEs are shown in appendix 5 in chapter 7).

In figure 40 we see images generated using two-color FISH. These pictures illustrate CTs, which may not be seen in Giemsa stained chromosomes. Another advantage is that with Isis it is possible to invert these pictures to grey-scale, so it is possible to count all kinds of CEs in same image, to get a whole picture of the chromosomal aberrations.

3.5.5.1 Effect of B-NHEJ inhibition in translocation formation in HCT116 cells

As translocations can be scored successfully using two-color FISH we wished to investigate the effect of PARP inhibition on the frequency of such translocations. For this study HCT116 wt and *Lig4*$^{-/-}$ cells were employed. To see the effect of PARP inhibition one set of cells was treated 1 h before irradiation with PJ34 before 2 Gy IR.

In all previously shown results the cells were collected from 1 to 5 h after irradiation to cover mostly G2 cells. In this set of experiments the time window was extended to cover also other phases of the cell cycle i.e. G1- and S-phase. Aiming to score cells in G2-phase 3 to 5 h, for S-phase 12 to 14 h and for G1 cells 28 to 30 h post IR time points were chosen.

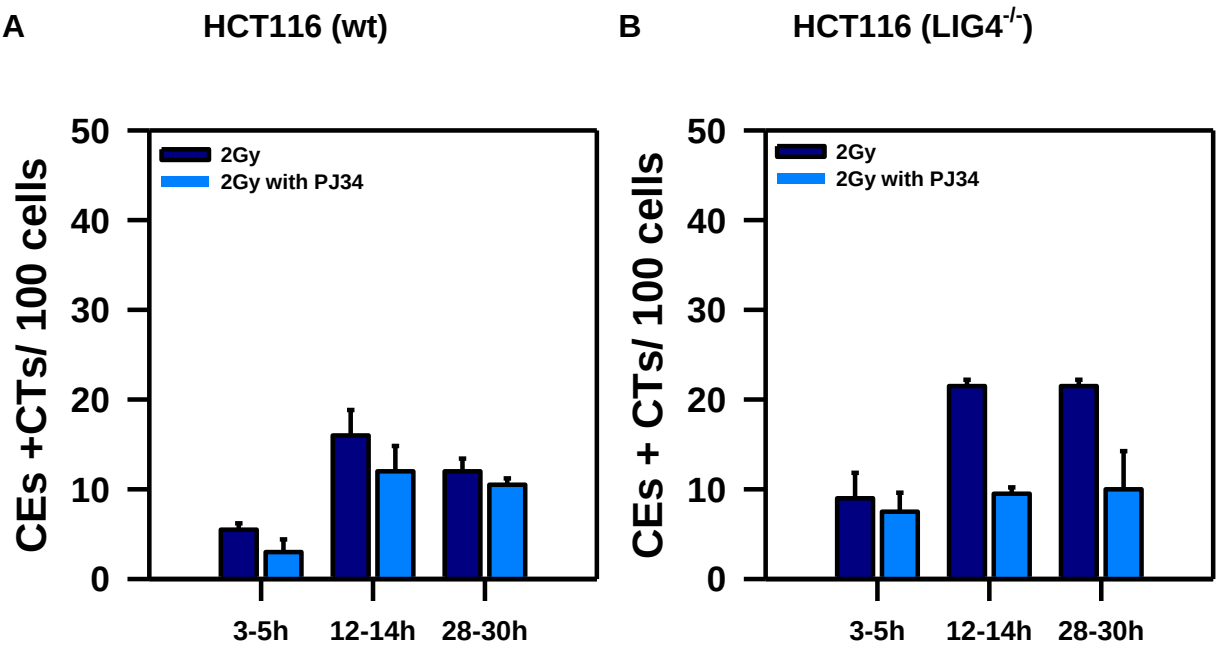

Figure 41: Effect of B-NHEJ inhibitor PJ34 on the formation of CEs in exponentially growing Human colorectal carcinoma cells irradiated with 2 Gy X-rays. One set of cells is untreated and the other set was treated with the indicated concentration of PJ34 for 1 h before irradiation and allowed to repair for 3 to 5, 12 to 14 and 28 to 30 h. PJ34 was maintained in the culture medium during the entire experiment. (A) Effect of 5 µM PJ34 on CE and CT formation in wild type and (B) in *Lig4*$^{-/-}$ cells.

The highest frequency of CEs and CTs in wild type cells is in the S- and G1-phase, with 16 and 12 CEs per 100 cells, respectively. No color switches could be observed during 3 to 5 h only CEs were scored (fig 41A). The *Lig4*$^{-/-}$ cells showed relatively higher numbers of CTs plus CEs, about 21 per 100 cells in S- and G1-cells (fig 41B). Since B-NHEJ is active in G1-phase to back up D-NHEJ there is an equal number of CEs and CTs compared to S-phase.

Here we could show again that PARP-1 inhibition resulted in a decrease of CEs plus CTs in both cells lines over the cell cycle, although the effect is more robust in D-NHEJ deficient cells.

4 Discussion

4.1 Is there a dose dependent switch of repair pathway choice?

For the repair of IR induced DNA DSBs the cell has the possibility to choose between several pathways (Kennedy and D'Andrea, 2006). Here we focus on the three main DSB repair pathways in higher eukaryotes HRR, D-NHEJ and B-NHEJ (Nussenzweig and Nussenzweig, 2007).

These three repair pathways have different characteristics; D-NHEJ is simply joining the broken DNA ends, and because of this it is a very fast repair process, which works during the entire cell cycle. This can cause sequence alterations or in some cases translocations therefore it is considered as an error-prone repair pathway (Burma et al., 2006; Mladenov and Iliakis, 2011).

The other main repair pathway is HRR that works with slower repair kinetics than D-NHEJ. HRR is using an undamaged homologous template to faithfully repair the DSB; therefore it is considered as an error-free repair pathway. Since it needs a template for the repair and because there is strong preference for the use of the sister chromatid, it is only active through late S- and G2-phase of the cell cycle (Mladenov and Iliakis, 2011; Schipler and Iliakis, 2013).

The backup pathway, B-NHEJ, is also active throughout the cell cycle. In this case the DNA ends are again simply ligated, but with slower speed compared to D-NHEJ. This is the reason why this repair pathway has the highest probability to from translocations, as well as large deletions and sequence alterations at the junctions (Dueva and Iliakis, 2013; Nussenzweig and Nussenzweig, 2010).

Since the above mentioned three DSB repair pathways have different abilities to faithfully restore the genome, there has to be a mechanism through which the cell makes the decision, which repair pathway to choose for the repair of each individual DSB (Mladenov and Iliakis, 2011). However, it is still unknown how the cell makes this choice of pathways, even though many details on mechanism and also information about proteins involved are available (You and Bailis, 2010; Yun and Hiom, 2009; Zhang et al., 2009). There is a model for a possible competition between HRR and D-NHEJ, assuming that the pathway choice is not made by the

cell itself (Roth and Wilson, 1985). But in our lab earlier findings revealed a dependency of the repair pathways on radiation dose, since PFGE results demonstrate that HRR plays a minor role in the repair of DNA DSBs at 20 Gy. However other experiments revealed that HRR deficient cells are unable to repair G2-chromosomal breaks at low doses (0.5 – 2 Gy) and have RAD51 foci formation that saturates after exposure to higher doses. So we assumed that there is a dependency of repair pathway choice on dose.

4.2 D-NHEJ is extremely important for the repair of DSBs after exposure to high radiation doses

There is a clear repair defect in cells deficient in D-NHEJ and DSBs are repaired with slower kinetics (Wu et al., 2008b). This repair can be assigned to the backup pathway, B-NHEJ (DiBiase et al., 2000; Mladenov and Iliakis, 2011; Wu et al., 2008a). The results presented here show that D-NHEJ is a very efficient DSB repair pathway even after exposure to radiation doses as high as 80 Gy. When D-NHEJ is deficient the kinetics of DSB repair are slower, and this effect becomes stronger as the radiation dose increases. The latter effect suggests that B-NHEJ is not able to handle the increased load of DSBs as good as D-NHEJ. This may be due to the slow speed of DSB repair, which shows that the cell needs an active D-NHEJ pathway to handle the bulk of DSBs, particularly after exposure to extremly high doses of IR, e.g. 80 Gy.

4.2.1 B-NHEJ and/or D-NHEJ are able to repair G2-PCC breaks in HRR deficient G2 cells at higher doses

The fact that after high radiation doses (20 Gy) we do not see an effect on DSB repair in HRR deficient cells (DiBiase et al., 2000; Mladenov and Iliakis, 2011; Wu et al., 2008b); the fact that we see a very strong impairment on the repair of G2-chromosomal breaks at low doses (0.5 - 2 Gy) (Soni, 2010); and the fact that Rad51 foci formation saturates after exposure to radiation doses above 4 Gy (unpublished data), lead us to formulate the hypothesis that at different radiation doses different pathways may be activated and recruited for the repair of DSBs. All these observations, and the inherent contradictions they uncover, could somehow be related to the size of the radiation doses employed in each experimental end point.

First, PFGE experiments typically use high radiation doses (20 Gy), show that HRR plays a minor role in the repair of DNA DSBs. However, experiments carried out at low radiation doses (below 10 Gy), such as cell survival, repair of chromosome breaks and Rad51 foci formation show that HRR has a central role in DSB and chromosome break repair, as well as in cell survival. These results suggest that few DSBs, which are the precursors of chromosome breaks, are specifically processed by HRR. Indeed, unpublished results from our laboratory demonstrate that when doses well below 2 Gy are used, nearly 60% of DSBs are handled by HRR (unpublished data).

4.2.1.1 PFGE results hint to a contribution of slower repair pathways in the repair of DSBs after 5Gy of IR

The results obtained with PFGE when cells were exposed to 5 Gy provide hints that the repair kinetics in wild type cells is slower at low than at high radiation doses – possibly a hint for a switch to HRR. We could not detect this transition in the repair kinetics in HRR deficient cells, which may indicate that intact HRR is required for this transition. In order to investigate, which pathway is active in wild type cells after exposure to 5 Gy IR, different inhibitors of HRR and B-NHEJ were used. It was not possible to achieve a clear result with PFGE, when experiments were performed at radiation doses lower than 10 Gy. As a result these experiments interpreted conclusively. However, the results obtained hint to a contribution of a slower DSB repair pathway i.e. HRR or B-NHEJ at 5 Gy of IR in wt cells.

4.2.1.2 G2-PCC results suggest a switch from HRR to D-NHEJ and possibly to B-NHEJ at 5 Gy

The second method we used for the analyses of the present work was premature chromosome condensation during the G2-phase of the cell cycle. Here we raised the dose of IR to 5 Gy, to achieve an overlap with the lowest dose we use in PFGE. Since HRR deficient cells are radiosensitive in late S-phase, we used aphidicolin to prevent cells irradiated during the S-phase from entering G2-phase, which may mask G2-specific effects (Iliakis et al., 1982; Tamulevicius et al., 2007). These investigations revealed that the wild type cells repair the majority of breaks with fast kinetics and after 8 h repair the majority of chromosome damage is repaired. In

XRCC2 mutant cells, almost no repair takes place after exposure to low radiation doses (e.g. 1 Gy), an observation, which is in agreement with results obtained earlier (Soni, 2010). Surprisingly, in HRR deficient cells repair of almost all G2-PCC breaks, could be detected after exposure to 5 Gy; in fact, the repair kinetics obtained under these conditions is comparable to that measured in wild type cells. This may be evidence for a switch from HRR to some form of end-joining. Indeed, we could show that D-NHEJ does not play a role in the repair of chromatid breaks at low radiation doses (Soni, 2010), but now becomes likely that at higher radiation doses D-NHEJ contributes to the repair of G2-PCC breaks. After 5 Gy the initial damage is 4-fold to that obtained after 1 Gy. This leads to the assumption that with higher initial number of chromosome breaks, B-NHEJ and/or D-NHEJ engage in the repair of the G2-PCC breaks. Further evidence for this possibility is that after inhibition of both NHEJ pathways, overall chromosome break repair is strongly inhibited in cells exposed to 5Gy.

A hint for the increased involvement of B-NHEJ in the repair of G2-PCC breaks after higher doses of IR is also the formation of chromosomal exchanges (CEs). Indeed, CEs formation is increased almost 15-fold compared to cells irradiated with 1 Gy. B-NHEJ is directly implicated in the formation of CEs (Nussenzweig and Nussenzweig, 2010). To find out if the high frequency of CEs is due to B-NHEJ, PARP-1 was inhibited using small molecule inhibitors. This inhibition caused a strong reduction in the frequency of CEs. This may suggest that B-NHEJ is the DSB repair pathway, which is repairing chromosome damage in HRR deficient cells exposed to 5 Gy IR – i.e. B-NHEJ is acting as backup to HRR.

All above results show that there is a dose dependent switch among DSB repair pathways. This appears particularly evident from HRR at low doses to D-NHEJ and/or B-NHEJ as the dose of radiation increases. Furthermore, the results reveal that B-NHEJ is not only the backup for D-NHEJ, but it can also back up HRR in G2-PCC break repair. Why this only occurs at high but not at low doses of radiation needs further investigation.

A possible scenario for DSB repair pathway choice could be that after irradiation with low doses, HRR is mainly responsible for the repair of DSBs; after exposure to higher radiation doses i.e. 5 Gy or above, D-NHEJ is the major pathway for the

repair. When a cell is deficient in D-NHEJ, B-NHEJ is able to back up D-NHEJ, even without the need of end resection (Dueva and Iliakis, 2013). But after resection of the DNA ends and a failure of HRR, B-NHEJ will also backup HRR. It is indeed known that the initial end resection of a DSB can either be used by HRR or B-NHEJ. When HRR and D-NHEJ are active B-NHEJ is repairing only a small proportion of DSBs (Truong et al., 2013).

4.3 Contribution of PARP-1 to the formation of CTs in G2 cells

Here we show that B-NHEJ contributes to the repair of chromosomal breaks in HRR deficient cells after irradiation with 5 Gy. As already mentioned above it is now highly likely that the alternative pathway B-NHEJ is responsible for the formation of the majority of CEs and CTs (Iliakis et al., 2007), which are the hallmark of cancer (Alt et al., 2013; Bunting and Nussenzweig, 2013; Roukos et al., 2013). It has previously been shown that B-NHEJ is involved in the formation of translocations of site-directed DSBs (Simsek et al., 2011; Zhang and Jasin, 2011), but till now it has not been reported how B-NHEJ contributes to the formation of IR induced translocations in G2 cells.

The main components shown to be involved in the backup pathway are PARP-1, LIG3 and XRCC1. It has been stated that also LIG1 is able to support B-NHEJ (Arakawa et al., 2012). Recently it has been revealed that PARP-1 plays an important role in IR induced translocations in irradiated G1 cells (Wray et al., 2013), but its role in G2 needs still to be elucidated.

Starting from this background, the second goal of this thesis was to investigate the impact of PARP-1 inhibitors to the formation of CTs in G2 cells. These experiments were carried out in different D-NHEJ mutant cell lines from different species.

4.3.1 Lower frequency of CEs formation after PARP-1 inhibition hints to B-NHEJ as a backup of HRR

First of all it is noticeable that mouse, as well as human wild type cells, have a low rate of CEs formation. This might be due to the presence of highly active D-NHEJ (Wang et al., 2006). However we found a much higher frequency of CEs in G2-PCC in HRR deficient cells (Irs1tor) as compared to CEs in metaphases in wild type and D-NHEJ deficient cells. The same pattern could be reproduced in all species

investigated. Therefore it seems that in G2-phase of the cell cycle B-NHEJ is more the backup of HRR than of D-NHEJ. This finding fits to the fact that components of HRR i.e. NBS1 (Deriano et al., 2009), MRE11 (Rass et al., 2009; Xie et al., 2009) and CTIP (Zhang and Jasin, 2011) are involved in repair of B-NHEJ. It seems that B-NHEJ also works when HRR and D-NHEJ are active, since there are CEs formed in wild type cells, albeit at low numbers.

It has been suggested that B-NHEJ is microhomology dependent, which may derive from the fact that it backs up HRR in such a strong way, and as a result it could benefit from the DNA end resection occurring in early stages of HRR (McVey and Lee, 2008). However the error-prone nature of B-NHEJ results in CE formation with high probability in G2-phase cells (Iliakis et al., 2004). In cells where D-NHEJ is active the formation of chromosomal aberrations and translocations is reduced, which suggests that components of D-NHEJ are able to inhibit CEs formation (Difilippantonio et al., 2000; Ferguson et al., 2000; Weinstock et al., 2007). It has been suggested that Ku is the factor, which regulates pathway choice between B-NHEJ and D-NHEJ (Fattah et al., 2010). Furthermore it was shown, that Ku and PARP-1 compete for DNA ends (Wang et al., 2006).

In this thesis we used D-NHEJ deficient cells, which have a defect in *DNA-PKcs*, *Ku80* or a double mutant *Ku80/ DNA-PKcs*. If we compare the frequency of CE formation, it is noticeable that the cells, which have a knock out in *Ku80* show a higher frequency of CEs compared to cells with a knockout of *DNA-PKcs*. This is another evidence for a competition between Ku and PARP-1. When Ku is absent PARP-1 has a much higher chance for binding to DNA ends (Wang et al., 2006). In the double knock out we see an additive effect in CE formation.

4.3.2 PARP-1 is important for the formation of IR induced CEs and CTs in G2-phase cells at low doses

After inhibition of PARP-1 with PJ34 we see that CEs are reduced by at least 50%. This shows that PARP-1 plays not only an important role in the formation of IR induced translocations in cells irradiated in G1 (Wray et al., 2013), but also in the formation of CEs in G2 cells.

In addition, we wished to test if PARP-1 contributes to the CEs, as well as to CTs formation throughout the cell cycle, and particularly in G1-phase. For this purpose a human cell line was used, because human cells have a much longer G1-phase compared to mouse and Chinese hamster cells. Here we used two-chromosome FISH to analyze CTs involving chromosomes 1 and 2. The junctions could be either between these two chromosomes or between them and DAPI-stained chromosomes. We could also simultaneously score CEs.
After treatment with PJ34 the frequency of CEs plus CTs are only slightly decreased but compared to the cells, which are deficient in *Lig4*, we see much stronger inhibition in their formation.

Here we could show again that PARP-1 is involved in the formation of CEs as well as CTs in G1-phase of the cell cycle, but additionally we could show its involvement in G2-phase, in HRR and D-NHEJ deficient cells. This is important, because highly specific PARP inhibitors are getting more and more intensively considered in the treatment of cancer.

5 Conclusions

In this thesis we could demonstrate that the choice of DSB repair pathways is at least partly determined by the radiation dose applied. The inhibited repair of chromatid breaks in HRR deficient cells after exposure to low doses of IR (0.5 - 2 Gy) recovered after irradiation with higher doses (5 Gy). After 5 Gy IR, HRR deficient cells were able to repair chromatid breaks with kinetics comparable to that of wild type cells. These results suggest that at low doses of IR, HRR is the dominant DSB repair pathway.

Another DSB repair pathway that is also gaining importance in pathway choice is the backup pathway B-NHEJ. We show results suggesting that B-NHEJ can backup repair of G2-PCC breaks in HRR deficient G2 cells at higher doses (5 Gy and above, at least). Another hint that B-NHEJ is involved in DSB repair is that at higher doses the formation of CEs is increased almost 15-fold (30 CEs in 50 cells), as compared to that measured after exposure to 1 Gy (2 CEs in 50 cells).

The experiments with D-NHEJ deficient Mouse embryonic fibroblasts and Human colorectal tumor cells show that the frequency of CEs formation is much higher in cells, which are deficient in HRR compared to wild type and D-NHEJ deficient cells. This also shows that in G2-phase cells exposed to high doses, B-NHEJ is able to back up HRR as efficiently as D-NHEJ.

Finally, we show that PARP-1 plays an important role in the formation of CEs and CTs in G2-phase at clinically relevant doses i.e. 1 or 2 Gy.

6 Bibliography

Ackland, S.P., Schilsky, R.L., Beckett, M.A., and Weichselbaum, R.R. (1988). Synergistic cytoxicity and DNA strand break formation by bromodeoxyuridine and bleomycin in human tumor cells. Cancer Res *48*, 4244-4249.

Alt, Frederick W., Zhang, Y., Meng, F.-L., Guo, C., and Schwer, B. (2013). Mechanisms of Programmed DNA Lesions and Genomic Instability in the Immune System. Cell *152*, 417-429.

Arakawa, H., Bednar, T., Wang, M., Paul, K., Mladenov, E., Bencsik-Theilen, A.A., and Iliakis, G. (2012). Functional redundancy between DNA ligases I and III in DNA replication in vertebrate cells. Nucleic acids research *40*, 2599-2610.

Arnaudeau, C., Lundin, C., and Helleday, T. (2001). DNA double-strand breaks associated with replication forks are predominantly repaired by homologous recombination involving an exchange mechanism in mammalian cells. J Mol Biol *307*, 1235-1245.

Audebert, M., Salles, B., and Calsou, P. (2004). Involvement of Poly(ADP-ribose) Polymerase-1 and XRCC1/DNA Ligase III in an Alternative Route for DNA Double-strand Breaks Rejoining. J Biol Chem *279*, 55117-55126.

Aylon, Y., Liefshitz, B., and Kupiec, M. (2004). The CDK regulates repair of double-strand breaks by homologous recombination during the cell cycle. EMBO J *23*, 4868-4875.

Bailey, S.M., and Bedford, J.S. (2006). Studies on chromosome aberration induction: What can they tell us about DNA repair? DNA Repair *5*, 1171-1181.

Bartek, J., and Lukas, J. (2007). DNA damage checkpoints: from initiation to recovery or adaptation. Curr Opin Cell Biol *19*, 238-245.

Bender, M.A., Griggs, H.G., and Bedford, J.S. (1974). Mechanisms of chromosomal aberration production. III. Chemicals and ionizing radiation. Mutat Res *23*, 197-212.

Boboila, C., Jankovic, M., Yan, C.T., Wang, J.H., Wesemann, D.R., Zhang, T., Fazeli, A., Feldman, L., Nussenzweig, A., Nussenzweig, M.*, et al.* (2010a). Alternative end-joining catalyzes robust IgH locus deletions and translocations in the combined absence of ligase 4 and Ku70. Proc Natl Acad Sci USA *107*, 3034-3039.

Boboila, C., Yan, C., Wesemann, D.R., Jankovic, M., Wang, J.H., Manis, J., Nussenzweig, A., Nussenzweig, M., and Alt, F.W. (2010b). Alternative end-joining catalyzes class switch recombination in the absence of both Ku70 and DNA ligase 4. J Exp Med *207*, 417-427.

Bohgaki, T., Bohgaki, M., and Hakem, R. (2010). DNA double-strand break signaling and human disorders. Genome Integrity *1*, 15.

Bryant, P.E. (1984). Enzymatic restriction of mammalian cell DNA using Pvu II and Bam H1: evidence for the double-strand break origin of chromosomal aberrations. Int J Radiat Biol *46*, 57-65.

Bryant, P.E., Mozdarani, H., and Marr, C. (2008). G2-phase chromatid break kinetics in irradiated DNA repair mutant hamster cell lines using calyculin-induced PCC and colcemid-block. Mutat Res *657*, 8-12.

Bunting, S.F., and Nussenzweig, A. (2013). End-joining, translocations and cancer. Nat Rev Cancer *13*, 443-454.

Burma, S., Chen, B.P.C., and Chen, D.J. (2006). Role of non-homologous end joining (NHEJ) in maintaining genomic integrity. DNA Repair *5*, 1042-1048.

Caldecott, K.W. (2001). Mammalian DNA single-strand break repair: an X-ra(y)ted affair. BioEssays *23*, 447-455.

Chen, F., Nastasi, A., Shen, Z., Brenneman, M., Crissman, H., and Chen, D.J. (1997). Cell cycle-dependent protein expression of mammalian homologs of yeast DNA double-strand break repair genes *Rad51* and *Rad52*. Mutat Res *384*, 205-211.

Cheng, Q., Barboule, N., Frit, P., Gomez, D., Bombarde, O., Couderc, B., Ren, G.-S., Salles, B., and Calsou, P. (2011). Ku counteracts mobilization of PARP1 and MRN in chromatin damaged with DNA double-strand breaks. Nucleic acids research *39*, 9605-9619.

Cheong, N., Wang, X., Wang, Y., and Iliakis, G. (1994). Loss of S-phase dependent radioresistance in irs-1 cells exposed to x-rays. Mutat Res *314*, 77-85.

Ciccia, A., and Elledge, S.J. (2010). The DNA Damage Response: Making It Safe to Play with Knives. Mol Cell *40*, 179-204.

Conrad, M.F., Albadawi, H., Stone, D.H., Crawford, R.S., Entabi, F., and Watkins, M.T. (2006). Local Administration of the Poly ADP-Ribose Polymerase (PARP) Inhibitor, PJ34 During Hindlimb Ischemia Modulates Skeletal Muscle Reperfusion Injury. Journal of Surgical Research *135*, 233-237.

Convery, E., Shin, E.K., Ding, Q., Wang, W., Douglas, P., Davis, L.S., Nickoloff, J.A., Lees-Miller, S.P., and Meek, K. (2005). Inhibition of homologous recombination by variants of the catalytic subunit of the DNA-dependent protein kinase (DNA-PKcs). Proc Natl Acad Sci USA *102*, 1345-1350.

Della-Maria, J., Zhou, Y., Tsai, M.-S., Kuhnlein, J., Carney, J.P., Paull, T.T., and Tomkinson, A.E. (2011). Human Mre11/Human Rad50/Nbs1 and DNA Ligase IIIα/XRCC1 Protein Complexes Act Together in an Alternative Nonhomologous End Joining Pathway. J Biol Chem *286*, 33845-33853.

Denko, N., Giaccia, A., Peters, B., and Stamato, T.D. (1989). An asymmetric field inversion gel electrophoresis method for the separation of large DNA molecules. Analytical Biochemistry *178*, 172-176.

Deriano, L., Stracker, T.H., Baker, A., Petrini, J.H.J., and Roth, D.B. (2009). Roles for NBS1 in Alternative Nonhomologous End-Joining of V(D)J Recombination Intermediates. Mol Cell *34*, 13-25.

Dewey, W.C., Miller, H.H., and Leeper, D.B. (1971). Chromosomal aberrations and mortality of x-irradiated mammalian cells: Emphasis on repair. Proc Natl Acad Sci USA *68, No. 3*, 667-671.

DiBiase, S.J., Zeng, Z.-C., Chen, R., Hyslop, T., Curran, W.J., Jr., and Iliakis, G. (2000). DNA-dependent protein kinase stimulates an independently active, nonhomologous, end-joining apparatus. Cancer Res *60*, 1245-1253.

Difilippantonio, M.J., Zhu, J., Chen, H.T., Meffre, E., Nussenzweig, N.C., Max, E.E., Ried, T., and Nussenzweig, A. (2000). DNA repair protein Ku80 suppresses chromosomal aberrations and malignant transformation. Nature *404*, 510-514.

Drouet, J., Delteil, C., Lefrancois, J., Concannon, P., Salles, B., and Calsou, P. (2005). DNA-dependent Protein Kinase and XRCC4-DNA Ligase IV Mobilization in the Cell in Response to DNA Double Strand Breaks. J Biol Chem *280*, 7060-7069.

Dueva, R., and Iliakis, G. (2013). Alternative pathways of non-homologous end joining (NHEJ) in genomic instability and cancer. Transl Cancer Res *2*, 163-177.

Elmroth, K., Nygren, J., Martensson, S., Ismail, I.H., and Hammarsten, O. (2003). Cleavage of cellular DNA by calicheamicin γI. DNA Repair *2*, 363-374.

Essers, J., van Steeg, H., de Wit, J., Swagemakers, S.M., Vermeij, M., Hoeijmakers, J.H., and Kanaar, R. (2000). Homologous and non-homologous recombination differentially affect DNA damage repair in mice. EMBO J *19*, 1703-1710.

Fattah, F., Lee, E.H., Weisensel, N., Wang, Y., Lichter, N., and Hendrickson, E.A. (2010). Ku Regulates the Non-Homologous End Joining Pathway Choice of DNA Double-Strand Break Repair in Human Somatic Cells. PLoS Genet *6*, e1000855.

Ferguson, D.O., Sekiguchi, J.M., Chang, S., Frank, K.M., Gao, Y., DePinho, R.A., and Alt, F.W. (2000). The nonhomologous end-joining pathway of DNA repair is required for genomic stability and the suppression of translocations. Proc Natl Acad Sci USA *97*, 6630-6633.

Friedl, A.A., Kiechle, M., Fellerhoff, B., and Eckardt-Schupp, F. (1998). Radiation-Induced Chromosome Aberrations in Saccharomyces cerevisiae: Influence of DNA Repair Pathways. Genetics *148*, 975-988.

Goodhead, D.T. (1994). Initial events in the cellular effects of ionizing radiations: clustered damage in DNA. Int J Radiat Biol *65*, 7-17.

Gospodinov, A., and Herceg, Z. (2013). Chromatin structure in double strand break repair. DNA Repair *12*, 800-810.

Gostissa, M., Alt, F.W., and Chiarle, R. (2011). Mechanisms that Promote and Suppress Chromosomal Translocations in Lymphocytes. Annual Review of Immunology *29*, 319-350.

Greaves, M.J., and Wiemels, J. (2003). Origins of Chromosome Translocations in Childhood Leukaemia. Nat Rev Cancer *3*, 639-649.

Hada, M., Wu, H., and Cucinotta, F.A. (2011). mBAND analysis for high- and low-LET radiation-induced chromosome aberrations: A review. Mutation Research/Fundamental and Molecular Mechanisms of Mutagenesis *711*, 187-192.

Hakem, R. (2008). DNA-damage repair; the good, the bad, and the ugly. EMBO J *27*, 589-605.

Halazonetis, T.D., Gorgoulis, V.G., and Bartek, J. (2008). An Oncogene-Induced DNA Damage Model for Cancer Development. Science *319*, 1352-1355.

Hall, E.J., and Giaccia, A.J. (2006). Radiobiology for the Radiologist, Sixth Edition edn (Philadelphia, Baltimore, New York, London, Buenos Aires, Hong Kong, Sydney, Tokyo, Lippincott Williams & Wilkins).

Harper, J.W., and Elledge, S.J. (2007). The DNA Damage Response: Ten Years After. Mol Cell *28*, 739-745.

Helleday, T., Lo, J., van Gent, D.C., and Engelward, B.P. (2007). DNA double-strand break repair: From mechanistic understanding to cancer treatment. DNA Repair *6*, 923-935.

Heller, R.C., and Marians, K.J. (2006). Replication fork reactivation downstream of a blocked nascent leading strand. Nature *439*, 557-562.

Heyer, W.-D., Ehmsen, K.T., and Liu, J. (2010). Regulation of Homologous Recombination in Eukaryotes. Annual Review of Genetics *44*, 113-139.

Heyer, W.-D., Li, X., Rolfsmeier, M., and Zhang, X.-P. (2006). Rad54: the Swiss Army knife of homologous recombination? Nucleic acids research *34*, 4115-4125.

Huertas, P., Cortes-Ledesma, F., Sartori, A.A., Aguilera, A., and Jackson, S.P. (2008). CDK targets Sae2 to control DNA-end resection and homologous recombination. Nature *455*, 689-692.

Iliakis, G. (2009). Backup pathways of NHEJ in cells of higher eukaryotes: Cell cycle dependence. Radiother Oncol *92*, 310-315.

Iliakis, G., Nusse, M., and Bryant, P. (1982). Effects of aphidicolin on cell proliferation, repair of potentially lethal damage and repair of DNA strand breaks in Ehrlich ascites tumour cells exposed to x-rays. Int J Radiat Biol *42,*, 417-434.

Iliakis, G., Wang, H., Perrault, A.R., Boecker, W., Rosidi, B., Windhofer, F., Wu, W., Guan, J., Terzoudi, G., and Pantelias, G. (2004). Mechanisms of DNA double strand

break repair and chromosome aberration formation. Cytogenetic and Genome Research *104*, 14-20.

Iliakis, G., Wu, W., Wang, M., Terzoudi, G.I., and Pantelias, G.E. (2007). Backup Pathways of Nonhomologous End Joining May Have a Dominant Role in the Formation of Chromosome Aberrations. In Chromosomal Alterations, G. Obe, Vijayalaxmi, ed. (Berlin, Heidelberg, New York, Springer Verlag), pp. 67-85.

Iliakis, G.E., Pantelias, G.E., Okayasu, R., and Blakely, W.F. (1992). Induction by H_2O_2 of DNA and interphase chromosome damage in plateau phase CHO cells. Radiat Res *131*, 193-203.

Ira, G., Pellicioli, A., Balijja, A., Wang, X., Fiorani, S., Carotenuto, W., Liberi, G., Bressan, D., Wan, L., Hollingsworth, N.M.*, et al.* (2004). DNA end resection, homologous recombination and DNA damage checkpoint activation require CDK1. Nature *431*, 1011-1017.

Jackson, S.P. (2002). Sensing and repairing DNA double-strand breaks. Carcinogenesis *23*, 687-696.

Jackson, S.P., and Bartek, J. (2009). The DNA-damage response in human biology and disease. Nature *461*, 1071-1078.

Jazayeri, A., Falck, J., Lukas, C., Bartek, J., Smith, G.C.M., Lukas, J., and Jackson, S.P. (2006). ATM- and cell cycle-dependent regulation of ATR in response to DNA double-strand breaks. Nat Cell Biol *8*, 37-45.

Jeggo, P.A. (1998). Identification of genes involved in repair of DNA double-strand breaks in mammalian cells. Radiat Res *150 (Suppl)*, S80-S91.

Jeggo, P.A., Geuting, V., and Löbrich, M. (2011). The role of homologous recombination in radiation-induced double-strand break repair. Radiother Oncol *101*, 7-12.

Johnson, R.D., and Jasin, M. (2000). Sister chromatid gene conversion is a prominent double-strand break repair pathway in mammalian cells. EMBO J *19*, 3398-3407.

Kadhim, M.A., Hill, M.A., and Moore, S.R. (2006). Genomic instability and the role of radiation quality. Radiation Protection Dosimetry *122*, 221-227.

Kadyk, L.C., and Hartwell, L.H. (1992). Sister Chromatids Are Preferred Over Homologs as Substrates for Recombinational Repair in Saccharomyces cerevisiae. Genetics *132*, 387-402.

Kastan, M.B., and Bartek, J. (2004). Cell-cycle checkpoints and cancer. Nature *432*, 316-323.

Kennedy, R.D., and D'Andrea, A.D. (2006). DNA Repair Pathways in Clinical Practice: Lessons From Pediatric Cancer Susceptibility Syndromes. J Clin Oncol *24*, 3799-3808.

Kim, J.-S., Krasieva, T.B., Kurumizaka, H., Chen, D.J., Taylor, A.M.R., and Yokomori, K. (2005). Independent and sequential recruitment of NHEJ and HR factors to DNA damage sites in mammalian cells. J Cell Biol *170*, 341-347.

Kurimasa, A., Kumano, S., Boubnov, N.V., Story, M.D., Tung, C.-S., Peterson, S.R., and Chen, D.J. (1999). Requirement for the kinase activity of human DNA-dependent protein kinase catalytic subunit in DNA strand break rejoining. Mol Cell Biol *19*, 3877-3884.

Lee-Theilen, M., Matthews, A.J., Kelly, D., Zheng, S., and Chaudhuri, J. (2011). CtIP promotes microhomology-mediated alternative end joining during class-switch recombination. Nat Struct Mol Biol *18*, 75-79.

Lengauer, C., Kinzler, K.W., and Vogelstein, B. (1998). Genetic instabilities in human cancers. Nature *396*, 643-649.

Lieber, M.R. (2008). The Mechanism of Human Nonhomologous DNA End Joining. J Biol Chem *283*, 1-5.

Lieber, M.R. (2010). NHEJ and its backup pathways in chromosomal translocations. Nat Struct Mol Biol *17*, 393-395.

Limbo, O., Chahwan, C., Yamada, Y., de Bruin, R.A.M., Wittenberg, C., and Russell, P. (2007). Ctp1 Is a Cell-Cycle-Regulated Protein that Functions with Mre11 Complex to Control Double-Strand Break Repair by Homologous Recombination. Mol Cell *28*, 134-146.

Ma, Y., Pannicke, U., Schwarz, K., and Lieber, M.R. (2002). Hairpin Opening and Overhang Processing by an Artemis/DNA-Dependent Protein Kinase Complex in Nonhomologous End Joining and V(D)J Recombination. Cell *108*, 781-794.

Mansour, W.Y., Rhein, T., and Dahm-Daphi, J. (2010). The alternative end-joining pathway for repair of DNA double-strand breaks requires PARP1 but is not dependent upon microhomologies. Nucleic acids research *38*, 6065-6077.

McVey, M., and Lee, S.E. (2008). MMEJ repair of double-strand breaks (director's cut): deleted sequences and alternative endings. Trends Genet *24*, 529-538.

Meek, K., Gupta, S., Ramsden, D.A., and Lees-Miller, S.P. (2004). The DNA-dependent protein kinase: the director at the end. Immunological Reviews *200*, 132-141.

Mimitou, E.P., and Symington, L.S. (2008). Sae2, Exo1 and Sgs1 collaborate in DNA double-strand break processing. Nature *455*, 770-774.

Mladenov, E., and Iliakis, G. (2011). Induction and Repair of DNA Double Strand Breaks: The Increasing Spectrum of Non-homologous End Joining Pathways. Mutation Research/Fundamental and Molecular Mechanisms of Mutagenesis *711*, 61-72.

Natarajan, A.T., and Obe, G. (1978). Molecular mechanisms involved in the production of chromosomal aberrations. 1. Utilization of neurospora endonuclease for the study of aberration production in G2 stage of the cell cycle. Mutat Res *52*, 137-149.

Natarajan, A.T., and Palitti, F. (2008). DNA repair and chromosomal alterations. Mutation Research/Genetic Toxicology and Environmental Mutagenesis *657*, 3-7.

Nikjoo, H., O'Neill, P.O., Terrissol, M., and Goodhead, D.T. (1999). Quantitative modelling of DNA damage using Monte Carlo track structure method. Radiat Environm Biophys *38*, 31-38.

Nussenzweig, A., and Nussenzweig, M.C. (2007). A Backup DNA Repair Pathway Moves to the Forefront. Cell *131*, 223-225.

Nussenzweig, A., and Nussenzweig, M.C. (2010). Origin of Chromosomal Translocations in Lymphoid Cancer. Cell *141*, 27-38.

O'Neill, P., and Wardman, P. (2009). Radiation chemistry comes before radiation biology. Int J Radiat Biol *85*, 9-25.

Olive, P.L. (1998). The Role of DNA Single- and Double-Strand Breaks in Cell Killing by Ionizing Radiation. Radiat Res *150 (Suppl.)*, S42-S51.

Pastink, A., Eeken, J.C.J., and Lohman, P.H.M. (2001). Genomic integrity and the repair of double-strand DNA breaks. Mutat Res *480-481*, 37-50.

Paul, K., Wang, M., Mladenov, E., Bencsik-Theilen, A.A., Bednar, T., Wu, W., Arakawa, H., and Iliakis, G. (2013). DNA ligases I and III cooperate in alternative non-homologous end-joining in vertebrates. PLoS One *8*, e59505.

Paull, T.T., Rogakou, E.P., Yamazaki, V., Kirchgessner, C.U., Gellert, M., and Bonner, W.M. (2000). A critical role for histone H2AX in recruitment of repair factors to nuclear foci after DNA damage. Curr Biol *10*, 886-895.

Perrault, R., Wang, H., Wang, M., Rosidi, B., and Iliakis, G. (2004). Backup Pathways of NHEJ Are Suppressed by DNA-PK. J Cell Biochem *92*, 781-794.

Povirk, L.F. (2012). Processing of Damaged DNA Ends for Double-Strand Break Repair in Mammalian Cells. ISRN Molecular Biology *2012*, Article: ID 345805.

Prevo, R., Fokas, E., Reaper, P.M., Charlton, P.A., Pollard, J.R., McKenna, W.G., Muschel, R.J., and Brunner, T. (2012). The novel ATR inhibitor VE-821 increases sensitivity of pancreatic cancer cells to radiation and chemotherapy. Cancer Biol Ther *13*, 1-10.

Price, Brendan D., and D'Andrea, Alan D. (2013). Chromatin Remodeling at DNA Double-Strand Breaks. Cell *152*, 1344-1354.

Rass, E., Grabarz, A., Plo, I., Gautier, J., Bertrand, P., and Lopez, B.S. (2009). Role of Mre11 in chromosomal nonhomologous end joining in mammalian cells. Nat Struct Mol Biol *16*, 819-825.

Richardson, C., Horikoshi, N., and Pandita, T.K. (2004). The role of the DNA double-strand break response network in meiosis. DNA Repair *3*, 1149-1164.

Richardson, C., Moynahan, M.E., and Jasin, M. (1998). Double-strand break repair by interchromosomal recombination: suppression of chromosomal translocations. Genes & Development *12*, 3831-3842.

Rieder, C.L., and Cole, R.W. (1998). Entry into Mitosis in Vertebrate Somatic Cells Is Guarded by a Chromosome Damage Checkpoint That Reverses the Cell Cycle When Triggered during Early but Not Late Prophase. J Cell Biol *142*, 1013-1022.

Roth, D.B., and Wilson, J.H. (1985). Relative rates of homologous and nonhomologous recombination in transfected DNA. Proc Natl Acad Sci USA *82*, 3355-3359.

Roukos, V., Voss, T.C., Schmidt, C.K., Lee, S., Wangsa, D., and Misteli, T. (2013). Spatial Dynamics of Chromosome Translocations in Living Cells. Science *341*, 660-664.

San Filippo, J., Sung, P., and Klein, H. (2008). Mechanism of Eukaryotic Homologous Recombination. Ann Rev Biochem *77*, 229-257.

Sancar, A., Lindsey-Boltz, L.A., Ünsal-Kacmaz, K., and Linn, S. (2004). Molecular Mechanisms of Mammalian DNA Repair and the DNA Damage Checkpoints. Ann Rev Biochem *73*, 39-85.

Sax, K. (1940). An analysis of X-ray induced chromosomal aberrations in tradescantia. Genetics *25*, 41-68.

Schipler, A., and Iliakis, G. (2013). DNA double-strand-break complexity levels and their possible contributions to the probability for error-prone processing and repair pathway choice. Nucl Acids Res *41*, 7589-7605.

Shrivastav, M., De Haro, L.P., and Nickoloff, J.A. (2008). Regulation of DNA double-strand break repair pathway choice. Cell Res *18*, 134-147.

Simsek, D., Brunet, E., Wong, S.Y.-W., Katyal, S., Gao, Y., McKinnon, P.J., Lou, J., Zhang, L., Li, J., Rebar, E.J.*, et al.* (2011). DNA Ligase III Promotes Alternative Nonhomologous End-Joining during Chromosomal Translocation Formation. PLoS Genet *7*, e1002080.

Simsek, D., and Jasin, M. (2010). Alternative end-joining is suppressed by the canonical NHEJ component Xrcc4-ligase IV during chromosomal translocation formation. Nat Struct Mol Biol *17*, 410-416.

Singh, S.K., Bednar, T., Zhang, L., Wu, W., Mladenov, E., and Iliakis, G. (2012). Inhibition of B-NHEJ in Plateau-Phase Cells Is Not a Direct Consequence of Suppressed Growth Factor Signaling. Int J Radiat Oncol Biol Phys *84*, e237-e243.

Singh, S.K., Wu, W., Wu, W., Wang, M., and Iliakis, G. (2009). Extensive Repair of DNA Double-Strand Breaks in Cells Deficient in the DNA-PK Dependent Pathway of NHEJ after Exclusion of Heat-Labile Sites. Radiat Res *172*, 152-164.

Singh, S.K., Wu, W., Zhang, L., Klammer, H., Wang, M., and Iliakis, G. (2011). Widespread Dependence of Backup NHEJ on Growth State: Ramifications for the Use of DNA-PK Inhibitors. Int J Radiat Oncol Biol Phys *79*, 540-548.

Soni, A. (2010). The Role of Homologous Recombination Repair in the processing of G2-chromosomal breaks and maintenance of G2-checkpoint. DuEPublico *PhD thesis*.

Stephens, P.J., Greenman, C.D., Fu, B., Yang, F., Rignell, G.R., Mudie, L.J., Pleasance, E.D., Lau, K.W., Beare, D., Stebbings, L.A.*, et al.* (2011). Massive Genomic Rearrangement Acquired in a Single Catastrophic Event during Cancer Development. Cell *144*, 27-40.

Stephens, P.J., McBride, D.J., Lin, M.-L., Varela, I., Pleasance, E.D., Simpson, J.T., Stebbings, L.A., Leroy, C., Edkins, S., Mudie, L.J.*, et al.* (2009). Complex landscapes of somatic rearrangement in human breast cancer genomes. Nature *462*, 1005-1010.

Sutherland, B.M., Bennett, P.V., Sidorkina, O., and Laval, J. (2000). Clustered DNA damages induced in isolated DNA and in human cells by low doses of ionizing radiation. Proc Natl Acad Sci USA *97*, 103-108.

Symington, L.S., and Gautier, J. (2011). Double-Strand Break End Resection and Repair Pathway Choice. Annual Review of Genetics *45*, 247-271.

Takata, M., Sasaki, M.S., Sonoda, E., Morrison, C., Hashimoto, M., Utsumi, H., Yamaguchi-Iwai, Y., Shinohara, A., and Takeda, S. (1998). Homologous recombination and non-homologous end-joining pathways of DNA double-strand break. EMBO J *17*, 5497-5508.

Tamulevicius, P., Wang, M., and Iliakis, G. (2007). Homology-Directed Repair is Required for the Development of Radioresistance during S Phase: Interplay between Double-Strand Break Repair and Checkpoint Response. Radiat Res *167*, 1-11.

Thompson, L.H., and Schild, D. (2001). Homologous recombinational repair of DNA ensures mammalian chromosome stability. Mutat Res *477*, 131-153.

Truong, L.N., Li, Y., Shi, L.Z., Hwang, P.Y.-H., He, J., Wang, H., Razavian, N., Berns, M.W., and Wu, X. (2013). Microhomology-mediated End Joining and Homologus Recombination share the initial end resection step to repair DNA double-strand breaks in mammalian cells. Proc Natl Acad Sci USA *in press*.

van Gent, D.C., Hoeijmakers, J.H.J., and Kanaar, R. (2001). Chromosomal stability and the DNA double-stranded break connection. Nature Reviews Genetics *2*, 196-206.

Verkaik, N.S., Esveldt-van Lange, R.E.E., van Heemst, D., Brüggenwirth, H.T., Hoeijmakers, J.H.J., Zdzienicka, M.Z., and van Gent, D.C. (2002). Different types of V(D)J recombination and end-joining defects in DNA double-strand break repair mutant mammalian cells. European Journal of Immunology *32*, 701-709.

Wang, H., Perrault, A.R., Takeda, Y., Qin, W., Wang, H., and Iliakis, G. (2003). Biochemical evidence for Ku-independent backup pathways of NHEJ. Nucleic acids research *31*, 5377-5388.

Wang, H., Rosidi, B., Perrault, R., Wang, M., Zhang, L., Windhofer, F., and Iliakis, G. (2005). DNA Ligase III as a Candidate Component of Backup Pathways of Nonhomologous End Joining. Cancer Res *65*, 4020-4030.

Wang, H., Zeng, Z.-C., Bui, T.-A., Sonoda, E., Takata, M., Takeda, S., and Iliakis, G. (2001). Efficient rejoining of radiation-induced DNA double-strand breaks in vertebrate cells deficient in genes of the RAD52 epistasis group. Oncogene *20*, 2212-2224.

Wang, M., Wu, W., Wu, W., Rosidi, B., Zhang, L., Wang, H., and Iliakis, G. (2006). PARP-1 and Ku compete for repair of DNA double strand breaks by distinct NHEJ pathways. Nucleic acids research *34*, 6170-6182.

Ward, J.F. (1988). DNA damage produced by ionizing radiation in mammalian cells: Identities, mechanisms of formation, and reparability. Progress in Nucleic Acid Research *35*, 95-125.

Ward, J.F. (1990). The yield of DNA double-strand breaks produced intracellularly by ionizing radiation: a review. Int J Radiat Biol *57*, 1141-1150.

Ward, J.F., Blakely, W.F., and Joner, E.I. (1985). Mammalian cells are not killed by DNA single-strand breaks caused by hydroxyl radiacals from hydrogen peroxide. Radiat Res *103*, 383-392.

Weinstock, D.M., Brunet, E., and Jasin, M. (2007). Formation of NHEJ-derived reciprocal chromosomal translocations does not require Ku70. Nat Cell Biol *9*, 978-981.

West, S.C. (2003). Molecular views of recombination proteins and their control. Nat Rev Mol Cell Biol *4*, 1-11.

Weterings, E., and Chen, D.J. (2008). The endless tale of non-homologous end-joining. Cell Res *18*, 114-124.

Windhofer, F., Wu, W., and Iliakis, G. (2007a). Low Levels of DNA Ligases III and IV Sufficient for Effective NHEJ. Journal of Cellular Physiology *213*, 475-483.

Windhofer, F., Wu, W., Wang, M., Singh, S.K., Saha, J., Rosidi, B., and Iliakis, G. (2007b). Marked dependence on growth state of backup pathways of NHEJ. Int J Radiat Oncol Biol Phys *68*, 1462-1470.

Wray, J., Williamson, E.A., Singh, S.B., Wu, Y., Cogle, C.R., Weinstock, D.M., Zhang, Y., Lee, S.-H., Zhou, D., Shao, L.*, et al.* (2013). PARP1 is required for chromosomal translocations. Blood *in press*.

Wu, W., Wang, M., Mussfeldt, T., and Iliakis, G. (2008a). Enhanced Use of Backup Pathways of NHEJ in G_2 in Chinese Hamster Mutant Cells with Defects in the Classical Pathway of NHEJ. Radiat Res *170*, 512-520.

Wu, W., Wang, M., Wu, W., Singh, S.K., Mussfeldt, T., and Iliakis, G. (2008b). Repair of radiation induced DNA double strand breaks by backup NHEJ is enhanced in G2. DNA Repair *7*, 329-338.

Wyman, C., and Kanaar, R. (2006). DNA Double-Strand Break Repair: All's Well that Ends Well. Annual Review of Genetics *40*, 363-383.

Xie, A., Kwok, A., and Scully, R. (2009). Role of mammalian Mre11 in classical and alternative nonhomologous end joining. Nat Struct Mol Biol *16*, 814-818.

Yang, H., Li, Q., Fan, J., Holloman, W.K., and Pavietich, N.P. (2005). The BRCA2 homologue Brh2 nucleates RAD51 filament formation at a dsDNA-ssDNA junction. Nature *433*, 653-657.

You, Z., and Bailis, J.M. (2010). DNA damage and decisions: CtIP coordinates DNA repair and cell cycle checkpoints. Trends in Cell Biology *20*, 402-409.

Yun, M.H., and Hiom, K. (2009). CtIP-BRCA1 modulates the choice of DNA double-strand-break repair pathway throughout the cell cycle. Nature *459*, 460-463.

Zhang, Y., and Jasin, M. (2011). An essential role for CtIP in chromosomal translocation formation through an alternative end-joining pathway. Nat Struct Mol Biol *18*, 80-84.

Zhang, Y., Shim, E.Y., Davis, M., and Lee, S.E. (2009). Regulation of repair choice: Cdk1 suppresses recruitment of end joining factors at DNA breaks. DNA Repair *8*, 1235-1241.

Zhong, Q., Chen, C.-F., Chen, P.-L., and Lee, W.-H. (2002). BRCA1 Facilitates Microhomology-mediated End Joining of DNA Double Strand Breaks. J Biol Chem *277*, 28641-28647.

Zou, L., and Elledge, S.J. (2003). Sensing DNA Damage Through ATRIP Recognition of RPA-ssDNA Complexes. Science *300*, 1542-1548.

7 Appendix

Appendix 1: Study of S-phase block in Chinese hamster wild type and HRR mutants by flow cytometry. Two sets of exponentially growing cells, the first set is untreated and the cells of the second set are block in S-phase by treating with Aphidicolin. In every set there are cells, which were irradiated with 0, 1 and 5 Gy X-rays. We analyzed the experiment by flow cytometry at 0, 0.5, 2, 6, and 8 h post-irradiation and looked at the BrdU-positive S-phase and BrdU-negative G2-phase cells gated in the density plots.

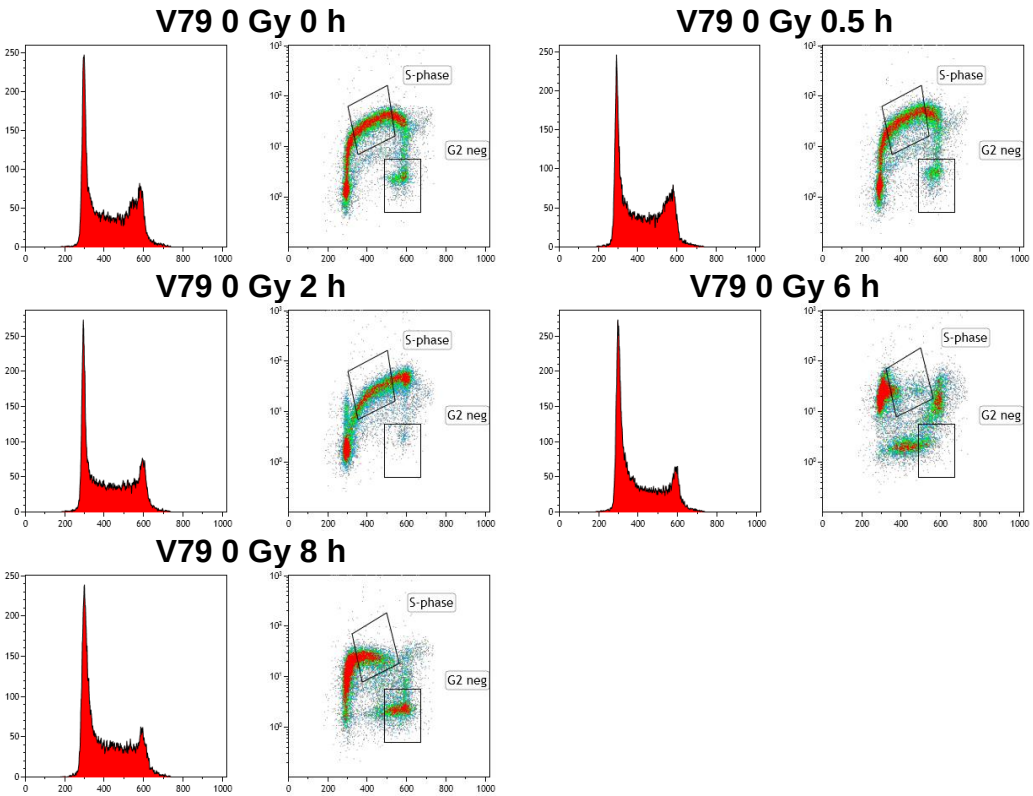

Figure 42: V79 without irradiation

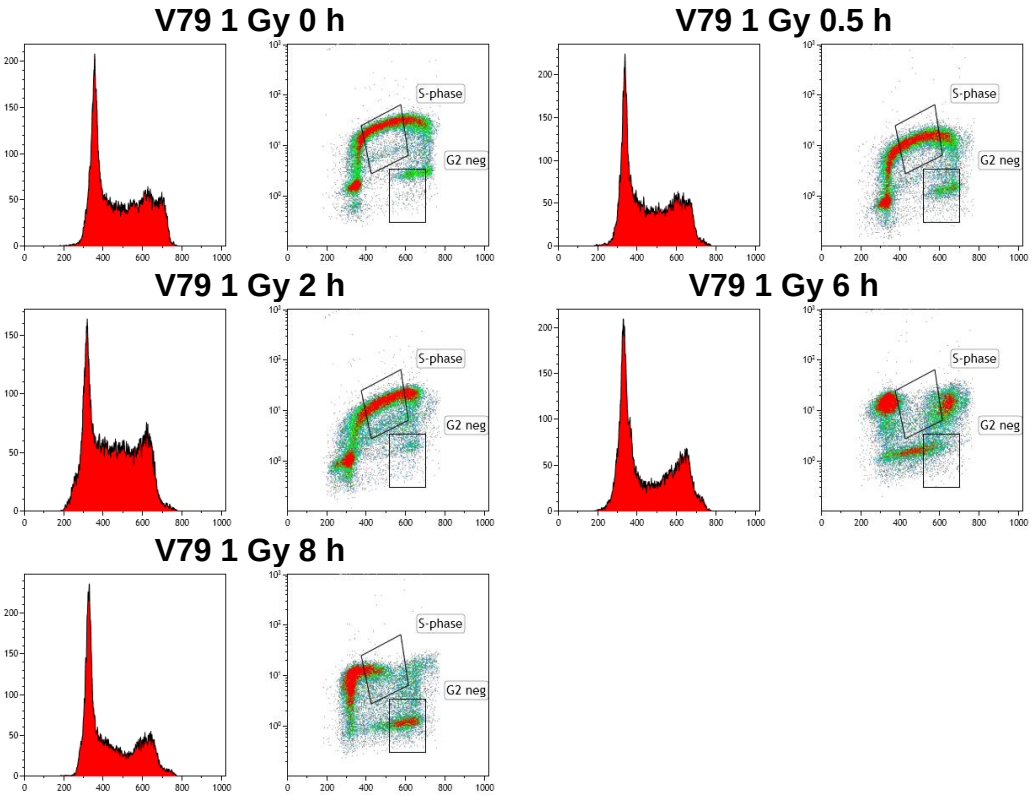

Figure 43: V79 irradiated with1 Gy of IR

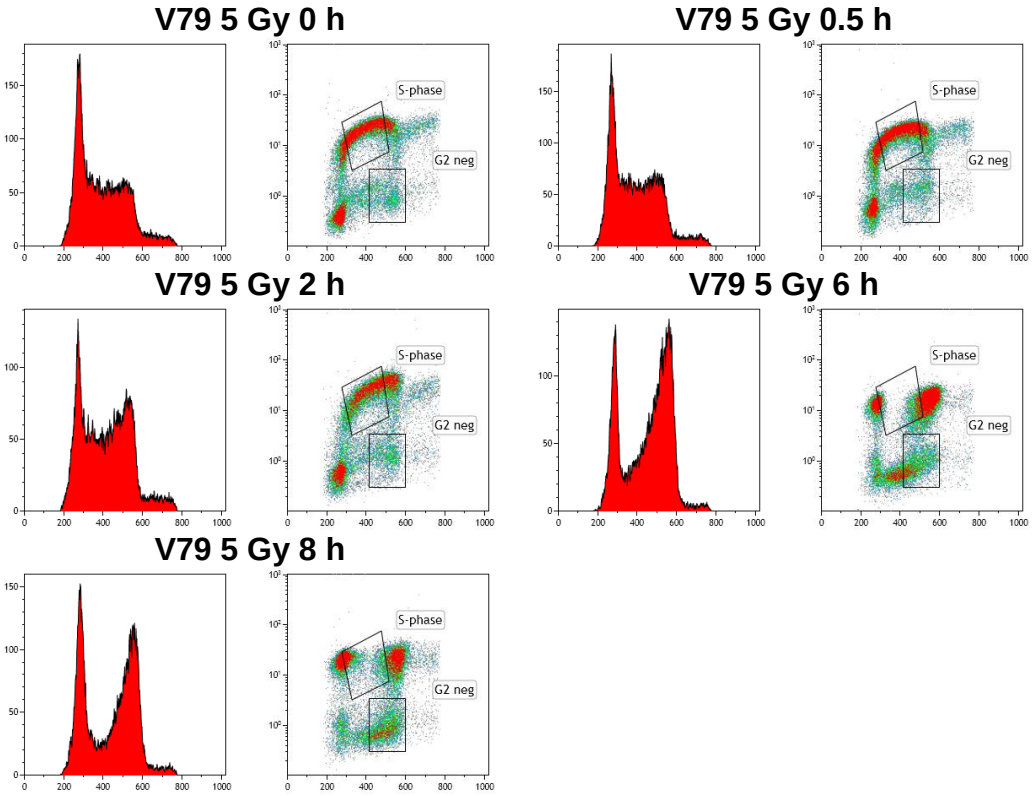

Figure 44: V79 irradiated with 5 Gy of IR

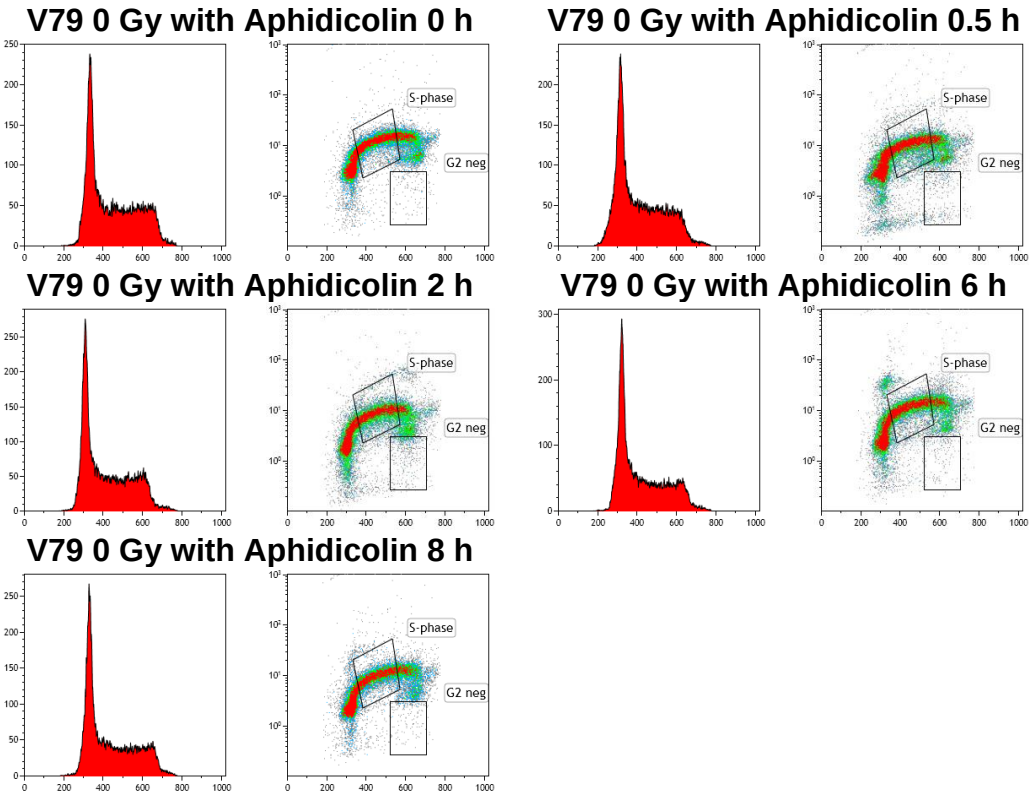

Figure 45: V79 with Aphidicolin-block without irradiation

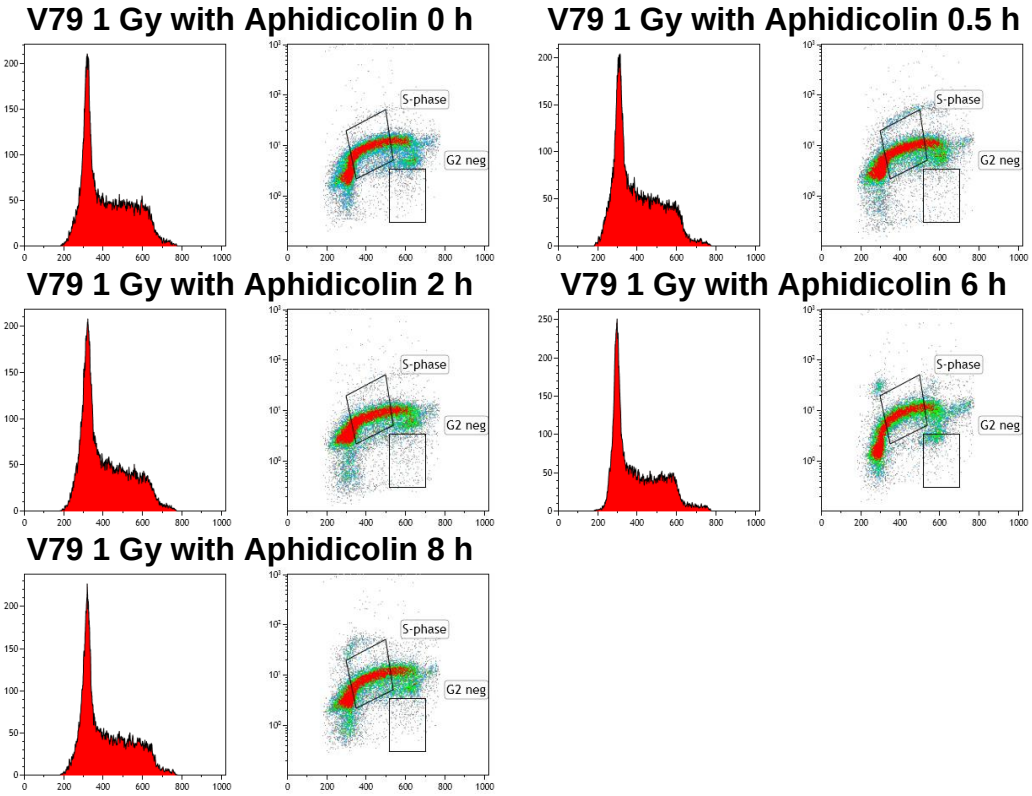

Figure 46: V79 with Aphidicolin-block irradiated with 1 Gy of IR

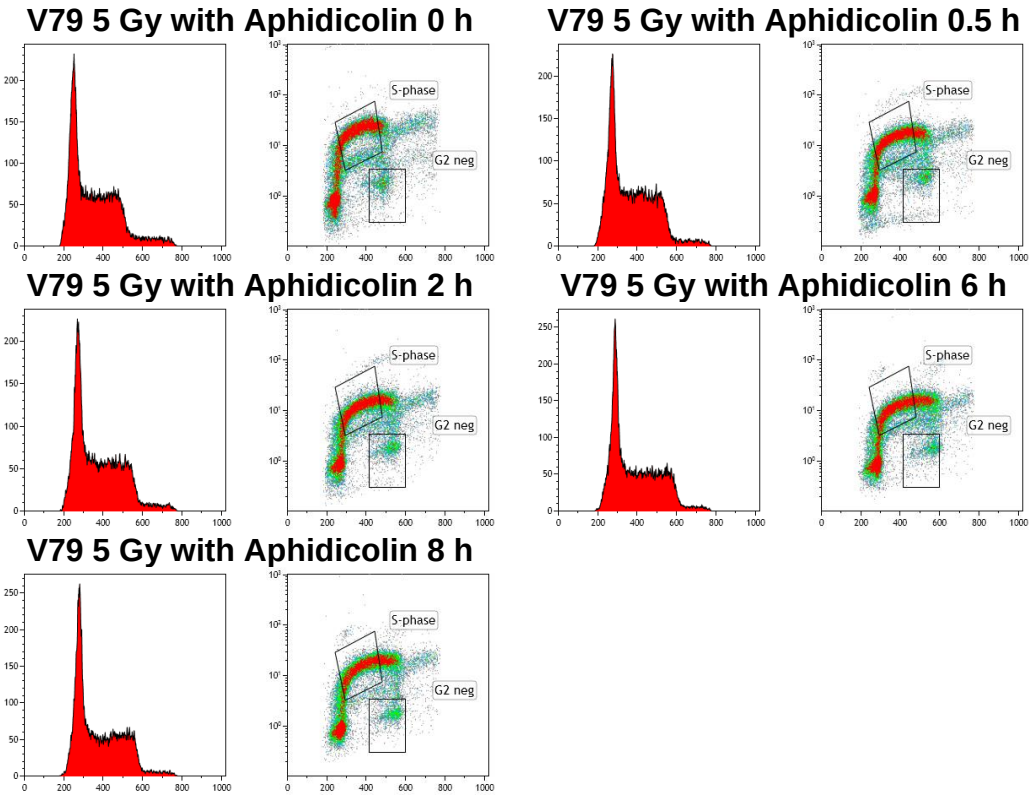

Figure 47: V79 with Aphidicolin-block irradiated with 5 Gy of IR

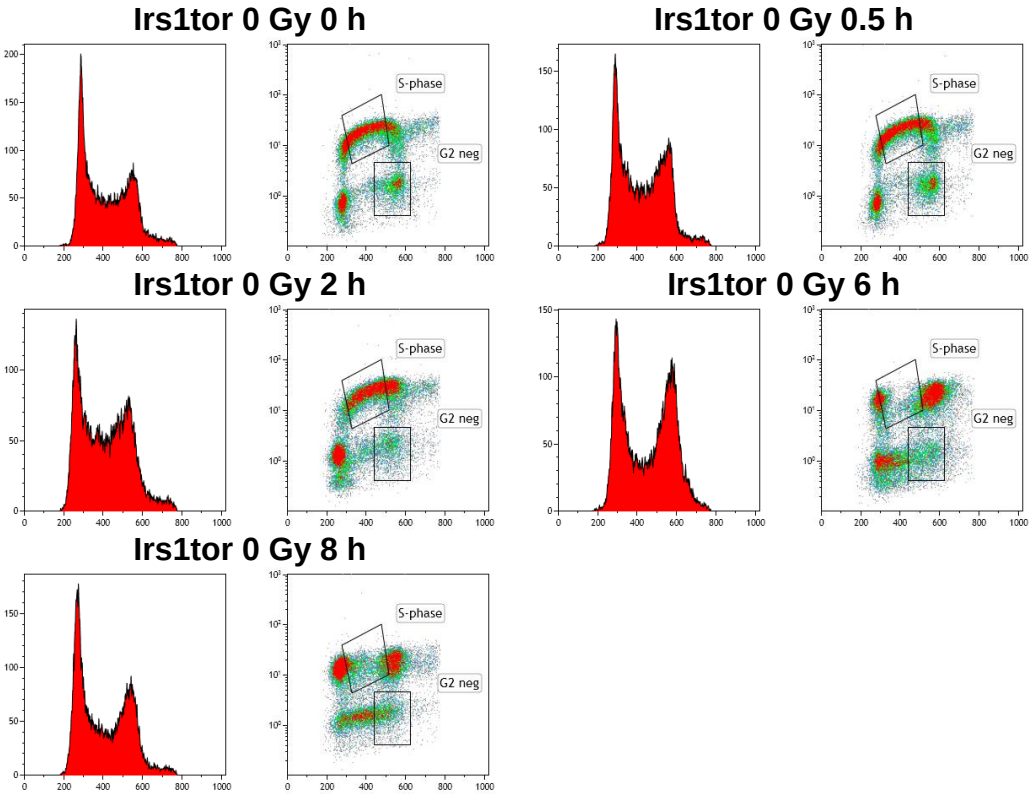

Figure 48: Irs1tor without irradiation

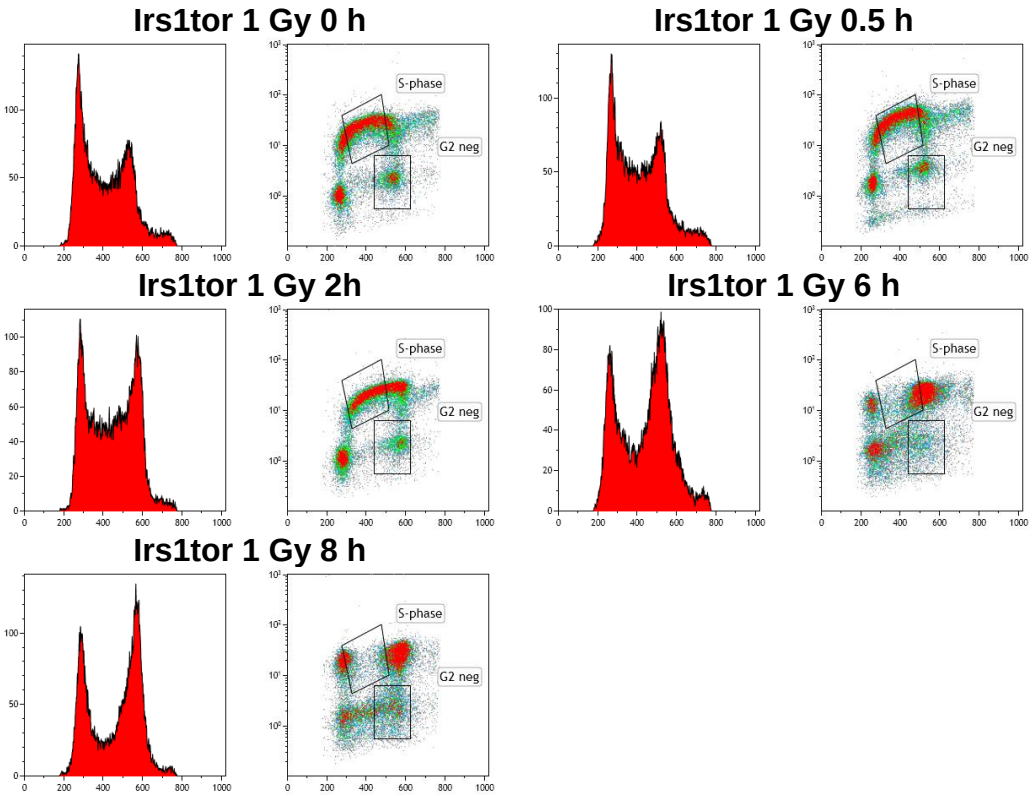

Figure 49: Irs1tor irradiated with 1 Gy of IR

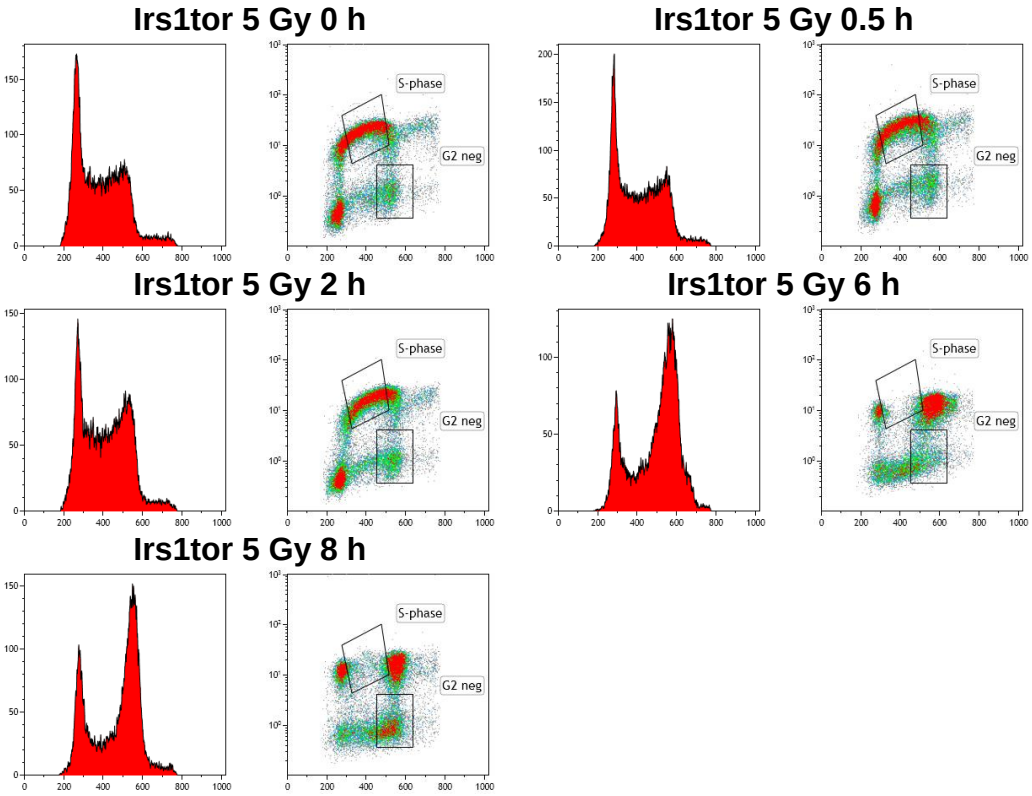

Figure 50: Irs1tor irradiated with 5 Gy of IR

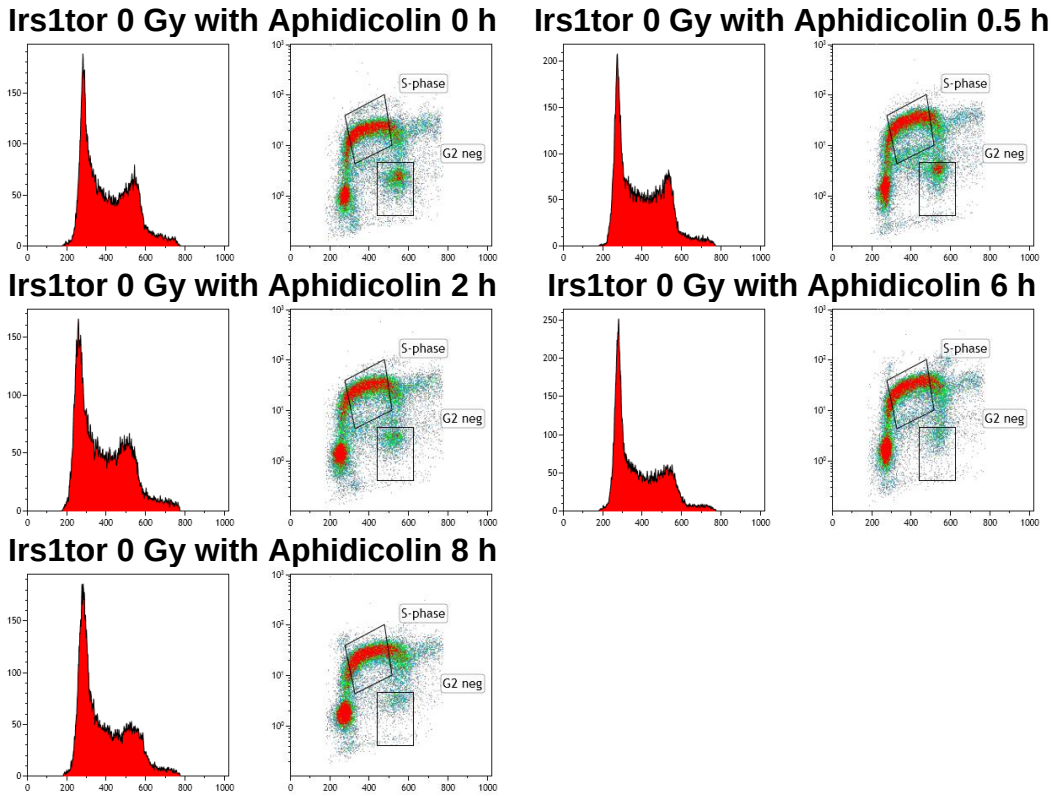

Figure 51: Irs1tor with Aphidicolin-block without irradiation

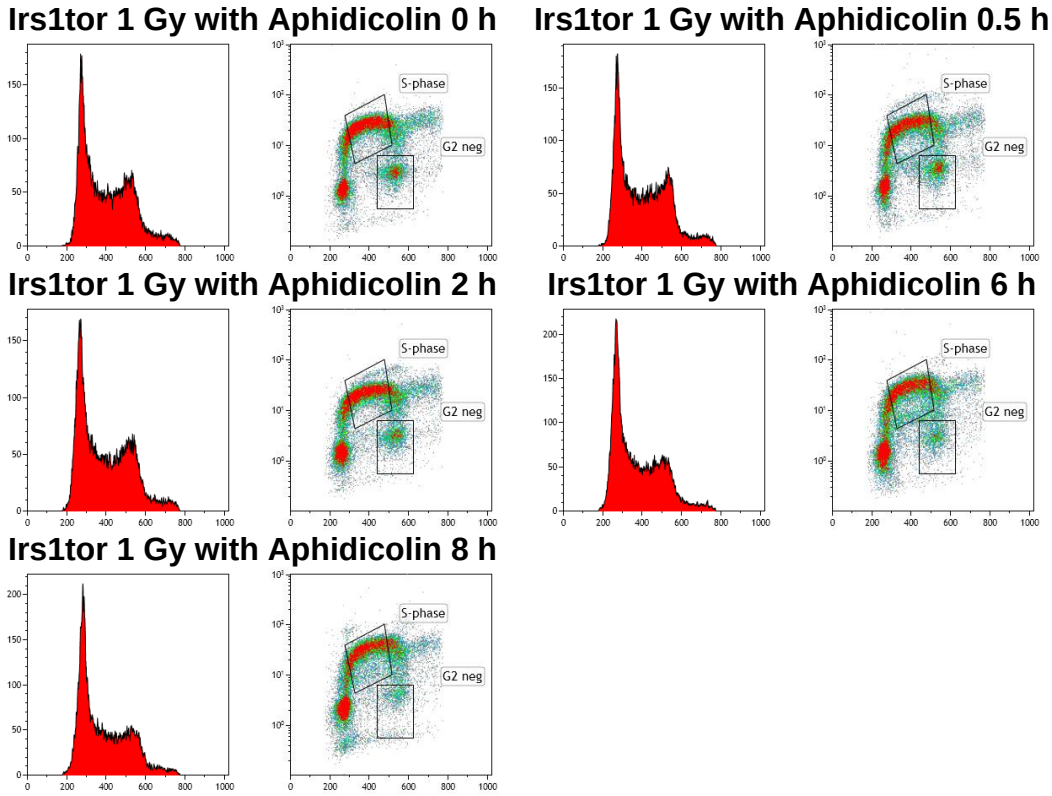

Figure 52: Irs1tor with Aphidicolin-block irradiated with 1 Gy of IR

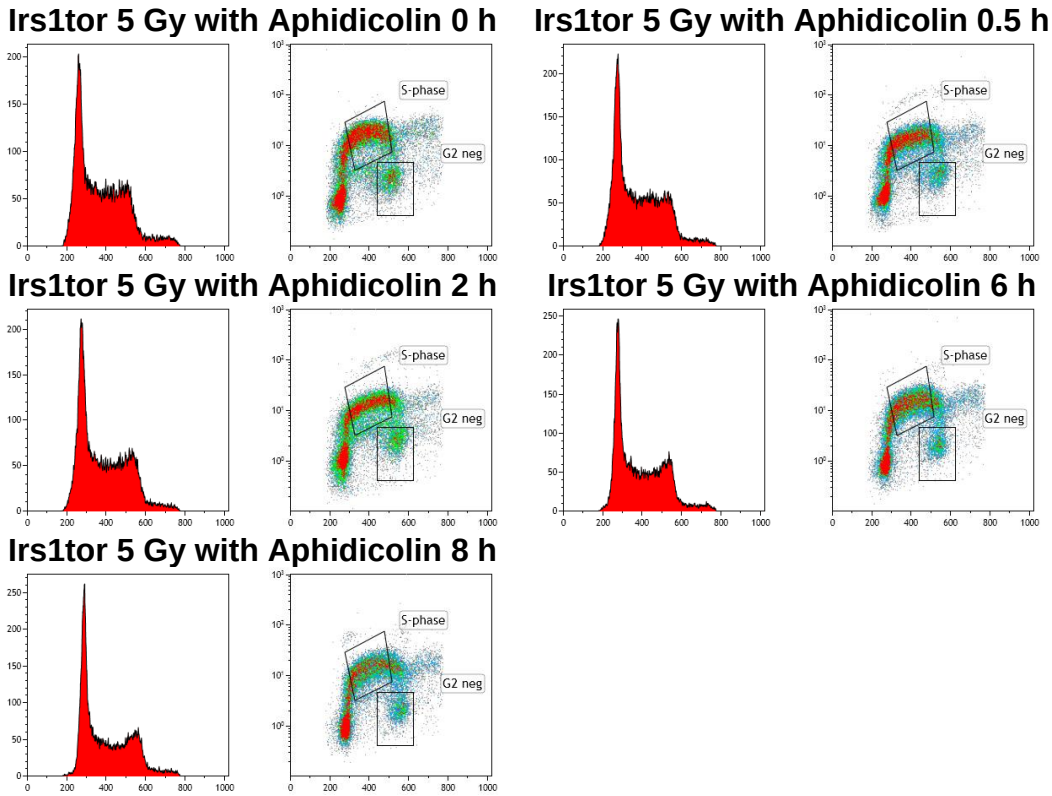

Figure 53: Irs1tor with Aphidicolin-block irradiated with 5 Gy of IR

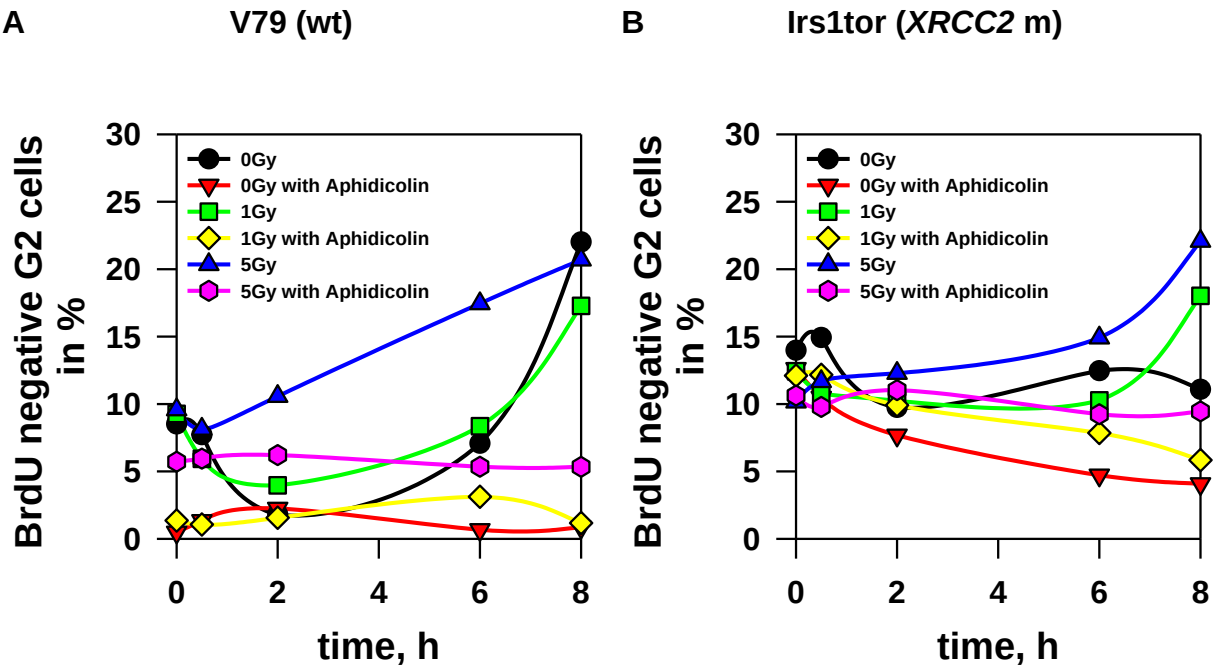

Figure 54: BrdU negative G2-phase cells

Appendix 2: Pictures of Aphidicolin treated G1-, S- and G2-phase cells after Calyculin A induced G2-PCC in Chinese hamster cells.

G1-phase cell

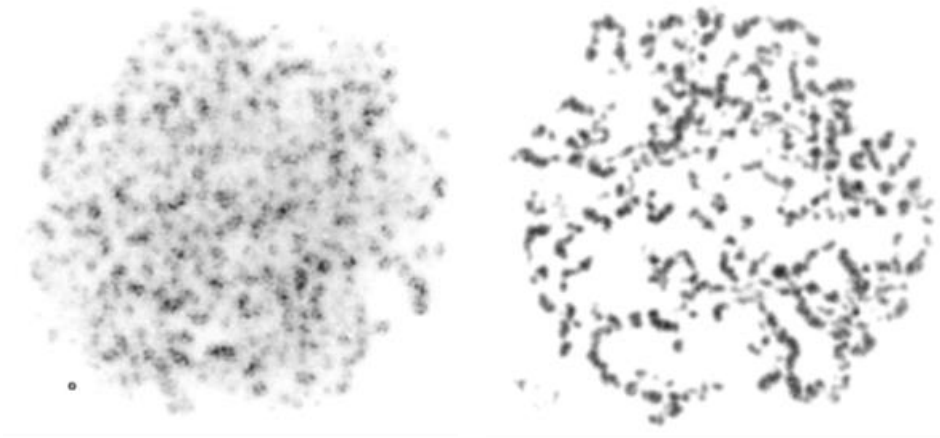

G2-phase cells

S-phase cells

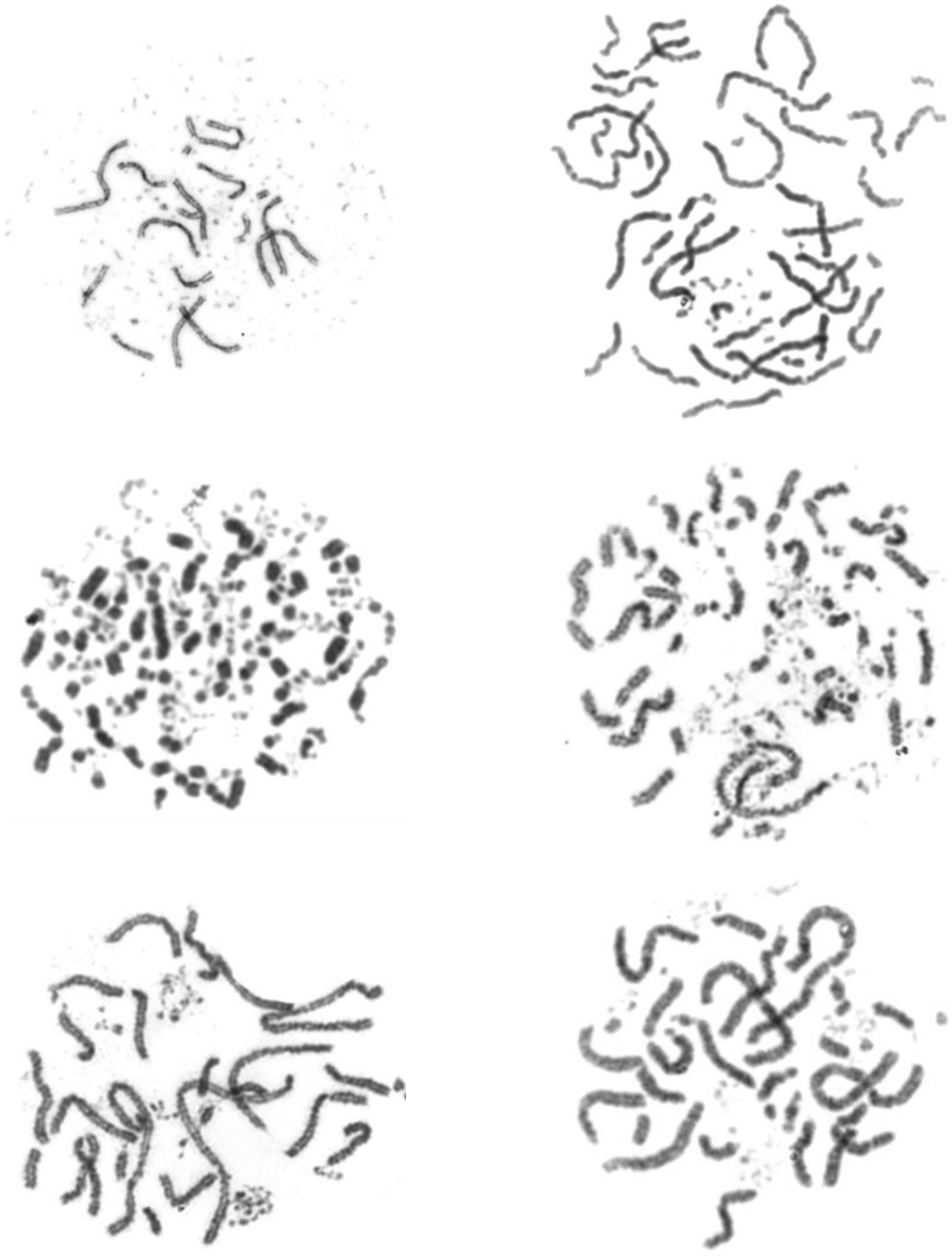

Appendix 3: Exemplary pictures of G2-PCC breaks and exchanges in Chinese hamster cells (red arrows display G2-PCC breaks and red circles point to exchanges).

G2-PCC breaks	**G2-PCC exchanges**
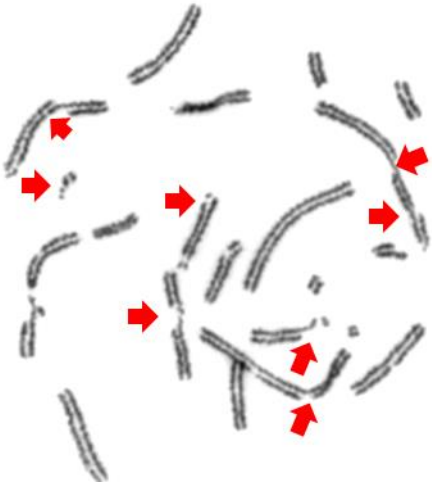	
	
	

Appendix 4: Metaphase pictures of chromatid exchanges (CEs) in Mouse embryonic fibroblasts (MEF) and Human colorectal tumor cells (HCT) irradiated with 1Gy X-rays (red circles represent CEs).

Mef Metaphases control

Mef Metaphases CE

Mef Metaphases CE

Mef Metaphases CE

Mef Metaphases CE

Mef Metaphases CE

HCT Metaphases control

HCT Metaphases CE

HCT Metaphases CE

Appendix 5: Fluorescence metaphase pictures of chromatid exchanges (CEs) and translocations (CTs) in Human colorectal tumor cells (HCT) irradiated with 2 Gy X-rays (white circles represent CEs as well as CTs).

HCT Metaphases control

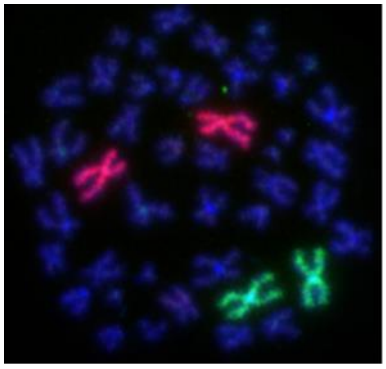

HCT Metaphases CE

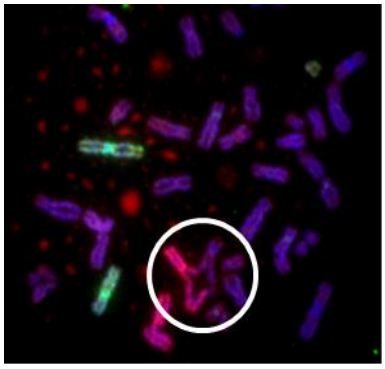

HCT Metaphases CE

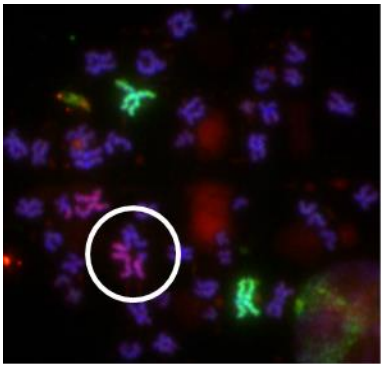

HCT Metaphases CT

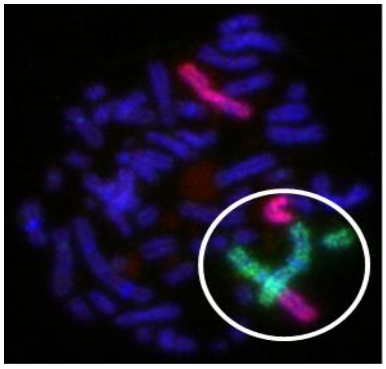

HCT Metaphases CT

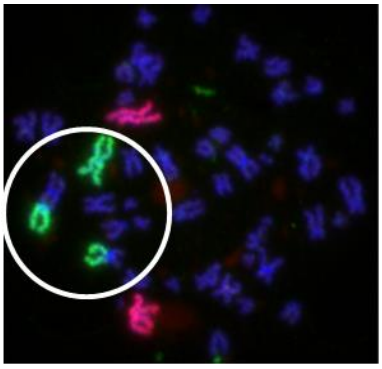

HCT Metaphases CT

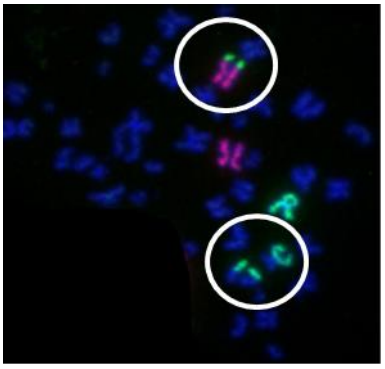

Acknowledgments

First of all I would like to thank the “**Deutsche Forschungsgemeinschaft**” that I could be a part of the DFG graduate training program 1431 **“Transcription, chromatin structure and DNA repair in development and differentiation”** and for the financial support of my thesis.

My special gratitude goes to my mentor **Prof. Dr. George Iliakis** for giving me the opportunity to do my PhD in the Institute of Medical Radiation Biology. I thank you for the support during my thesis on scientific as well as on personal matters. I enjoyed being part of this great team.

I also would like to thank the members of my promotional committee **Prof. Dr. Ann Ehrenhofer-Murray**, **Prof. Dr. Hemmo Meyer** and **PD Dr. Jürgen Thomale** for their helpful suggestions and critical comments during the meetings of the promotional committee.

Dr. Aashish Soni you were my lab-guru, without you the time of my thesis certainly would not have been the same. Thank you for teaching, supervising and advising me in lab and personal life and also for helping me during my writing phase!

I would like to thank **Dr. Aashish Soni**, **Dr. Agnes Schipler**, **Dr. Katja Paul, Dr. Emil Mladenov** and **Tamara Murmann** for the critical reading of my thesis, the useful suggestions and for the help in formatting the thesis.

I am very thankful to **Ms Jutta Müller**, for her excellent and timely administrative assistance and **Prof. Dr. Wolfgang-Ulrich Müller** for giving me insights into radiation protection and laboratory safety.

I also would like to thank **Tamara Mussfeldt** and **Malihe Mesbah** for all the technical support and **Ms Lander** for the lab organization, and that you all had always an open ear also for personal matter. Furthermore I want to thank all the other members of the lab. I always felt good to be part of this wonderful team. Special thanks goes to the cooking evening girls, in particular to **Agnes, Katja, Swetlana** and **Theresa**. I am happy to get to know such good friends.

I am very lucky to have my family, without you I would not be the kind of person that I am. Thank you **Mama** and **Papa** for giving me always unreserved support and that you always helped me to fulfill all my dreams so far. I also want to thank my sisters **Stefanie** and **Johanna** and my brothers **Christian**, **Martin** and **Michael,** I known that life was not always easy with me…

And of course I have to thank all my **friends** all over the world, especially **Tina, Anna, Anja R., Britta, Carina, Claudia, Daniela, Lisa, Lydia, Sonja**, **Vera** and the girls from the GRK1431, especially **Anne, Bernadette** and **Stephanie**, it is good to have you around.

And last but not least I want to thank my lovely relatives "**Siemanns**". I am happy that you are always there for me and my family!

„Der Lebenslauf ist in der Online-Version aus Gründen des Datenschutzes nicht enthalten.“